NOVEL ROLES FOR ENTERIC GLIA IN THE SYNAPSE-SPECIFIC CONTROL OF INTESTINAL MOTOR NEUROCIRCUITS AND THE PATHOGENESIS OF CHRONIC INTESTINAL PSEUDO-OBSTRUCTION

By

Mohammad Mustafa Ahmadzai

A DISSERTATION

Submitted to
Michigan State University
in partial fulfillment of the requirements
for the degree of

Physiology – Doctor of Philosophy

2020

ABSTRACT

NOVEL ROLES FOR ENTERIC GLIA IN THE SYNAPSE-SPECIFIC CONTROL OF INTESTINAL MOTOR NEUROCIRCUITS AND THE PATHOGENESIS OF CHRONIC INTESTINAL PSEUDO-OBSTRUCTION

By

Mohammad Mustafa Ahmadzai

Motility is an essential feature of gastrointestinal (GI) physiology that is necessary for life. Defects in motility are seen in a spectrum of GI diseases including functional GI disorders (FGIDs), which are prevalent throughout the world and are associated with reduced quality of life. FGIDs remain a substantial social burden that continues to exact tremendous personal and economic costs. Effective treatments for FGIDs are currently lacking due, in part, to an incomplete understanding of the mechanisms regulating GI motility.

The motility of the GI tract is controlled by the enteric nervous system (ENS) through neural circuits embedded within the gut wall. Enteric neurons serve effector and regulatory functions and are subject to dynamic and reciprocal input from surrounding populations of enteric glia. Enteric glia are specialized peripheral glial cells that sense neural circuit activity through neurotransmitter receptors and reciprocally modify their function through gliotransmitter release. While interactions between neurons and glia of the central nervous system (CNS) are remarkably synapse-specific, whether this sophisticated degree of neurocircuit modulation occurs in the ENS has never been explored. The overarching objective of this dissertation was to characterize the mechanisms by which enteric glia modulate activity within enteric motor circuits and to elucidate the role of enteric glia in the pathogenesis of FGIDs.

In the first part of this dissertation, we developed a novel mouse model that combined chemogenetics and optogenetics to characterize network-level activity in ENS motor circuits. We report here the first evidence that enteric glia are functionally committed to specific circuit pathways of the ENS. In the second part of this dissertation, we combine Ca^{2+} imaging, genetic,

immunohistochemistry, *ex vivo* and *in vivo* motility techniques to demonstrate a novel role the type I lysophosphatidic acid receptor (LPAR1) in the regulation of GI motility by enteric glia. Our study reveals a striking reduction in glial LPAR1 expression in chronic intestinal pseudo-obstruction (CIPO), a severe FGID in which failure in GI motility leads to life-threatening episodes of bowel obstruction. Together, our studies shed new light on the mechanisms by which enteric glia regulate ENS motor activity under physiological conditions and how dysregulations in glial signaling can drive GI dysmotilities like CIPO.

ACKNOWLEDGEMENTS

I would like to express my utmost gratitude and appreciation for my advisor, Dr. Brian Gulbransen. Brian has been an outstanding mentor who made me feel welcome from the moment I joined his lab. His support has been unconditional and unwavering. He has given me the latitude and freedom to explore my ideas and make the most of my experience – always pushing me to aim high. He has had an incredibly positive outlook that I thrived off and is a true role model that I one day hope to emulate. I have grown immensely under his mentorship, and I thank him for being patient with me throughout my many learning experiences.

I would also like to thank my esteemed committee members, Dr. Jim Galligan, Dr. Narayanan Parameswaran, Dr. Julia Busik and Dr. Joe Beatty. My work would not have been possible without their incredibly valuable feedback, support, and patience. Their doors were always open, and they always took the time to give me the guidance I needed.

I would like to thank my family – particularly my mom and my dad, who sacrificed much and endured it all with beautiful patience. You were my first teachers and my first mentors, and I would not be the person I am today without you. I am forever grateful for each of you and I will always cherish you in my heart.

I also feel an incredible amount of gratitude towards current and past members of the Gulbransen lab: Jonathon, David, Wilmarie, Vlado, Christine, Aaron, and Luisa. It was a genuine pleasure getting work with each of you! To Jonathon in particular: thank you for always being willing to help and for your incredible patience. A special thank you as well to my dear friends who did their part in keeping me mindful of the things that matter most. That list is long, and I could not do it justice to name you all – but you know who you are.

Lastly, I would like to thank the MSUCOM DO/PhD Program, particularly Dr. Justin McCormick, Bethany Heinlen, Dr. Brian Schutte and Michelle Volker for their immense support

throughout the highs and lows of this very long journey. A special thank you to Jasmine and Elvira for helping me navigate the web of bureaucracy and keeping me on the straight and narrow.

TABLE OF CONTENTS

LIST OF FIGURES

KEY TO ABBREVIATIONS

Acetyl-Coenzyme A	acetyl-CoA
Acetylcholine	ACh
Adenosine diphosphate	ADP
After-hyperpolarization type	AH-type
Action potential	AP
Adenosine triphosphate	ATP
Calcium ion	Ca^{2+}
Choline acetyl transferase	ChAT
Chronic intestinal pseudo-obstruction	CIPO
Colonic migrating motor complex	CMMC
Circular muscle-myenteric plexus	CMMP
Clozepine-N-oxide	CNO
Central nervous system	CNS
Causes recombination	Cre
4',6-diamidino-2-phenylindole	DAPI
Dinitrobenzene sulphonic acid	DNBS
Designer receptor exclusively activated by designer drug	DREADD
Electrical field stimulation	EFS
Ectonucleotide pyrophosphatase type 2	Enpp2
Enteric nervous system	ENS
Fast excitatory post-synaptic potential	fEPSP
Functional gastrointestinal disorder	FGID
Field of view	FOV
Focal tract stimulation	FTS
Genetically encoded calcium indicator	GECI
Glial fibrillary acidic protein	GFAP
Gastrointestinal	GI

G-protein coupled receptor	GPCR
Irritable bowel syndrome	IBS
Inhibitory concentration, half-max	IC_{50}
Intrinsic primary afferent neuron	IPAN
Potassium channel, calcium-dependent	K_{Ca}
Lower esophageal sphincter	LES
Longitudinal muscle-myenteric plexus	LMMP
Lysophosphatidic acid	LPA
Lysophosphatidic acid receptor, type I	LPAR1
Major histocompatibility complex, type II	MHCII
Myenteric plexus	MP
Neuronal nitric oxide synthase	nNOS
Nitric oxide	NO
Purinergic receptor, type 2X	P2X
Purinergic receptor, type 2Y1	P2Y1
Standard error of the mean	SEM
Small intestinal bacterial overgrowth	SIBO
Sub-mucosal plexus	SMP
Synaptic type	S-type
Tandem dimeric derivative of dsRed	tdT
Vasoactive intestinal peptide	VIP
Wingless family member, type I	Wnt1

CHAPTER 1: INTRODUCTION

GENERAL OVERVIEW

The gastrointestinal (GI) tract is a motile organ specialized in the digestion of food, absorption of nutrients and excretion of waste products[1]. The enteric nervous system (ENS) is a division of the peripheral nervous system that controls all aspects of GI function through intrinsic neurocircuits embedded within the gut wall. ENS control of GI motility is fundamentally autonomous but subject to dynamic regulation from the central nervous system (CNS) through extrinsic neural pathways. Nevertheless, pathology affecting the ENS is sufficient to compromise gut motility and contributes to a spectrum of GI diseases. Overall, GI diagnoses impose a substantial economic burden and account for 12% of all visits to the emergency department in the United States[2]. A deeper understanding of the fundamental physiology of the ENS neurocircuitry is therefore crucial towards developing better treatments for GI motility disorders.

Enteric neurons serve effector roles in coordinating the motility of the GI tract. As such, enteric neuropathy is a hallmark feature of GI dysmotility[3]. Primary etiologies include heritable diseases like mitochondrial neurogastrointestinal encephalomyopathy, which presents early in life, while secondary causes include metabolic (diabetes), infectious (Chagas) or vascular (stroke) disturbances. Enteric neurons are necessary for gut motility, but it is now clear that they do not act in isolation. Rather, they are subject to ongoing and reciprocal input from surrounding populations of enteric glia located throughout the ENS.

Enteric glia are unique non-myelinating peripheral glial cells that serve indispensable roles in GI physiology. Enteric glia modulate intestinal secretion, vascular tone and motility through a number of direct and indirect mechanisms. Enteric glia have also been shown to serve pathological roles by promoting the death of enteric neurons during colitis, though the full breadth of their pathological roles remain poorly understood, particularly as it relates to their regulation of the ENS motor circuitry. This dissertation investigates novel mechanisms through which enteric glia regulate intestinal motor neurocircuits and GI motility.

NEURAL CONTROL OF GI MOTILITY

Extrinsic pathways

The CNS provides regulatory input to the GI tract through extrinsic neural pathways (**Fig 1.1**)[4]. Parasympathetic input to the GI tract originates within vagal motor nuclei of the caudal medulla and is primarily stimulatory in nature. The proximal GI tract (esophagus, stomach, pancreas, and proximal colon) consequently receives parasympathetic input via the vagus nerve while the distal colon receives parasympathetic input via pelvic nerves emerging at spinal levels S2-4. In contrast, sympathetic control of the GI tract originates within hypothalamic nuclei and conveyed via splanchnic nerves emerging at spinal levels T8-L2[5]. Sympathetic control of the GI tract is inhibitory in nature. Finally, somatosensory cortical centers provide conscious control of anal sphincter tone and are critical in mediating the defecation reflex. In this regard, elegant integration between the extrinsic and intrinsic neural circuit systems is seamless under physiological conditions but fundamentally dysregulated during GI pathologies.

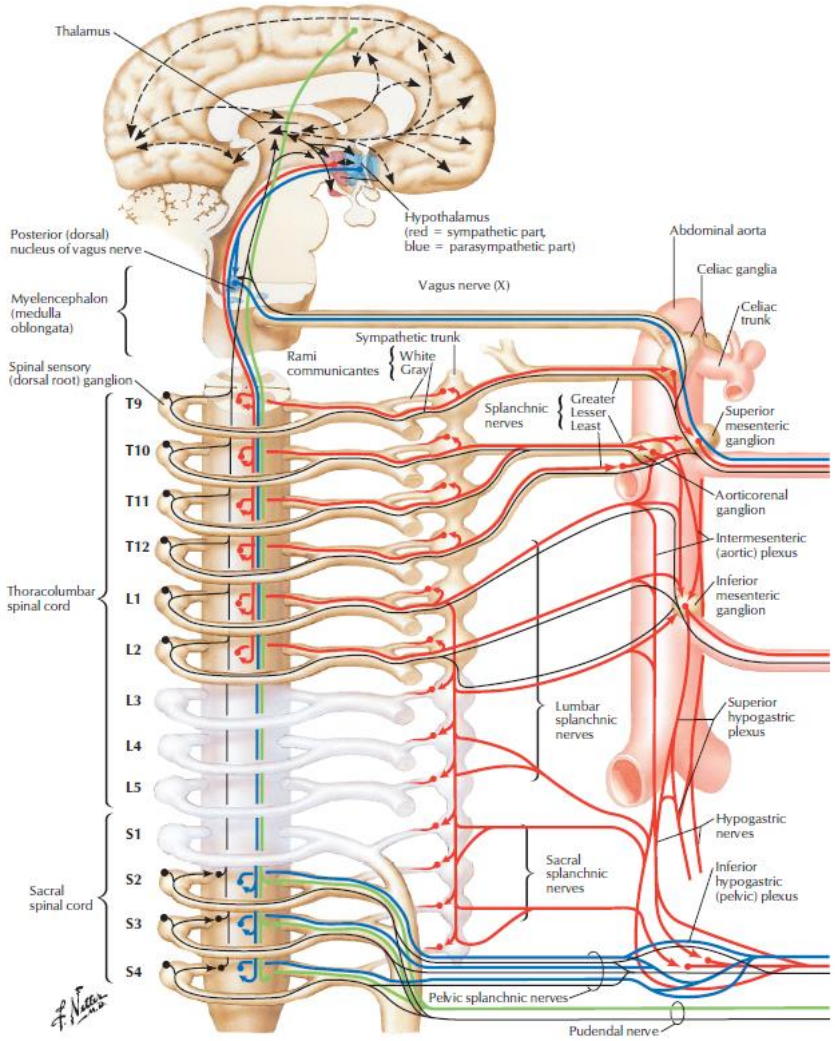

Figure 1.1. Extrinsic innervation of the gastrointestinal (GI) tract. Descending control from the CNS arises from parasympathetic and sympathetic nuclei of the vagal nucleus and hypothalamus, respectively. These constituent nerves associated with each of these autonomic pathways are distinct, though both require spinal tracts to varying extents. Parasympathetic innervation via the vagus nerve provides stimulatory, mostly cholinergic input to the proximal GI tract. Preganglionic parasympathetic fibers are long, traversing through abdominal ganglia (celiac and superior mesenteric ganglia) before synapsing onto post-ganglionic neurons within the target organ. In the lower GI tract, parasympathetic fibers coursing through the anterolateral horn emerge via pelvic splanchnic nerves. Parasympathetic activities facilitate digestive processes, including gastric acid secretion and peristaltic contractions in the post-prandial state. In contrast, sympathetic input courses through the thoraco-lumbar network and arrives via greater, lesser, and least splanchnic nerves. Sympathetic innervation attenuates GI contractility, utilizing noradrenaline as the neurotransmitter to modulate activity of effector neurons within the target tissue. Image adapted from Felton et. al. (2016)[6].

Intrinsic pathways

The intrinsic neural circuitry of the ENS affects all aspects of GI physiology including epithelial barrier integrity, secretion, absorption, motility, blood flow and neuro-immune interactions. In this regard, ENS neurocircuits are custom tailored to fit the needs of the needs of the specific gut region. For instance, the ENS stimulates chaotic patterns of gut contraction in the proximal small bowel that are non-propulsive in nature and serve to promote mixing, digestion, and absorption of food. In contrast, contractility in the colon is more ordered, serving the singular purpose of propelling lumen contents (waste) in an oral-to-aboral direction.

The ENS is anatomically sub-divided into two distinct ganglionated plexuses: the sub-mucosal plexus (SMP) and the myenteric plexus (MP; **Fig 1.2**). The SMP is located subjacent to the epithelium, where its proximity to the gut lumen allows it to actively monitor lumen chemistry and mounts context-appropriate physiological responses. Thus, the SMP regulates local blood flow and the transepithelial flux of nutrients. The SMP is absent from the esophagus and stomach but otherwise present throughout the remainder of the GI tract.

The MP is situated deep between the inner circular and outer longitudinal smooth muscle layers of the muscularis propria. By comparison, the MP is dramatically larger than the SMP, housing roughly 2/3rd of the total population of enteric neurons. The cell bodies of enteric neurons are housed within myenteric ganglia, which are interconnected by inter-ganglionic fiber tracts. Thus, the MP forms a vast, continuous neural network in which axonal projections link oral and distal gut segments. Ultimately, the MP provides local intrinsic motor control to the GI smooth musculature pertinent to motility. The MP innervates all gut segments beginning in the lower 1/3rd of the esophagus and proceeding aborally to the internal anal sphincter. The cellular constituents of the MP and SMP include enteric neurons and enteric glia, though these differ drastically in terms of functional characteristics and fundamental physiology according to the GI segment in question.

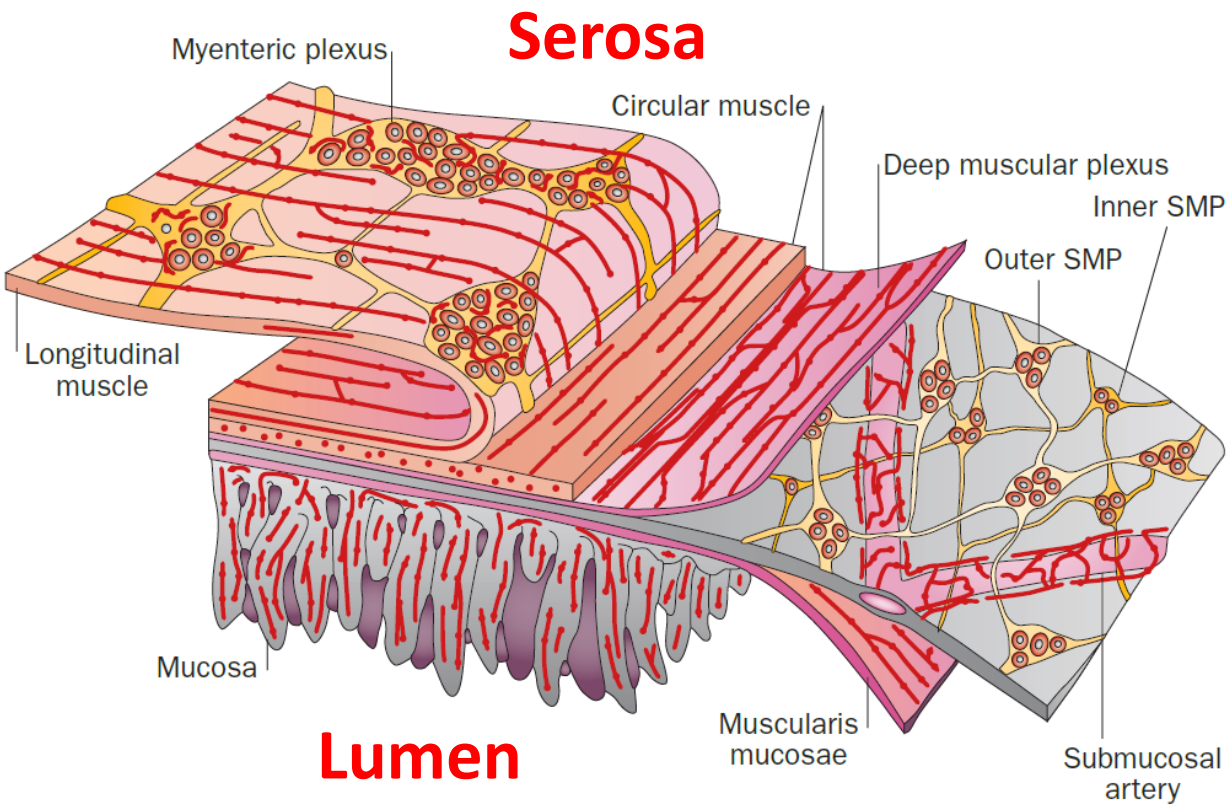

Figure 1.2. In situ arrangement of the enteric nervous system (ENS). The two anatomic division of ENS neurocircuitry include the myenteric plexus (MP) and the sub-mucosal plexus (SMP). Both plexuses feature ganglia that house cell bodies of intrinsic neurons, although SMP ganglia are in general smaller and less dense overall. The SMP is located deep to the muscularis mucosa but superficial to the plane of the circular musculature and can be further subdivided in accordance to its location relative to the plane of the submucosal vasculature. As such, the outer SMP is closer to the vascular bed and controls blood flow. The inner SMP is closer to the epithelium, and thus modulates secretive and absorptive processes during digestion. The MP is located between the inner circular and outer longitudinal smooth muscle layers. The ganglia of the MP are much larger than their SMP counterparts and thus better equipped to modulate tone within vast territories of intestinal smooth musculature. Though not shown here, the constituent neuronal cell bodies within these myenteric ganglia correspond to one of 3 functional classes: intrinsic primary afferent neurons (IPANs), interneurons, and motor neurons. Image adapted from Furness, 2012.[7]

ENTERIC NEURONS

The neural circuitry of the ENS is best understood in terms of the functional roles of its constituent neurons during motor reflex activity. Thus, enteric neurons fall into one of three possible categories: intrinsic primary afferent neurons (IPANs), which are sensory in function; interneurons, which elicit activity in target neurons; and motor neurons, which are efferent in function and modulate activity of the gut musculature. This functional approach is particularly useful because it describes a neuron's role within a physiological meaningful context while also providing a framework for understanding prior classification systems.

Morphological classification

Dogiel provided the initial classification of enteric neurons, which was based on morphological characteristics and subsumes at least two subtypes: Dogiel type I and Dogiel type II. Although several additional subtypes have been described (reviewed elsewhere[8] in greater detail), this discussion will primarily focus on these two major subtypes.

Dogiel Type I neurons (**Fig 1.3a**) are unipolar in appearance and characterized by a singular axon that projecting to the muscle tissue or local ganglia. The cell bodies range in size from and are on average 24 (major-axis) by 15 (minor-axis) microns, giving them an oblong appearance. In general, Dogiel I neurons serve excitatory or inhibitory roles as motor neurons or interneurons within the ENS reflex circuitry (see *Functional classification*). In contrast, Dogiel type II (**Fig 1.3b**) neurons are larger, with somas measuring on average 35 (major-axis) by 18 (minor-axis) microns. Dogiel II neurons are characterized by their multi-polar appearance, with one axon projecting to the mucosa and a second contacting neighboring ganglia. In this regard, Dogiel type II neurons are thought to sub-serve a predominantly sensory role within the ENS. Overall, both Dogiel type I and II are found in both the SMP and MP, with some variation in the proportions vary

according to the organ region in question with some overlap in the functional roles of these different classes.

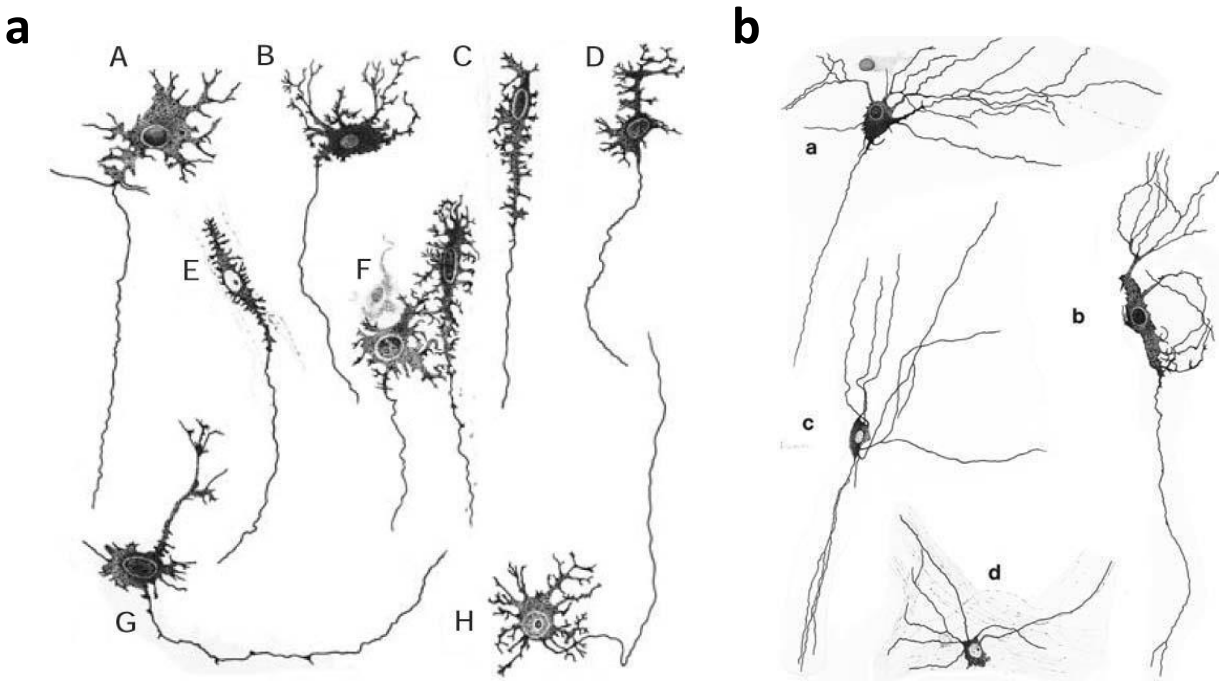

Figure 1.3. Morphological characteristics of enteric neurons. a, Dogiel type I neurons exhibit a mono-polar appearance and a dense network of short, flat dendritic projections that terminating near the cell soma. Dogiel I neurons correspond to interneurons and motor neurons of the ENS circuitry. b, Dogiel II neurons have multiple axonal projections. One axon projects to the mucosa while the remaining axons synapse with neurons located within the same or adjacent ganglia. Original images by Dogiel, 1899 and adapted from Furness, 2007.[8]

Electrophysiological classification

Enteric neurons are classified into two electrophysiologically distinct categories defined by the kinetics of their action potentials (APs). The first category subsumes S-type neurons, which fire fast APs with a short after-hyperpolarization period lasting <100ms in duration and sensitive to the sodium channel blocker, tetrodotoxin. Activation of S-type neurons primarily evokes fast excitatory post-synaptic potentials (fEPSPs). S-type neurons possess Dogiel I morphology and thus functionally correspond to interneurons or motor neurons of the ENS, but are never sensory neurons[8]. In contrast, AH-type neurons fire action potentials characterized by a slow, prolonged after-hyperpolarization period (hence the "AH" classification) that can last up to 30s in duration[9,10]. The ionic component responsible for this characteristically slow response is carried by maximum conductance calcium-sensitive potassium channels (K_{Ca}), which are exclusively expressed within AH-neurons. By this token, AH-neurons set the gain of the system and alterations in K_{Ca} channel activity are seen with disease states. During inflammation, for example, myenteric neurons of the distal colon exhibit reduced K_{Ca} channel activation, resulting in an overall increase in neuronal excitability[11]. AH-neurons thus serve as sensory neurons within the ENS motor reflex, and morphologically correspond to Dogiel type II neurons.

Neurochemical classification

Enteric neurons are sub-divided according to the neurochemical markers they express[12]. Acetylcholine (Ach) is the major excitatory neurotransmitter in the ENS that is consequently synthesized by IPANs, all interneurons and orally-projecting, excitatory motor neurons. All these neurons are immunoreactive for the parent enzyme, choline acetyltransferase (ChAT), which catalyzes Ach production from choline and acetyl-CoA. The primary inhibitory neurotransmitter of the ENS is nitric oxide (NO), which is released by aborally-projecting inhibitory motor neurons to elicit relaxation of smooth muscle. These neurons are immunoreactive for neuronal nitric oxide

synthase (nNOS) but may also secrete vasoactive intestinal peptide (VIP) and/or adenosine triphosphate (ATP) as co-transmitters. Given the widespread expression of ChAT, sensory neurons are particularly distinguishable by the high expression of calcium-binding proteins, calretinin or calbindin, which are absent in other neuronal subtypes.

FUNCTIONAL CIRCUITS OF THE ENS

Enteric neurons of the MP monitor luminal contents, epithelial distortion and gut distension via afferent endings that innervate the mucosal and muscular compartments[4]. The ganglia in which these neurons reside are signal integration sites where context-appropriate, efferent reflexes are generated. In the simplest reflex arc (**Fig 1.4**), IPAN activation concomitantly recruits ascending and descending neural pathways to simultaneously evoke contraction and relaxation of the gut's musculature, respectively[13]. The resultant contraction of proximal gut segments coincides with relaxation of distal gut segments, the net effect being the forward propulsion of gut lumenal contents. This fundamental paradigm is recapitulated along the length of the GI tract, with ascending networks being predominantly cholinergic and descending networks being predominantly nitrergic, with purinergic co-transmission also being common.

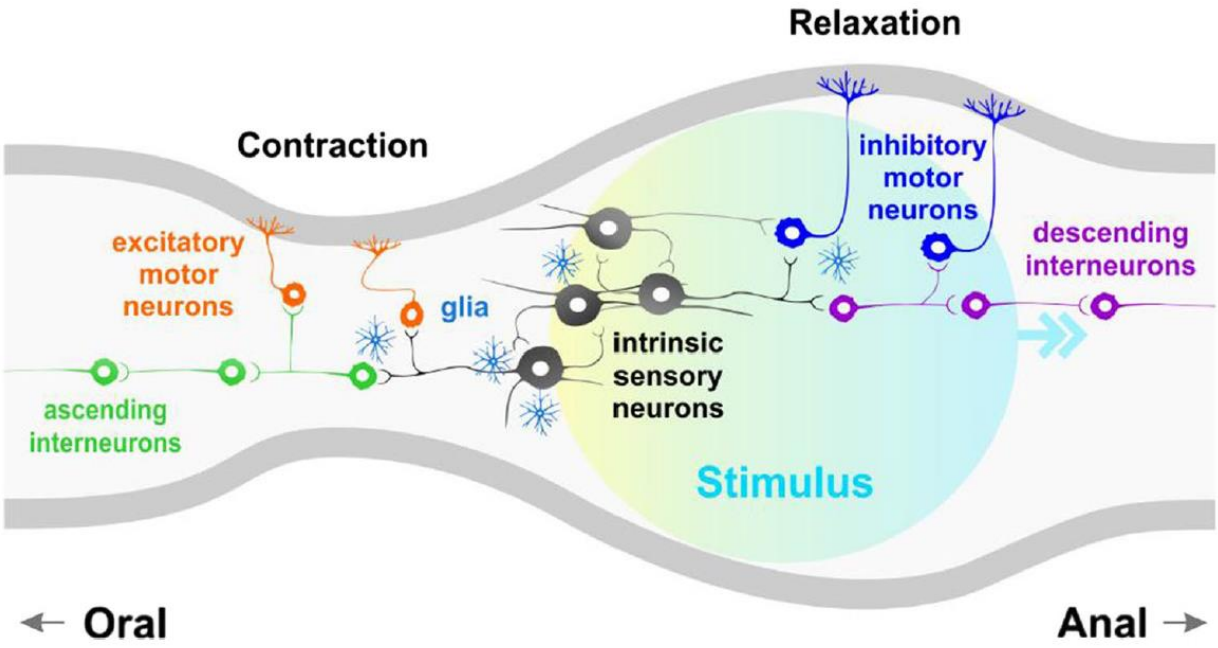

Figure 1.4. Structural arrangement of enteric neurons of the myenteric plexus. The synaptic connectivity of the six functional sub-classes of enteric neurons serves to provide temporally and spatially precise control of gut motility through reflex circuits capable of functioning autonomously. Activation of afferent endings of intrinsic sensory neurons (IPANs) projecting into the mucosa monitor lumenal contents. Activation of IPANs triggers bi-directional activation of the reflex circuitry. The ascending division of these response synapses onto ascending interneurons and excitatory motor neurons. Activation of these targets is achieved via predominantly fast cholinergic signaling acting at nicotinic acetylcholine receptors. The result is contraction of orally located gut wall musculature. By contrast, concomitant activation of descending interneurons and inhibitory motor neurons occurs via fast cholinergic and purinergic signaling mechanisms, which culminates in production of nitric oxide (NO) and relaxation of aborally-located gut segments. Image adapted from Fung & Vandenberghe (2020)[13].

ENTERIC GLIA

Even though the properties of individual enteric neuronal subtypes have been well-described (see above), a full appreciation for the functional sophistication of the ENS cannot be gleaned by considering its neuronal elements in isolation. Indeed, enteric glia residing at synaptic foci throughout the MP are now known to play a central role in modulating the activity of enteric neurons. In addition to orchestrating passive support roles within neurocircuits (including neurotransmitter biosynthesis[14,15], degradation of synaptic material[16–20]), enteric glia express receptors for several neurotransmitters, including the M1 and M3 muscarinic acetylcholine[21], bradykinin[22] and P2X receptors[23], enabling them to actively sense neuronal activity. In addition, enteric glia can secrete gliotransmitters, chiefly purines, to stimulate activity within enteric neurons[24].

Cholinergic activation of enteric glia serves physiological roles in GI motility by driving colonic contractions[21], but glial purine release during acute colitis promotes enteric neuron death[24]. But because enteric glia also express the type II major histocompatibility complex (MHCII), they may be equally well-equipped to act as antigen presenting cells and thereby contribute to long term inflammatory processes[25].

Synapse-specific regulation of neurocircuits

Some view the ENS to be an evolutionary precursor to the CNS[26] and so it is unsurprising that enteric glia possess many of the sensory and effector mechanisms seen in neuroglia of the brain. Nevertheless, there is mounting evidence that neuroglial regulation of CNS neurocircuits is incredibly precise, though whether this constitutes a highly evolved function unique to CNS glia or is a fundamental feature of enteric glia remains to be seen.

In the basal ganglia, astrocytes are functionally committed to one of two (D1 of D2) well-characterized dopaminergic pathways[27]. In this neural circuit, astrocytes couple networked pairs

of D1-D1 or D2-D2 (homotypic) neurons to the exclusion heterotypic interactions. More recently, astrocytes of the nucleus accumbens were shown to exhibit robust Ca^{2+} responses following synaptic activation or amphetamine application, and the ensuring astrocytic release of purines was singularly responsible for presynaptic inhibition of the reward circuitry[28]. Together, these studies highlight potential roles for circuit-specific glia in the pathogenesis of human disease. But whether enteric glia regulate ENS activity in a similar way has never been shown and is the central focus of the first chapter of this dissertation.

Functional dysmotilities as connectopathies of the ENS neurocircuitry

Despite how extensively enteric neurons have been characterized, drug treatment options for GI motility disorders remain limited in scope and inconsistent in their therapeutic benefit[29]. Understanding how enteric glia modulate neuronal activity in an intact, fully networked system may be a crucial step in progressing from “synapse-to-connectome” and developing a truer-to-life model of GI motility.

To these ends, functional gastrointestinal disorders (FGIDs) comprise a broad family of common GI motility disorders that are defined by aberrant gut-brain interactions[30] and can affect any gut region. Although often accompanied by psychosocial disturbances[31] (e.g. anxiety and depression), alterations in gut microflora[32], genetic predisposition[33], the pathophysiological basis of FGIDs remain poorly understood though a combination of events likely contribute to the process. Nevertheless, the most common FGIDs are characterized by alterations in motility[34], with irritable bowel syndrome (IBS) being the most common one to affect the gut.

In contrast, chronic intestinal pseudo-obstruction (CIPO) constitutes the most severe FGID, which results in life-threatening GI obstruction in the absence of mechanical blockade[35]. CIPO is an extreme example of a gut dysmotility in which there are no known neuronal defects in

the ENS in at least 50% of patients, and yet some failure in the gut's contractile apparatus drives the substantial morbidity, mortality and high complication rate seen in this disease[35].

In a recent study, CIPO was linked to alterations in gut epithelial-blood vascular barrier abnormalities[36] but these findings are largely non-specific and are otherwise also seen in several unrelated GI pathologies in which pseudo-obstruction rarely occurs. Rather, FGIDs are now thought to be associated with an initial inflammatory insult that results in acute ENS hyperexcitability, which is consolidated into long-term functional changes via neuroplastic mechanisms during establishment of disease.

CNS glia express the type I lysophosphatidic acid receptor (LPAR1; see **Fig 1.5**), which binds biolipid mediators of inflammation to sensitize peripheral nerves during the pathogenesis of neuropathic pain[37]. LPA1R is a G-protein coupled receptor that modulates several physiological processes in the GI tract, including fluid absorption/secretion[38], barrier function[39] and sphincter tone[40]. Although cultured enteric glia express LPAR1, its biological relevance to motility is entirely unknown. Thus, the putative role of enteric glia in bridging acute and chronic inflammation has never been explored and is the focus of the second chapter of this dissertation.

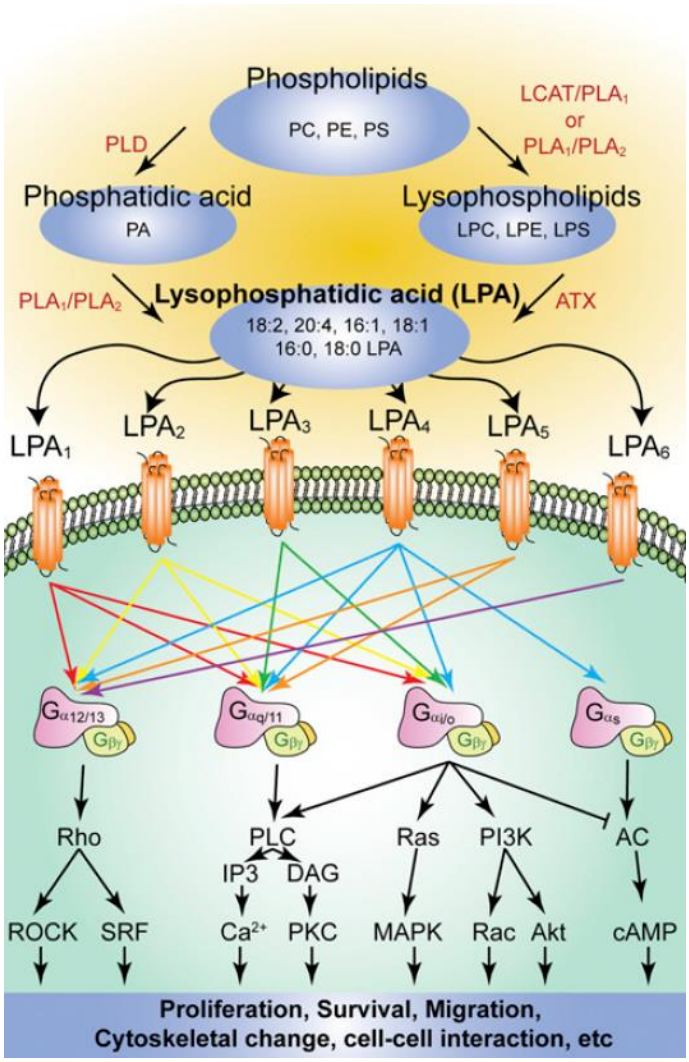

Figure 1.5. Lysophosphatidic acid receptor (LPAR) pharmacology. The LPAR family of G-protien coupled receptor (GPCR) receptors binds a broad range of bioactive lipid molecule that are generated via distinct extracellular and intracellular pathways (only extracellular sources are shown here). There are a total of six LPAR receptor subtypes, denoted $LPAR_{1\text{-}6}$, which couple to $G_{q/11}$, $G_{\alpha/s}$, $G_{\alpha/i}$, and $G_{\alpha12/13}$ secondary signal transduction cascades. Although all LPARs bind lysophosphatidic acid molecules, they exhibit promiscuous binding with some ligand-receptor interactions being of greater affinity. Overall, LPAR1 demonstrates pleiotropically tissue expression but it iss particularly involved in axonal guidance roles and thus mediates alterations in cell morphology. In the context of the CNS, LPAR1 expressed by glia serves a central role in the development CNS circuits controlling suckling behaviors and mood regulation. Image adapted from Yung et. al. (2014)[41].

SUMMARY AND AIMS OF DISSERTATION

The ENS controls GI motility through neural networks that receive dynamic regulatory input from enteric glia. The signaling pathways used by enteric glia to regulate ENS excitability are important to the normal physiological control of gut motility. Ultimately, some molecular and biochemical elements of CNS glia are found within enteric glia, but whether they share the same capacity to modulate neurocircuit activity on a synapse-specific basis has never been shown. Chapter 2 consequently describes the role of enteric glia as circuits-specific regulators of enteric motor neurocircuits, thereby attempting to reframe the GI motor reflex as a network-level phenomenon governed by a "connectome"[42] of discrete synapse-level interactions.

In addition, the putative role of enteric glia in the pathogenesis of CIPO, a severe functional GI disorder, has never been explored but may result from aberrant responses to biolipid mediators of inflammation at the earliest stages of the disease. Thus, Chapter 3 explores the role of enteric glial biolipid signaling in GI motility and the pathogenesis of CIPO. Together, this dissertation serves to highlight novel roles for enteric glia in the ENS circuitry controlling gut motility.

REFERENCES

REFERENCES

1. Greenwood-Van Meerveld, B., Johnson, A. C. & Grundy, D. Gastrointestinal physiology and function. *Handb. Exp. Pharmacol.* **239**, (2017).

2. Myer, P. A. *et al.* Clinical and economic burden of emergency department visits due to gastrointestinal diseases in the United States. *Am. J. Gastroenterol.* **108**, 1496–1507 (2013).

3. De Giorgio, R. *et al.* Inflammatory neuropathies of the enteric nervous system. *Gastroenterology* **126**, 1872–1883 (2004).

4. Furness, J. B. The enteric nervous system and neurogastroenterology. *Nat. Rev. Gastroenterol. Hepatol.* **9**, 286–294 (2012).

5. Furness, J. B., Callaghan, B. P., Rivera, L. R. & Cho, H. J. The enteric nervous system and gastrointestinal innervation: Integrated local and central control. *Adv. Exp. Med. Biol.* **817**, 39–71 (2014).

6. Felten, D. L. *et al. Atlas of Neuroscience*. (Elsevier, 2016).

7. Furness, J. B. The enteric nervous system and neurogastroenterology. *Nat. Rev. Gastroenterol. Hepatol.* **9**, 286–294 (2012).

8. Furness, J. B. *The Enteric Nervous System*. *The Enteric Nervous System* (Blackwell Publishing, 2007). doi:10.1002/9780470988756.

9. Mao, Y., Wang, B. & Kunze, W. Characterization of myenteric sensory neurons in the mouse small intestine. *J. Neurophysiol.* **96**, 998–1010 (2006).

10. Iyer, V. *et al.* Electrophysiology of guinea-pig myenteric neurons correlated with immunoreactivity for calcium binding proteins. *J. Auton. Nerv. Syst.* **22**, 141–150 (1988).

11. Krauter, E. M., Linden, D. R., Sharkey, K. A. & Mawe, G. M. Synaptic plasticity in myenteric neurons of the guinea-pig distal colon: Presynaptic mechanisms of inflammation-induced synaptic facilitation. *J. Physiol.* **581**, 787–800 (2007).

12. Furness, J. B. Types of neurons in the enteric nervous system. *J. Auton. Nerv. Syst.* **81**, 87–96 (2000).

13. Fung, C. & Vanden Berghe, P. Functional circuits and signal processing in the enteric nervous system. *Cell. Mol. Life Sci.* **1**, 3 (2020).

14. Kato, H. *et al.* Immunocytochemical characterization of supporting cells in the enteric nervous system in Hirschsprung's disease. *J. Pediatr. Surg.* **25**, 514–519 (1990).

15. Giaroni, C. *et al.* Evidence for a glutamatergic modulation of the cholinergic function in the human enteric nervous system via NMDA receptors. *Eur. J. Pharmacol.* **476**, 63–69 (2003).

16. Rühl, A., Hoppe, S., Frey, I., Daniel, H. & Schemann, M. Functional expression of the peptide transporter PEPT2 in the mammalian enteric nervous system. *J. Comp. Neurol.* **490**, 1–11 (2005).

17. Fletcher, E. L., Clark, M. J. & Furness, J. B. Neuronal and glial localization of GABA

transporter immunoreactivity in the myenteric plexus. *Cell Tissue Res.* **308**, 339–346 (2002).

18. Lavoie, E. G. *et al.* Ectonucleotidases in the digestive system: Focus on NTPDase3 localization. *Am. J. Physiol. - Gastrointest. Liver Physiol.* **300**, (2011).

19. Gulbransen, B. D. *et al.* Activation of neuronal P2X7 receptor-pannexin-1 mediates death of enteric neurons during colitis. *Nat. Med.* **18**, 600–604 (2012).

20. Braun, N. *et al.* Association of the Ecto-ATPase NTPDase2 with Glial Cells of the Peripheral Nervous System. *Glia* **45**, 124–132 (2004).

21. Delvalle, N. M., Fried, D. E., Rivera-Lopez, G., Gaudette, L. & Gulbransen, B. D. Cholinergic activation of enteric glia is a physiological mechanism that contributes to the regulation of gastrointestinal motility. *Am. J. Physiol. - Gastrointest. Liver Physiol.* **315**, G473–G483 (2018).

22. Murakami, M., Ohta, T., Otsuguro, K. I. & Ito, S. Involvement of prostaglandin E2 derived from enteric glial cells in the action of bradykinin in cultured rat myenteric neurons. *Neuroscience* **145**, 642–653 (2007).

23. Vanderwinden, J.-M., Timmermans, J.-P. & Schiffmann, S. N. Glial cells, but not interstitial cells, express P2X7, an ionotropic purinergic receptor, in rat gastrointestinal musculature. *Cell Tissue Res.* **312**, 149–154.

24. Brown, I. A. M., McClain, J. L., Watson, R. E., Patel, B. A. & Gulbransen, B. D. Enteric Glia Mediate Neuron Death in Colitis Through Purinergic Pathways That Require Connexin-43 and Nitric Oxide. *CMGH* **2**, 77–91 (2016).

25. Chow, A. K. & Gulbransen, B. D. Potential roles of enteric glia in bridging neuroimmune communication in the gut. *Am. J. Physiol. - Gastrointest. Liver Physiol.* **312**, G145–G152 (2017).

26. Furness, J. B. & Stebbing, M. J. The first brain: Species comparisons and evolutionary implications for the enteric and central nervous systems. *Neurogastroenterology and Motility* vol. 30 (2018).

27. Martín, R., Bajo-Grañeras, R., Moratalla, R., Perea, G. & Araque, A. Circuit-specific signaling in astrocyte-neuron networks in basal ganglia pathways. *Science (80-.).* **349**, 730–734 (2015).

28. Corkrum, M. *et al.* Dopamine-Evoked Synaptic Regulation in the Nucleus Accumbens Requires Astrocyte Activity. *Neuron* **105**, 1036-1047.e5 (2020).

29. Nurko, S. & Saps, M. Treating constipation with prucalopride: One size does not fit all. *Gastroenterology* **147**, 1214–1216 (2014).

30. Holtmann, G., Shah, A. & Morrison, M. Pathophysiology of Functional Gastrointestinal Disorders: A Holistic Overview. *Dig. Dis.* **35**, 5–13 (2018).

31. Longstreth, G. F. *et al.* Functional Bowel Disorders. *Gastroenterology* **130**, 1480–1491 (2006).

32. Drossman, D. A. Functional gastrointestinal disorders: History, pathophysiology, clinical features, and Rome IV. *Gastroenterology* **150**, 1262-1279.e2 (2016).

33. Canavan, C., West, J. & Card, T. The epidemiology of irritable bowel syndrome. *Clin.*

Epidemiol. **6**, 71–80 (2014).

34. Tack, J. Prokinetics and fundic relaxants in upper functional GI disorders. *Current Opinion in Pharmacology* vol. 8 690–696 (2008).

35. De Giorgio, R., Cogliandro, R. F., Barbara, G., Corinaldesi, R. & Stanghellini, V. Chronic Intestinal Pseudo-Obstruction: Clinical Features, Diagnosis, and Therapy. *Gastroenterol. Clin. North Am.* **40**, 787–807 (2011).

36. Boschetti, E. *et al.* Gut epithelial and vascular barrier abnormalities in patients with chronic intestinal pseudo-obstruction. *Neurogastroenterol. Motil.* 1–11 (2019) doi:10.1111/nmo.13652.

37. Inoue, M. *et al.* Initiation of neuropathic pain requires lysophosphatidic acid receptor signaling. *Nat. Med.* **10**, 712–719 (2004).

38. Lin, S. *et al.* Lysophosphatidic Acid Stimulates the Intestinal Brush Border Na+/H+ Exchanger 3 and Fluid Absorption via LPA5 and NHERF2. *Gastroenterology* **138**, 649–658 (2010).

39. Lin, S. *et al.* Lysophosphatidic Acid Receptor 1 Is Important for Intestinal Epithelial Barrier Function and Susceptibility to Colitis. *Am. J. Pathol.* **188**, 353–366 (2018).

40. Feng, Y. & Liu, J. F. Expression of lysophosphatidic acid receptors in the human lower esophageal sphincter. *Exp. Ther. Med.* **7**, 423–428 (2014).

41. Yung, Y. C., Stoddard, N. C. & Chun, J. LPA receptor signaling: Pharmacology, physiology, and pathophysiology. *Journal of Lipid Research* vol. 55 1192–1214 (2014).

42. Swanson, L. W. & Lichtman, J. W. From Cajal to Connectome and beyond. *Annu. Rev. Neurosci.* **39**, 197–216 (2016).

CHAPTER 2: CIRCUIT-SPECIFIC ENTERIC GLIA REGULATE INTESTINAL MOTOR NEUROCIRCUITS

ABSTRACT

Glia in the central nervous system exert precise spatial and temporal regulation over neural circuitry on a synapse-specific basis, but it is unclear if peripheral glia share this exquisite capacity to sense and modulate circuit activity. In the enteric nervous system (ENS), glia control gastrointestinal motility through bidirectional communication with surrounding neurons. Here, we developed a novel mouse model that combines chemogenetic and optogenetic techniques to study network-level activity in the intact myenteric plexus (MP) of the proximal colon. Stimulation of aborally and orally projecting neural fiber tracts activated distinct populations of enteric glia, producing more robust overall responses in the ascending pathway. Pharmacological manipulation of glial purinergic and cholinergic signaling differentially altered neuronal responses in these circuits in a sex-dependent manner. Collectively, our findings establish that enteric glia regulate ENS circuit activity in a synapse-specific manner, providing profound new insights into the functional breadth and versatility of peripheral glia.

INTRODUCTION

The nervous system controls essential body functions through neuronal circuits that display exquisite temporal and spatially precise regulation. An emerging body of evidence suggests that glia, which respond to neurotransmitters and release substances that modulate neurotransmission[1,2], are response for at least some of this precision. Glial recruitment by synaptic activity was once considered a general phenomenon that reflects metabolic demands in active neural networks[3,4]. While this may be partially true, more recent data show that signaling in networks of neurons and glia is unexpectedly precise. Astrocytes in particular have emerged as circuit-specific cells that tune neurotransmission on a synapses-by-synapse basis[5–8]. These observations provide strong support for the concept that, rather than acting in a purely supportive role, glia serve integral regulatory functions in synaptic circuits. Yet whether the circuit-specific attributes of astrocytes represent highly evolved functions that emerge in certain circuits in the brain or reflect a more general role of glia in synaptic signaling is not understood.

The enteric nervous system (ENS) is the largest and most complex division of the peripheral nervous system. “Brain-like” neurocircuits composed of enteric neurons and glia are intrinsic to the intestine and function to control reflexive activities of the digestive tract such as patterns of intestinal movement[9]. The neuronal component of the enteric circuitry is well described, and the characteristics of intrinsic sensory neurons (primary afferent neurons), interneurons, and motor neurons that compose enteric motor circuits are known[10]. The basic organization of enteric neurons into functional circuits that control peristalsis is also understood and involves activation of intrinsic primary afferent neurons, which recruit ascending excitatory and descending inhibitory pathways that evoke contractions above and relaxations below the point of stimulation, respectively[10]. Although less understood, enteric glia are involved in enteric motor circuits and modulate reflex strength through bidirectional communication with enteric neurons[11–13]. During reflexive activities, enteric neurons recruit enteric glia[11,12], which release

transmitters that influence neurotransmission[13,14]. Enteric glia are necessary[14] to control the strength of enteric motility reflexes, but whether subpopulations of enteric glia are devoted to specific synaptic pathways is unknown. Enteric glia not only outnumber enteric neurons, they are also particularly localized at synaptic foci—an optimal site for regulating the flow of information within the ENS. Here, Ca^{2+} responses originating within a single cell can readily propagate between adjacent populations of enteric glia[14], but how these interactions ultimately modulate activity within distinct branches of the ENS reflex circuitry remains unclear.

The polarized arrangement of enteric synaptic pathways and the ability of isolated preparations to maintain their integrity offers an ideal system for studying the synaptic precision of glia in an integrated yet tractable network. Here, we leveraged this system to test the hypothesis that enteric glia function in a circuit-specific manner. To this end, we evoked activity in overlapping, but distinct, synaptic pathways and recorded calcium (Ca^{2+}) responses elicited in the enteric neuron-glial networks involved using genetically encoded Ca^{2+} indicators. We combined this approach with glial chemogenetics to assess whether enteric glia exert specific effects on neural pathways and used selective drugs to manipulate cholinergic and purinergic transmitter systems. Our data show that subpopulations of enteric glia are committed to specific ascending or descending neural circuits that control intestinal motility. Further, glial activation exerts differential effects on adjacent, overlapping synaptic pathways. The dedication of glia to a particular enteric neurocircuit depends, at least in part, on cholinergic and purinergic transmitter systems that constrain subsets of glia to a particular pathway, effects that are sex dependent. Therefore, bidirectional enteric glia-neuron signaling selectively occurs between specific populations of enteric glia, neurons, and synapses.

MATERIALS & METHODS

Animal use

All animal experiments were conducted in accordance with the standards established by the National Institutes of Health Guide for the Care and Use of Laboratory Animals. Institutional ethics approval was obtained from the Michigan State University Institutional Animal Care and Use Committee.

Mouse models

Transgenic male and female mice were generated on a C57/Bl6 background and used between 10 and 14 wk of age for all Ca^{2+}-imaging studies. Animals were housed in a temperature-controlled facility with a 12-h light:dark cycle and were provided *ad libitum* access to standard chow and water. Mice expressing the genetically encoded Ca^{2+} sensor, GCaMP5g, in enteric neurons and glia were generated by breeding B6;*129S6-Polr2a*$^{Tn(pb\text{-}CAG\text{-}GCaMP5g,\text{-}tdTomato)Tvrd}$/J mice (herein referred to as *GCaMP5g-tdT* mice; The Jackson Laboratory, stock #024477; RRID:IMSR_JAX:024477)[43] with B6.Cg-E2f1$^{Tg(Wnt1\text{-}cre)2Sor}$/J mice (herein referred to as *Wnt1*^{Cre} mice; The Jackson Laboratory, stock #022501; RRID:IMSR_JAX:022501)[19,44]. In the resulting offspring, denoted here as *Wnt1*^{Cre}*;GCaMP5g-tdT* mice, expression of the Ca^{2+} indicator GCaMP5g and the tdTomato reporter is driven by Cre recombinase activity in $Wnt1^{+}$ neural crest cells, such as enteric neurons and glia[45]. GCaMP5g expression is robust in both enteric neurons and glia in this line, but tdT expression is high in enteric glia and nearly undetectable in neurons (**Appendix Fig. 2.6**). This feature permits cell type identification based on tdT expression during subsequent analyses (**Appendix Figs. 2.7** and **2.9**). Experiments testing the effects of glial stimulation on enteric circuitry involved novel triple-transgenic mice expressing GCaMP5g in neurons and glia (as above) together with the $G_{q/11}$-coupled designer receptor exclusively

activated by designer drugs (DREADD) hM3Dq in enteric glia. This line was generated by breeding *Wnt1^{Cre};GCaMP5g-tdT* mice with *GFAP::hM3Dq$^{+/-}$* mice (a gift from Dr. Ken McCarthy, University of North Carolina at Chapel Hill; RRID: MMRRC_042286-UNC)[13,26,29]. The resultant triple-transgenic offspring used for experiments are denoted here as *Wnt1^{Cre};GCaMP5g-tdT;GFAP::hM3Dq* mice (see **Fig. 2.4** for functional and immunohistochemical characterization)[26]. These transgenic mice provide an excellent model for selectively provoking glial responses while concurrently visualizing Ca^{2+} levels in both neurons and glia. Mouse genotypes were verified commercially by Transnetyx Inc. (Cordova, TN).

Tissue isolation, dissection, fixation, and preparation

Mice were euthanized by cervical dislocation and decapitation in accordance with ethical guidelines of the Michigan State University Ethic Committee. Colonic tissue was then rapidly collected in Dulbecco's modified Eagle medium (DMEM) containing 3 μM nicardipine, included to limit smooth muscle contractions during dissection and imaging[13]. Colonic segments were opened along the length of the mesentery and the tissue was secured with insect pins in a 35-mm Sylgard-coated dish. All experiments utilized segments harvested from the proximal colon, identified based on the presence of aborally directed epithelial involutions that begin at the mesenteric border and encompass two-thirds of the colonic circumference. Segments used in immunohistochemical experiments were preserved in Zamboni's fixative overnight at 4°C. Whole-mount circular muscle-myenteric plexus (CMMP) preparations, used for live-cell imaging experiments, were obtained by microdissecting the mucosa and longitudinal muscle to expose the myenteric plexus[46]. Tissue orientation was carefully maintained during the dissection process. The resulting CMMP preparation maintains most of the functional connectivity in the myenteric plexus as well as connections with target tissue (smooth muscle).

Field and focal tract stimulation

Electrical field stimulation (EFS) was used to drive broad neuronal depolarization within enteric networks. In these experiments, tissues were stimulated with +70V voltage (10 Hz) using two platinum wires positioned on either side of the tissue preparation. Focal tract stimulation (FTS) was used to stimulate interganglionic myenteric nerve bundles in experiments designed to assess ascending and descending synaptic pathways. In these experiments, a custom-assembled tungsten bipolar electrode (World Precision Instruments Inc., Sarasota, FL) was placed on an interganglionic nerve bundle[47] located immediately oral or aboral to the field of view (FOV) containing the ganglion of interest. Because oral and aboral segments of the preparation are readily discernible, the focal stimulator could be moved to proximal and distal regions flanking the FOV. For both EFS and FTS, tissues were stimulated with 1-s depolarizing pulses using a GRASS S9E Electrical Stimulator (Quincy, MA) with the parameters, 70V, 10Hz and 0.1 ms duration.

Local drug application

Filamented borosilicate glass microelectrodes were fabricated using a pipette puller (P-87 Flaming-Brown Micropipette Puller, Sutter Instruments Corporation, Novato, CA, USA) and back-filled with drug-containing Kreb's buffer. Drugs were then puffed onto the surface of ganglia using very slight positive pressure applied with a 1-mL syringe connected to a pipette holder. This approach delivers a volume of drug-containing solution in the picoliter range and provides the novel advantage of allowing responses within multiple ganglia to be studied in a single preparation. Since certain enteric neurons are mechanosensitive[48], we confirmed that the force of fluid ejection *per se* was not capable of activating neurons or glia within myenteric ganglia using our experimental parameters (**Appendix Fig. 2.7**). During recordings, enteric glial responses were evoked with either ADP (3 mM) or CNO (100 μM). Higher concentrations of drug were required than in bath application experiments because of dilution by the volume of the bath[13].

Ca^{2+}-imaging studies

Tissues were continuously superfused with fresh, prewarmed (37°C) Kreb's buffer at a constant rate of 2–3 mL/min for the duration of all imaging experiments. The perfusate was removed at a constant rate using a Peri-Star Pro peristaltic pump (World Precision Instruments Inc.) to avoid oscillations in fluid levels within the recording chamber. Myenteric ganglia were visualized through a 20x wide-field water-immersion objective lens (Olympus XLUMPLFLN20xW, 1.0 numerical aperture) on an upright Olympus BX51WI fixed-stage microscope (Center Valley, PA). Ganglia were identified based on their plexiform appearance and high expression of the fluorescent tdTomato reporter in resident glial cells. Illumination for fluorescence imaging was supplied by a DG4 Xenon light source (Sutter Instrument, Novato, CA). The light used to excite GCamp5g was filtered through a 485/20-nm band-pass filter, and emitted light was filtered through a 515-nm long-pass filter. The tdTomato channel was excited by light filtered through a 535/20-nm band-pass filter, and reflected tdTomato signals were filtered through a 610/75-nm band-pass emission filter prior to detection[19]. Imaging data were acquired at a frame rate of 1 frame per second using a Neo sCMOS camera (Andor, South Windsor, CT) and saved on a personal computer running Windows 10 (Microsoft Corporation, WA) and MetaMorph (Molecular Devices, Sunnyvale, CA) software. Images were saved as *.tiff* files, and recordings were exported as *.tiff* stacks for subsequent analysis. In some cases, confocal fluorescence video microscopy was conducted using a Nikon A1R HD25 confocal spinning-disk microscope (Nikon, Tokyo, Japan) to obtain higher spatial and temporal resolution of Ca^{2+} responses during validation of our genetic models. In these cases, tissues were prepared as described above and imaged through a 20x Nikon objective lens (CFI Apochromat LWD Lambda20xC WI, 0.95 numerical aperture). Confocal images were captured using a Nikon DS-Ri2 digital camera (Nikon, Tokyo, Japan) and recorded using NIS-Elements C software (Nikon). Confocal video recordings were saved as *.tiff* stacks and exported for analysis as described above.

Whole-mount immunohistochemistry

Fixed colonic tissue was dissected for immunohistochemical studies as described previously[14]. Briefly, epithelium and circular smooth muscle layers were removed by microdissection, generating longitudinal muscle-myenteric plexus (LMMP) whole-mount preparations consisting of myenteric plexus lying atop longitudinal muscle. A 1-cm^2 sample of the LMMP was then washed three times in 0.1% Trixon X-100 in phosphate buffered saline (PBS). Tissues were then blocked for 45 min in blocking solution containing 4% normal donkey serum, 0.4% Triton X-100 and 1% bovine serum albumin dissolved in PBS. Tissue preparations were then probed overnight at 4°C with the following primary antibodies: chicken anti-GFAP (1:1000; Cat#ab4674, Abcam, Cambridge, UK), rabbit anti-hemagglutinin (1:500; Cat#3724, Cell Signaling, Danvers, MA) and rabbit anti-dsRed (1:1000; Cat#632496, Takara Bio USA Inc., Mountain View, CA). Prior to imaging, tissues were incubated for 2 h with Alexa Fluor 488-conjugated donkey anti-chicken (Cat#703-545-155, Jackson, Westgrove, PA) or Alexa 594-conjugated donkey anti-rabbit (Cat#711-585-152; Jackson, Westgrove, PA) secondary antibodies, as appropriate, diluted 1:400. The specificity of all antibodies used has been previously confirmed[26].

Solutions and chemicals

DMEM was obtained from Life Technologies (Carlsbad, CA). Unless otherwise noted, all regents were obtained from Sigma (St. Louis, MO). The composition of Kreb's solution used during imaging experiments was as follows: 121 mM Na^+, 4.9 mM K^+, 25 mM $NaCO_3^-$, 1.2 mM Mg^{2+}, 2.5 mM $CaCl_2$, 1.2 mM $NaHPO_3^-$, 11 mM D-glucose, and 1 mM pyruvate. Kreb's solution was titrated to pH 7.4 with NaOH.

Data analysis and statistics

Recordings were analyzed using Fiji software (NIH) as previously described[49]. Briefly, videos were background-subtracted and, where necessary, stabilized using the StackReg plugin (http://bigwww.epfl.ch/thevenaz/stackreg/). The tdT channel image obtained at the outset of the experiment was used to confirm the identity and location of glial cells for all experiments and to generate corresponding regions of interest (ROIs). To do this, the tdT image was band-passed filtered using Fiji's Free Fourier transform (FFT) and subsequently auto-thresholded. Glial ROIs were auto-detected using the resultant binary masks and were more specific for glial cells (**Appendix Figs. 2.7** and **2.9a**). We confirmed the functional validity of this approach by comparing the magnitude of the peak Ca^{2+} responses evoked by application of ADP (**Appendix Fig. 2.9b**), a potent agonist of the P2Y1 receptor, which is highly expressed on enteric glia[14,17]. Neuronal ROIs were manually selected after exclusion of auto-generated glial ROIs based on morphology and responsiveness to electrical stimuli, as depicted in spatio-temporal response maps (**Fig. 2.1e**; **Appendix Fig. 2.7**). This approach provides a visual indication of "activity over time", a well-described parameter used in previous studies of Ca^{2+} responses[50]. All glial and neuronal ROIs were saved. Ca^{2+} responses were then measured and exported to Microsoft Excel (Microsoft Corporation, WA). Final data values were quantified as fold-change in mean cellular fluorescence intensity relative to baseline florescence intensity ($\Delta F/F_o$) within a given cell. Unless otherwise noted, values are presented as means ± standard error of the mean (s.e.m.). For population recruitment studies evaluating the proportions of neurons or glia activated by FTS, a positive response was defined as a peak fluorescence value > 5 standard deviations above the average baseline Ca^{2+} level measured within a given cell for a fixed recording duration.

Unless otherwise stated, sample size refers to the number of cells that responded under given experimental conditions; the number of mice utilized is also indicated where appropriate. For all experiments, approximately 30–40 neurons and a comparable number of glia were studied

per ganglion, with at least 1–2 ganglia utilized per mouse under each recording condition. Statistical outliers were computed using two-tailed Grubb's test, and values were excluded from the final analysis only when they surpassed a threshold of $\alpha = 0.05$. Values from identical experimental setups were pooled after confirming equality of sample variances using a two-tailed *f*-test ($\alpha = 0.001$). In most cases, statistical analyses involved two-tailed Student's *t*-tests comparing baseline-adjusted peak Ca^{2+} response values with those in controls, with pairing of responses in select cases (i.e., pre- and post-CNO application) and application of Welch's correction when standard deviations were found to be unequal between treatment groups. Chi-square goodness-of-fit tests were used to compare the number of glia and neurons recruited as part of ENS circuits pathway(s) (ascending, descending, both or neither). For these purposes, positive glial or neuronal recruitment events were defined as those in which the peak Ca^{2+} response was 5 standard deviations greater than baseline. Shifts in the proportion of cells recruited by ascending, descending, both or neither circuit pathway(s) were assessed by generating contingency tables for cell recruitment under each condition and applying Fisher's two-tailed exact test to compare differences relative to control conditions. Data figures were generated using GraphPad Prism 5 (GraphPad Software Inc., La Jolla, CA), and illustrations were created using BioRender software (https://biorender.com/).

RESULTS

The ENS controls intestinal motility through neuronal circuitry composed of polarized ascending excitatory and descending inhibitory nerve pathways[15] (**Fig. 2.1a**). Enteric glia sense[12,16] and modulate[13,14] enteric neuron activity, but whether they do so in a synapse-specific manner is unclear. To determine whether enteric glia display selectivity in their responsiveness to neurons associated with either ascending or descending pathways, we used focal electrical stimulation to activate overlapping ascending and descending synaptic pathways and recorded responses in associated neuron-glia networks of *Wnt1^{Cre};GCaMP5g-tdT* mice. We tested the selectivity of glia-to-neuron signaling by combining this approach with glial chemogenetics in *Wnt1^{Cre};GCaMP5g-tdT;GFAP-hM3Dq* mice, which express a modified $G_{q/11}$ protein-coupled M3 muscarinic DREADD (designer receptor exclusively activated by designer drug) that is activated by clozapine-N-oxide (CNO) but not by the natural agonist acetylcholine (ACh).

Bidirectional enteric neuron-glial communication

Before addressing the question of enteric glial synapse-specificity, we determined the potential breadth of glial recruitment by enteric neurons. For these experiments, we used electrical field stimulation (EFS) as a broad neuronal stimulus and recorded evoked Ca^{2+} responses in networks of enteric neurons and glia in samples of myenteric plexus from the colons of *Wnt1^{Cre};GCaMP5g-tdT* mice (**Fig. 2.1a**). This mouse line expresses the genetically encoded Ca^{2+} indicator, GCaMP5g, in both enteric neurons and glia, while allowing differentiation of neurons and glia based on tdTomato expression, which is high in glia and nearly undetectable in neurons (**Fig. 2.1b–c**; **Fig. 2.6**). Using an initial EFS pulse of 3 s, we observed broad activation of neurons and glia within myenteric ganglia (**Fig. 2.1d,e**). Under these conditions, 31.3% of myenteric glia were recruited by neuronal activity. However, the peak neuronal Ca^{2+} response was extreme ($\Delta F/F_o$ = 3.50 ± 0.18; n = 22 cells), indicating that this stimulus is excessive and may push the

system to the limits of physiological activity. In subsequent experiments, we titrated the EFS stimulus, identifying a 1-s pulse as an optimal stimulus that evoked responses that were still robust but which were more in line with physiological activity. Under these conditions, EFS elicited a 1.66 ± 0.06-fold increase in neuronal Ca^{2+} levels and activated 94.4% of all studied neurons (n = 216 cells from 6 mice; **Fig. 2.1f,g**). The onset of the neuronal Ca^{2+} response was immediate in all neurons visualized within the field of view, with peak responses occurring within 1–2 s following application of EFS. Neuronal depolarization was followed immediately by a phase of glial recruitment that typically occurred ~1–2 s after the onset of EFS. Glial Ca^{2+} responses were characterized by a lower peak magnitude relative to baseline ($\Delta F/F_o$ = 1.05 ± 0.06) that recruited 88.6% ± 3.37% of all glia (n = 182 cells from 6 mice). These data show that the majority of enteric glia in the myenteric plexus can be recruited by neuronal activity.

We conducted similar experiments to assess the ability of enteric glia to recruit enteric neurons by stimulating enteric glia with adenosine diphosphate (ADP) and assessing Ca^{2+} responses in glia and neurons (**Fig. 2.1h,i**). ADP stimulates robust Ca^{2+} responses in all myenteric glia in the mouse colon[17,18] and drives gliotransmitter release through connexin-43 hemichannels[19]. Local application of ADP to myenteric glia triggered an immediate 1.96 ± 0.10-fold increase in glial Ca^{2+} levels relative to baseline (**Fig. 2.1j,k**). Glial Ca^{2+} responses remained largely confined to the tdT-positive network of glial cells and propagated through the myenteric ganglion (**Fig. 2.1k**). Glial activation was simultaneously accompanied by a neuronal response featuring a peak $\Delta F/F_o$ = 0.58 ± 0.05 that recruited 42.5% ± 9.0% of all neurons within the ganglia. The peak neuronal response to ADP was substantially smaller in magnitude than its glial counterpart but exhibited similar overall kinetics. Thus, enteric glia are capable of recruiting at least a portion of enteric neurons.

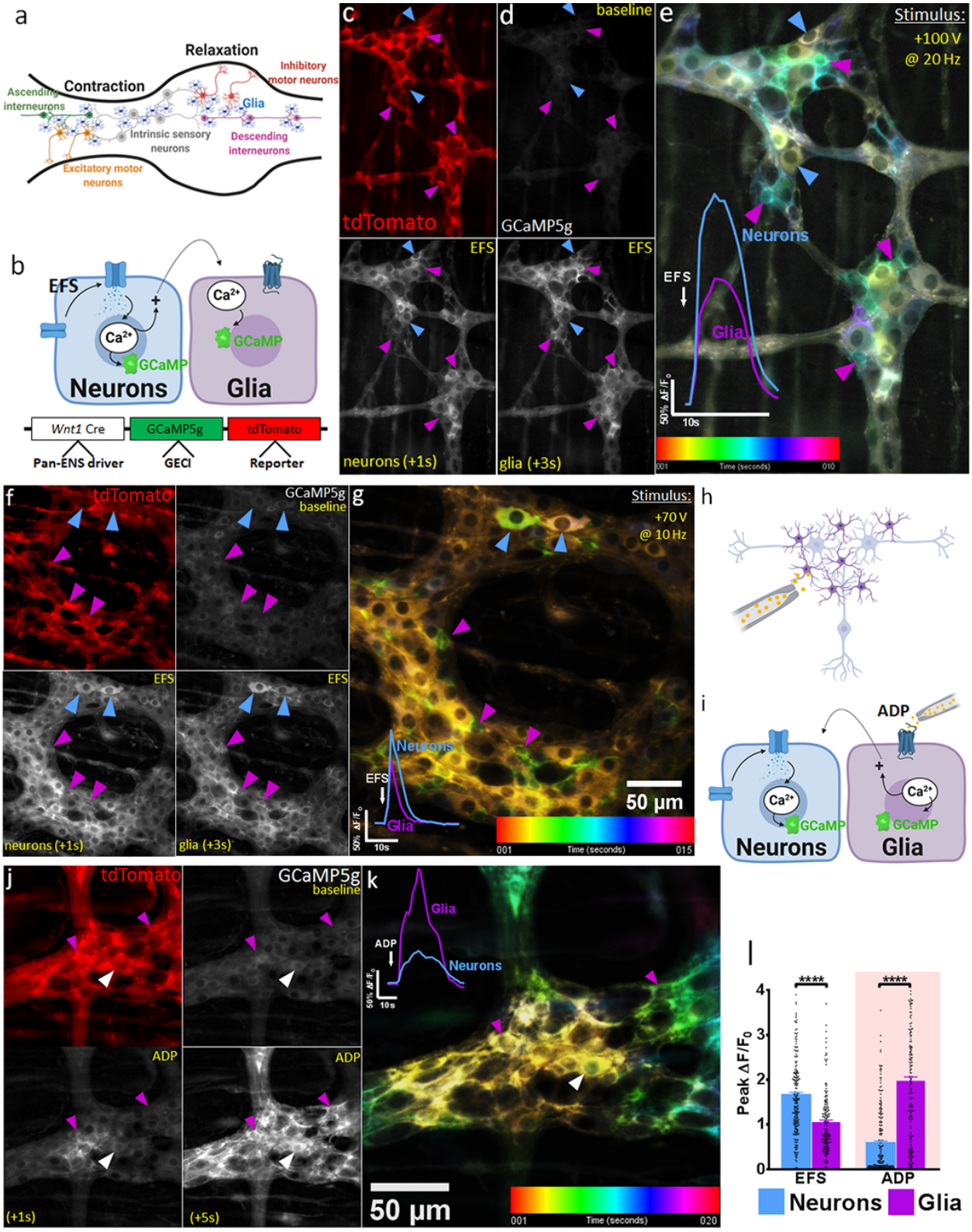

Figure 2.1. Bi-directional neuron-glia communication. a, The ENS circuitry controlling GI motility is composed of ascending and descending networks of neurons and glia. Intrinsic sensory neurons initiate reflex motility, synapsing onto neurons belonging to ascending and descending

Figure 2.1 (cont'd)
pathways. The descending circuitry promotes relaxation while the ascending circuitry promotes contraction. b, Experimental paradigm demonstrating neuron-to-glia communication (*top inset*) and genotypic schematic demonstrating expression of a genetically encoded Ca^{2+} indicator (GECI) in ENS cells under the control of the *Wnt1* neural-crest promoter (*bottom inset*). c, tdTomato expression is predominantly glial in this model (magenta arrowheads). d, GCaMP signals at baseline and following electrical field stimulation (EFS), which evokes a fast Ca^{2+} response in neurons (blue arrowheads) that is followed by glial responses (magenta arrowheads). e, Temporal color coding of enteric neuron and glial Ca^{2+} responses to +100V EFS applied at 20 Hz. Note that neuronal responses are red-yellow indicating early activation, and glial responses are green-blue indicating later responses. Traces show averaged responses of neurons and glia to EFS within the ganglion. Glial responses are activated by neurons. f, Stimulating the plexus with +70V EFS (at 10 Hz), a physiological stimulus intensity, achieves a similar Ca^{2+} response profile but mitigates tissue hyperexcitability. g, Color-coded temporal projection depicting EFS-mediated Ca^{2+} responses at +70V. Blue arrowheads indicate neurons and magenta arrowheads indicate glia. Representative tracings showing fold-change in average neuronal and glial fluorescence in 40 cells taken from a single ganglion, with similar results obtained in all animals (*bottom-left inset*). h, Experimental paradigm showing glia-to-neuron communication. i, ADP directly activates enteric glia and can indirectly recruit enteric neurons. j, Localized ADP application causes a dramatic glial Ca^{2+} response (magenta arrowheads). k, Color-coded temporal projection of the ADP response, which propagates along the glial network (magenta arrowheads) and is accompanied by a delayed neuronal recruitment phase (white arrowheads). Representative Ca^{2+} tracings showing neuronal and glial fluorescence in 40 cells taken from a single ganglion, with similar results obtained in all animals (*top-left inset*). l, Summary of average peak Ca^{2+} responses in neurons and glia consequent to stimulation with EFS or ADP. Bars depict means ± SEM (****$P < 0.0001$, unpaired Student's *t*-test).

Functionally specified networks of neurons and glia control intestinal reflexes

Results to this point show that enteric glia are responsive to neuronal activity in gut motor circuits and modulate a portion of neurons within these circuits. The gut motor reflex comprises overlapping neural programs in which ascending pathways promote gut contractility while descending pathways promote gut relaxation. In general, ascending circuit activity is mediated by cholinergic signaling while the descending circuitry involves nitrergic signaling together with purinergic co-transmission[20]. This polarized arrangement provides an ideal paradigm for testing whether enteric glia distinguish between activity in adjacent neural pathways. We therefore used a point stimulator to apply focal tract stimulation (FTS) to activate ascending and descending circuit pathways traveling through individual myenteric ganglia. This was accomplished by positioning a stimulating electrode on interganglionic nerve fiber bundles in the oral and aboral direction of the ganglion of interest (**Fig. 2.2a**). In this way, we could independently activate the descending or ascending reflex pathway associated with a given ganglion. Assessing the neuron-glial networks recruited under each condition allowed us to determine whether enteric glia are committed to specific synaptic pathways.

Like EFS, FTS evoked an immediate-onset Ca^{2+} response in neurons that peaked within 1 s and was accompanied by a glial recruitment phase that peaked 1–3 s following application of FTS. In general, stimulating ascending pathways elicited more robust Ca^{2+} responses in both neurons (~44% higher) and glia (~13% higher) compared with stimulation of descending pathways. This difference between pathways was more pronounced in neurons, in which activation of ascending pathways triggered a 1.44 ± 0.05-fold increase in basal Ca^{2+}, whereas activation of descending pathways evoked a 1.00 ± 0.03-fold increase (****$P < 0.0001$, n = 465 cells from 11 mice). In glia, descending pathway activation evoked a 0.40 ± 0.02-fold increase in basal Ca^{2+} levels, whereas ascending pathway activation triggered a 0.53 ± 0.03-fold increase (*$P < 0.05$, n = 560 cells from 11 mice; **Fig. 2.2b–d**).

The dramatic differences in Ca^{2+} response magnitudes between ascending and descending circuits were also associated with differences in the total numbers of neurons and glia activated within each pathway. Quantification of the number of neurons or glia recruited by FTS under various conditions revealed that, of 460 enteric neurons studied, 77% were activated by both ascending and descending FTS. On the other hand, 18% of all neurons were uniquely activated by ascending FTS, while only 4% were exclusively activated by descending FTS (**Fig. 2.2e**). Only 1% of neurons failed to respond to stimulation of either ascending or descending pathway. Glial population recruitment also differed between ascending and descending pathways. Of the 560 glial cells studied, 48% were recruited by both ascending and descending FTS. Ascending FTS recruited 13% of glia, whereas descending FTS recruited a different, non-overlapping subset of glia comprising 12% of the overall population (**Fig. 2.2e**); 27% of glia failed to respond to pathway stimulation in either direction. Thus, non-overlapping subpopulations of myenteric glia are functionally committed to either ascending or descending neural pathways.

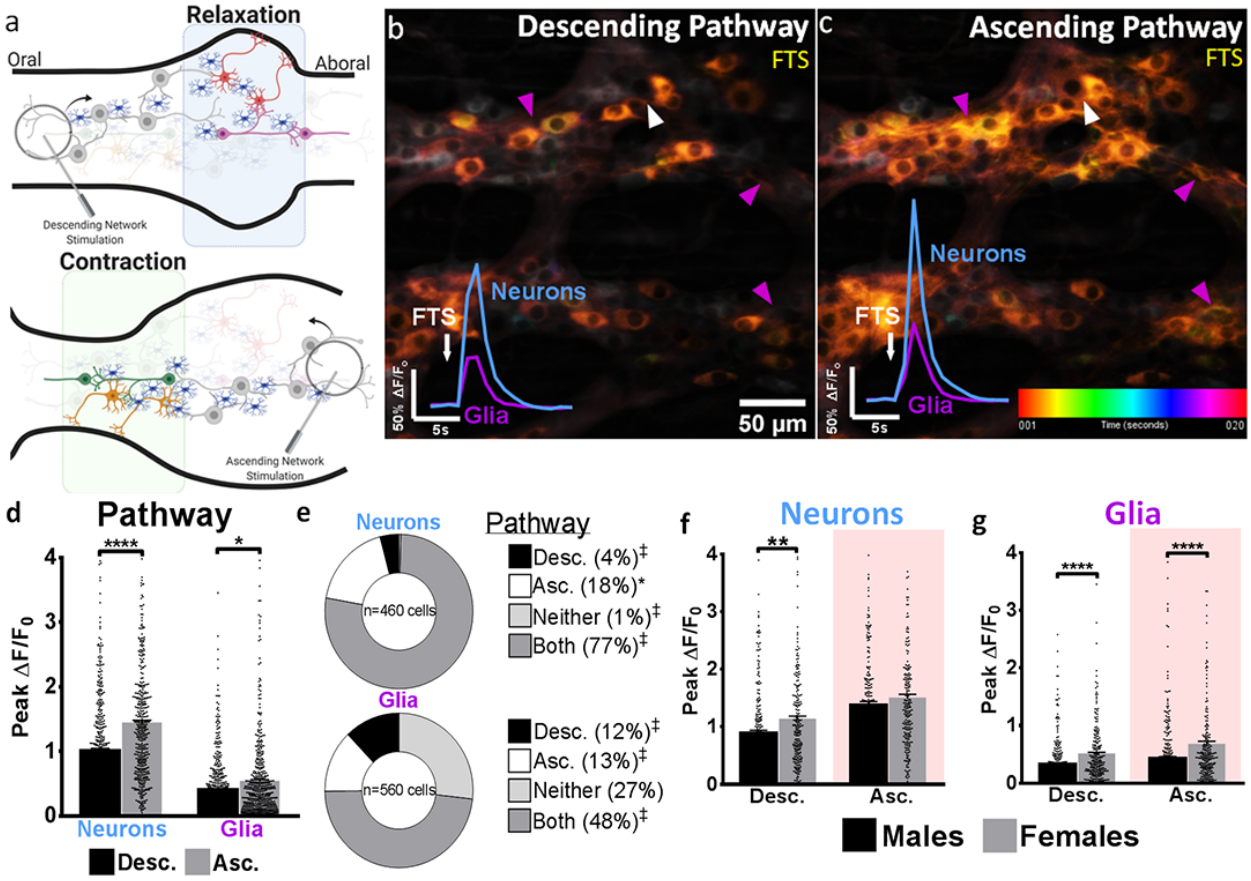

<u>Figure 2.2.</u> Functionally specified networks of neurons and glia control intestinal reflexes. a, Schematic diagram illustrating how the peristaltic reflex was experimentally manipulated using a concentric bipolar focal tract stimulator. Stimulating ganglia from the oral direction activates the descending neural circuitry associated with gut relaxation (*top panel*). Applying the same stimulus from the aboral side activates the ascending circuit pathway controlling gut contraction (*bottom panel*). Although not explicitly shown here, some populations of neurons and glia are functionally associated with both pathways. b, c, Color-coded temporal projections depicting Ca^{2+} responses provoked by descending or ascending FTS. Descending and ascending FTS stimulate distinct populations of neurons (white arrowhead) and glia (magenta arrowhead). Representative time-courses (*bottom-left insets*) demonstrate the average Ca^{2+} response evoked in the same population of neurons and glia. d, Compared to the descending pathway, ascending synaptic activity categorically provokes larger Ca^{2+} responses in both neurons and glia. e, Ascending and descending FTS recruit functionally distinct sub-populations of neurons and glia. Some neurons and glia are activated by both ascending and descending FTS ("Both"), whereas fewer neurons are exclusively activated by ascending ("Asc.") or descending ("Desc.") FTS alone. $^{‡}P < 0.0001$ and $^{*}P < 0.05$ by two-tailed Chi-square test comparing observed values with expected proportions. f, g, In the descending pathway, both neurons and glia are more robustly activated in females than males. In the ascending pathway, glia but not neurons are more robustly activated in females than males. Bars represent means ± SEM ($^{*}P < 0.05$, $^{**}P < 0.01$ and $^{****}P < 0.0001$, two-tailed unpaired Student's *t*-test).

Sex differences in ascending and descending circuit responses

Human functional gastrointestinal and motility disorders display sex differences[21], and glial-ablation studies in mice suggest that enteric glia can influence motility to different extents in males and females[22]. To address the possibility that the basic wiring of the ENS differs between sexes, we sub-stratified our pathway response data and found marked differences in the magnitudes of glial and neuronal Ca^{2+} responses between male and female mice (**Fig. 2.2f,g**). In neurons, descending pathway activation evoked larger Ca^{2+} responses in females ($\Delta F/F_o$ = 1.13 ± 0.06; n = 227) than in males ($\Delta F/F_o$ = 0.89 ± 0.05; n = 233) (**P* < 0.01; **Fig. 2.2f**). In glia, responses provoked by activation of ascending and descending pathways were globally more robust in females than in males. In 320 glial cells studied in 6 female mice, basal glial Ca^{2+} levels increased 0.50 ± 0.03-fold following descending FTS, whereas in 240 cells from 7 males, the same stimulus evoked a 0.33 ± 0.02-fold increase in glial Ca^{2+} levels (*****P* < 0.0001). Activation of the ascending pathway similarly triggered a more pronounced Ca^{2+} increase in female glia (0.67 ± 0.06-fold; n = 240 cells from 6 mice) than in males (0.43 ± 0.03-fold; n = 320 cells from 7 mice; *****P* < 0.0001). Thus, while the basic rules of glial and neuronal pathway selectivity remain constant in males and females, the magnitude of signals transduced by these pathways is governed by sex.

Cholinergic and purinergic transmitters dictate functional neuron-glial networks

Fast excitatory synaptic transmission in the myenteric plexus is mediated by ACh and purines[23]. In neurons, these transmitters contribute to the fast component of neurotransmission through activation of ionotropic nicotinic and purinergic receptors[24,25], whereas glial responses to synaptic activity are driven through metabotropic M3 and P2Y1 receptors[19,26]. Cholinergic signaling mediates ascending excitatory pathway activity and is abolished by nicotinic receptor blockade, which does not affect descending neuronal pathway responses[27]. In contrast,

destruction of descending fiber tracts abolishes purinergic neuronal activity[27], highlighting broad roles for cholinergic and purinergic transmission in the motor circuitry of the gut[28]. Given that our data show that ascending and descending synaptic pathways involve functionally specified networks of neurons and glia, we tested whether specific transmitters (i.e., ACh and purines) dictate glial pathway specificity.

To determine how neurotransmitter systems specify neuron-glia networks, we first tested the effects of blocking purinergic neuron-glia communication using the P2Y1 receptor antagonist, MRS2179 (1 μM)[17,19]. MRS2179 specifically and robustly inhibited ascending neural circuits, reducing peak neuronal responses to FTS by ~40% ($\Delta F/F_o$ = 1.44 ± 0.05 in controls [n = 465] vs. 0.84 ± 0.04 with MRS2179 [n = 181]; ****P < 0.0001; **Fig. 2.3a**), without affecting the magnitude of neuronal responses in descending pathways (P = 0.079). These alterations in neuronal responses were accompanied by changes in network-level connectivity within the myenteric plexus. Blocking glial P2Y1 receptors increased the proportion of neurons activated within descending circuits from 4% to 15% relative to controls (**Fig. 2.3c,e**; P < 0.0001). Conversely, MRS2179 did not affect the number of neurons activated within ascending circuits (19% vs. 18% in control, P = 0.897), but did reduce the proportion recruited by both pathways (62%) relative to controls (77%; P = 0.001). Consistent with a role for P2Y1 in the recruitment of glia by neurons, MRS2179 expanded the pool of FTS-unresponsive glia (“Neither”) from 27% (control) to 37% (P = 0.008), while simultaneously decreasing the proportion recruited by both ascending and descending pathways (“Both”) from 48% (control) to 38% (P = 0.015). These effects of MRS2179 were accompanied by a reduction in glial recruitment within descending pathways from 12% (controls) to 4% (P = 0.003) and an increase in glial recruitment within ascending pathways from 13% (controls) to 21% in the presence of MRS2179 (P = 0.022) (**Fig. 2.3b,d,f**). Together, these findings indicate that glial recruitment by purines functions to enhance ascending neural networks and constrain activity within descending networks (summarized in **Fig. 2.3g**).

Next, we tested how perturbing glial activation by ACh affects ascending and descending neuron-glia networks. ACh is the predominant excitatory neurotransmitter in the ENS, and glial responses to ACh are mediated through M3 mAChR receptors[26]. Therefore, we used the specific M3 mAChR antagonist J104129 (100 nM) to block glial recruitment without affecting fast cholinergic neurotransmission, which relies on nicotinic receptors. J104129 increased peak Ca^{2+} responses in neurons associated with descending pathways ($\Delta F/F_o$ = 1.35 ± 0.04 with J104129 [n = 239] vs. 1.00 ± 0.038 in controls [n = 460]; $P < 0.0001$; **Fig. 2.3a,d,e**) without affecting FTS-mediated neuronal responses in ascending pathways ($P = 0.896$). Similarly, J104129 increased the magnitude of glial peak Ca^{2+} responses triggered by descending FTS ($\Delta F/F_o$ = 0.589 ± 0.035 with J104129 vs. 0.405 ± 0.020 in controls; n = 240–560) and ascending FTS ($\Delta F/F_o$ = 0.544 ± 0.036 with J104129 vs. 0.663 ± 0.034 in controls [n = 240]; $P = 0.016$; **Fig. 2.3a,d,e**). Cholinergic blockade also altered neuronal and glial population recruitment dynamics. In the presence of J104129, 4% of activated glia were recruited by the descending pathway alone compared to 12% in controls ($P = 0.003$), whereas 1% were recruited by the ascending circuit following drug treatment compared with 13% in control conditions ($P < 0.0001$). These changes were accompanied by a dramatic increase in the number of glia that were responsive to both ascending and descending FTS from 48% under control conditions to 80% in the presence of J104129 ($P < 0.0001$). These results indicate that cholinergic transmission via the glial M3 receptor serves to constrain glial recruitment within the descending pathway and that loss of this inhibitory regulation permits glia to be activated by both ascending and descending circuits (**Fig. 2.3g**).

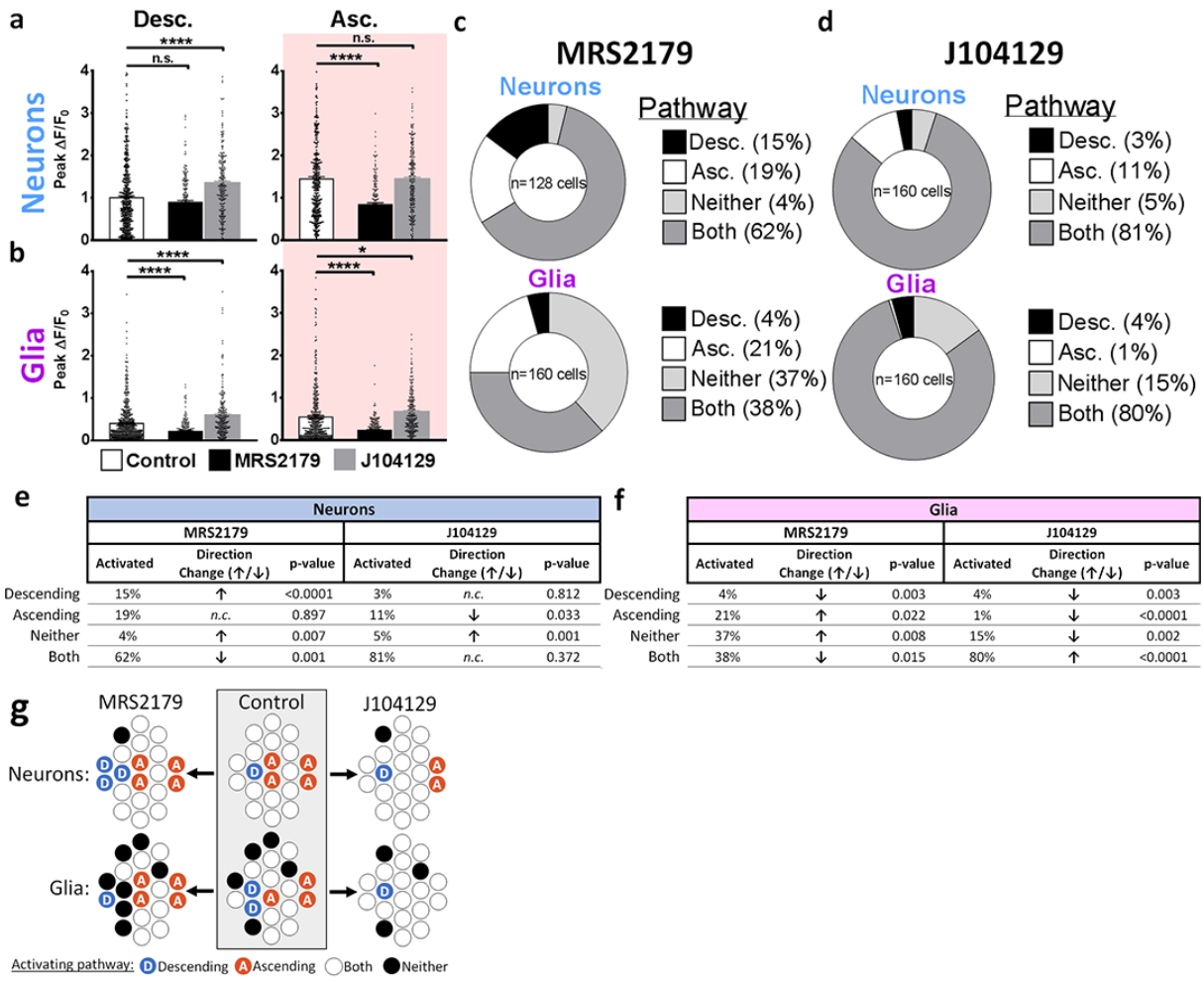

e

	Neurons					
	MRS2179			J104129		
	Activated	Direction Change (↑/↓)	p-value	Activated	Direction Change (↑/↓)	p-value
Descending	15%	↑	<0.0001	3%	*n.c.*	0.812
Ascending	19%	*n.c.*	0.897	11%	↓	0.033
Neither	4%	↑	0.007	5%	↑	0.001
Both	62%	↓	0.001	81%	*n.c.*	0.372

f

	Glia					
	MRS2179			J104129		
	Activated	Direction Change (↑/↓)	p-value	Activated	Direction Change (↑/↓)	p-value
Descending	4%	↓	0.003	4%	↓	0.003
Ascending	21%	↑	0.022	1%	↓	<0.0001
Neither	37%	↑	0.008	15%	↓	0.002
Both	38%	↓	0.015	80%	↑	<0.0001

Figure 2.3. Purinergic and cholinergic signaling differentially regulate ascending and descending divisions of the myenteric circuitry. a, *Left:* Under baseline conditions, descending FTS-provokes an increase in neuronal Ca^{2+} levels that is largely unaffected by the purinergic blocker MRS2179, but is augmented by the M3 cholinergic blocker, J104129. *Right*: J104129 does not affect the magnitude of the neuronal response evoked by ascending FTS, whereas MRS2179 reduces this response by nearly 40% compared with controls (black vs. white bars). b, *Left*: Glial Ca^{2+} responses triggered by descending FTS are reduced by MRS2179 and augmented by J104129. *Right*: Glial recruitment consequent to ascending FTS is attenuated by MRS2179 and augmented by J104129. All values represent means ± SEM. c, In the presence of MRS2179, approximately 15% of all responsive neurons were activated exclusively by descending FTS while only 4% of glia were recruited by the same stimulus. In contrast, 19% of neurons were activated exclusively by ascending FTS while 21% of glia were recruited by ascending FTS in the presence of MRS2179. d, In the presence of J104129, 3% of neurons were activated by descending FTS while 4% of glia were recruited by the same stimulus. Ascending FTS activated 11% of neurons within a myenteric ganglion in the presence of J104129 while 1% of glia were recruited under this condition. e, f, Summary table comparing proportions of neurons that are activated (e) and glia that are activated and recruited (f) by directional FTS in the presence of MRS2179 or J104129. g, Summary diagram recapitulating how cholinergic or purinergic

Figure 2.3 (cont'd)
blockade alters neuronal and glial population recruitment dynamics within each circuit pathway. MRS2179 abolishes neuronal recruitment by ascending pathways, which expands the pool of neurons associated with the descending circuitry (white→blue circles). J104129 bolsters neuron recruitment within the descending pathway, expanding the pool of neurons functionally affiliated with both pathways (orange→white circles).

Glial activation designates myenteric neurons to ascending or descending divisions of the motor reflex

Our data show that endogenous cholinergic and purinergic transmitter systems regulate specific motor pathways through glial signaling. However, it is possible that some of the observed effects could be due to M3 or P2Y1 receptor expression by enteric neurons. To circumvent this, we developed a chemogenetic mouse model that allows selective activation of enteric glia and asked how glial activation affects neurons in ascending and descending motor pathways. To this end, we crossed the *Wnt1^{Cre};GCaMP5g-tdT* mice used in the experiments above with *GFAP::hM3Dq* mice[13] to yield triple-transgenic *Wnt1^{Cre};GCaMP5g-tdT;GFAP::hM3Dq* mice in which the chemogenetic actuator hM3Dq is expressed by enteric glia (**Fig. 2.4a,b**) and GCaMP5g-tdT is expressed by both neurons and glia. Ca^{2+}-imaging and immunohistochemistry experiments conducted to confirm the function and specificity of this model revealed that hM3Dq receptor expression was co-localized with td-Tomato and GFAP (glial fibrillary acidic protein) expression in enteric glia (**Fig. 2.4c–e,l**) and that local CNO application produced robust Ca^{2+} responses in these same cells ($\Delta F/F_o$ = 1.24 ± 0.052, n = 219; **Fig. 2.4e**)[13,29]. Importantly, glial activation with CNO was followed by a Ca^{2+} response in neurons ($\Delta F/F_o$ = 0.298 ± 0.015, n = 746; **Fig. 2.4f,g**) that was offset relative to the glial phase, indicating that glia-to-neuron communication pathways remain preserved in our model.

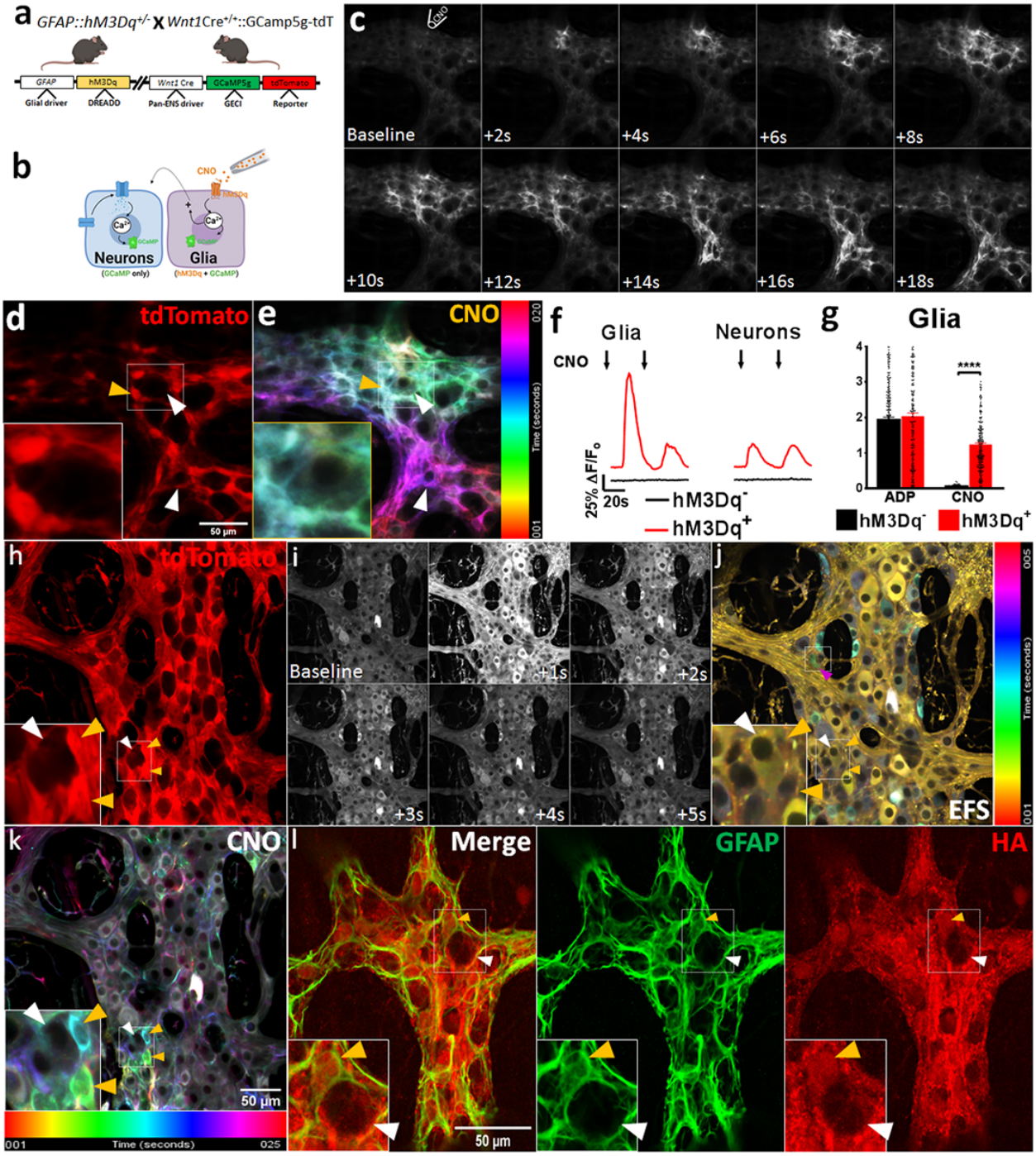

Figure 2.4. Development of a dual opto- and chemogenetic system for studying the effects of glial activation in enteric networks. a, Schematic diagram demonstrating mouse genotype. b, Enteric glia are directly activated by direct application of clozapine-N-oxide (CNO) to the ganglion. c, Still-frame montage depicting propagation of the CNO-induced Ca^{2+} response throughout the glial cell network, which is accompanied by eventual recruitment of enteric neurons within the vicinity. d, tdTomato expression is highest in glia. e, Color-coded temporal responses evoked by focal application of CNO overlap with glial tdTomato signals, confirming functional

Figure 2.4 (cont'd)

expression of the DREADD receptor in enteric glial cells (yellow arrowhead) but not enteric neurons (white arrowhead). Glial activation by CNO can nevertheless recruit neurons (lower white arrowhead), demonstrating intact glia-to-neuron recruitment pathways. f, *Left panel*: Representative tracings depict average Ca^{2+} response evoked by CNO (red tracings) in enteric glia compared with DREADD-null littermates (lower black traces). Time-courses shown are typical of the response evoked by CNO in enteric glia. *Right panel*: Representative neuronal response provoked by glial activation with CNO. g, Peak Ca^{2+} response evoked by glial agonists in DREADD-positive ($hM3Dq^{+}$) mice and DREADD-null littermates ($hM3Dq^{-}$). h, *In situ* expression of native tdTomato signals within the myenteric plexus of DREADD mice, imaged by confocal fluorescence microscopy. i, j, Time-lapse montage of EFS-induced Ca^{2+} responses. j, Color-coded temporal projection of responses in (i), with the top-most box depicting glial recruitment by neurons (magenta arrowhead), and preservation of neuro-glial communication pathways in this model. Inset showcases the neuronal response to EFS (white arrowhead) and the absence of a response in glia (orange arrowheads). k, Color-coded temporal responses to bath-applied CNO in enteric glia. CNO responses overlap with tdTomato signals and are absent in adjacent neurons. l, Immunohistochemical staining of a fixed myenteric plexus from a DREADD mouse. The plexus was probed for GFAP expression and hemagglutinin (HA; red channel), which is primarily expressed in $GFAP^{+}$ enteric glia (orange arrowheads; green channel). By comparison, enteric neurons (white arrowheads) express substantially lower levels of HA.

In line with our earlier demonstration that the magnitude of neuron and glial Ca^{2+} responses was larger in females, we observed that the magnitude of glial responses triggered by CNO were greater in females ($\Delta F/F_o$ = 0.937 ± 0.036, n = 430) than in males ($\Delta F/F_o$ = 0.747 ± 0.032, n = 357, $P < 0.0001$; **Fig. 2.5a**). Downstream neuronal responses triggered by CNO were also larger in females ($\Delta F/F_o$ = 0.386 ± 0.025, n = 390) compared with those in males (0.218 ± 0.016, n = 356; $P < 0.0001$), indicating that agonist-evoked glial activation is sex-dependent and that these putative differences in Ca^{2+} handling dynamics directly translate into more pronounced responses in female neurons. Whether this reflects the existence of signaling mechanisms unique to females (e.g., entirely different mediators) or simply indicates a greater degree of glial activation *per se* remains unclear. Further sub-stratification of CNO-mediated glial responses by pathway showed that sex differences were preserved only within the ascending circuitry (**Fig. 2.5a**). Despite this, CNO-mediated neuronal recruitment was unambiguously greater in both ascending and descending pathways in females (**Fig. 2.5a**), suggesting that in females, enteric glia that are functionally associated with the ascending circuitry are sufficient to modulate neuronal recruitment within ascending and descending pathways (**Fig. 2.5a**).

Having demonstrated that CNO-induced glial activation profiles differ based on sex and the circuit pathway involved, we next assessed the functional implications of these findings for neuronal excitability and investigated the role of cholinergic or purinergic transmission in this process. Under baseline conditions, descending pathway activation triggered a neuronal Ca^{2+} response ($\Delta F/F_o$) of 0.993 ± 0.033. This peak response was significantly reduced by CNO treatment ($\Delta F/F_o$ =0.916 ± 0.032, n = 335; P = 0.0012), suggesting that glial cholinergic signaling physiologically represses neuronal activity within the descending circuitry (**Fig. 2.5b**; **Appendix Fig. 2.8c**). This significant reduction in neuronal excitability, evoked by glial treatment with CNO, was unaffected by purinergic blockade since post-CNO treatment responses were lower in the presence of MRS2179 ($P < 0.0001$). This effect was abolished by J104129 (P = 0.685),

suggesting that the repressive effect of enteric glia on the descending pathway is mediated, in part, by M3 cholinergic signaling.

Neuronal responses to FTS were also reduced in the ascending pathway following glial activation with CNO ($\Delta F/F_o$ = 1.16 ± 0.039 in control vs. 0.945 ± 0.037 following CNO treatment, P<0.0001; n = 366), suggesting that cholinergic signaling from the descending pathway exerts cross-inhibitory regulation of ascending circuits (**Fig. 2.5b,d**). As such, M3 cholinergic blockade with J104129 does not prevent cross-inhibition of the ascending network, explaining why neuronal responses in this pathway were attenuated by CNO treatment (post-CNO $\Delta F/F_o$ = 1.12 ± 0.084, P<0.0001; and n = 80). Baseline neuronal excitability was lower in the presence of MRS2179 compared with that under control conditions ($\Delta F/F_o$ = 0.864 ± 0.064, P<0.0001; n = 53), demonstrating that purinergic signaling plays an important role in bolstering neuronal recruitment in this circuit. Interestingly, glial stimulation with CNO in the presence of MRS2179 did not further repress neuronal Ca^{2+} responses compared with effects of CNO alone (*P* = 0.111), indicating that loss of glial purinergic signaling is sufficient to abolish a large component of ascending neural circuit excitability (**Fig. 2.5b**).

In keeping with the repressive effects of glial cholinergic signaling on neural circuit activity, pretreatment with J104129 augmented CNO-mediated glial Ca^{2+} responses, increasing $\Delta F/F_o$ from 0.857 ± 0.024 under control conditions (n = 786 cells, both sexes and pathways combined) to 1.074 ± 0.037 (n = 159; *P* < 0.0001), whereas MRS2179 abolished CNO-mediated responses, reducing $\Delta F/F_o$ to 0.545 ± 0.043 (n = 148; *P* < 0.0001; **Appendix Fig. 2.8b**). The decreased glial responsiveness in the presence of MRS2179 might reflect a reduction in feed-forward glial network recruitment through purinergic P2Y1 activation[12], while the increased excitability observed in the presence of J104129 is consistent with loss of glial repressive activity at the network level[14].

The effects of CNO on each pathway highlight a regulatory role for glial cholinergic signaling in the ENS, particularly with regards to modulation of descending circuit excitability.

Since our initial findings clearly delineate a sex-dependent glial synapse-specificity within the ENS (**Fig. 2.2f,g**), we further sub-stratified the effects of CNO on neuronal excitability within each pathway by sex. As shown in **Fig. 2.5c**, the repressive effect of cholinergic activation was absent within the descending pathway in males ($P = 0.723$; $n = 182$) but persisted in females ($\Delta F/F_o = 1.107 \pm 0.046$ at baseline vs. 0.965 ± 0.043 post-CNO [$n = 193$]; $P < 0.0001$), suggesting that the descending cholinergic circuitry in particular is subject to sex-dependent effects. With regards to the ascending pathway, there was no difference in the effect of CNO-induced glial activation on neuronal excitability between males and females. Taken together, these data demonstrate that glial activation through purinergic or cholinergic mechanisms alters neuronal recruitment in ascending and descending pathways, and that these neurotransmitters serve opposing roles in the myenteric circuitry (**Fig. 2.5d**).

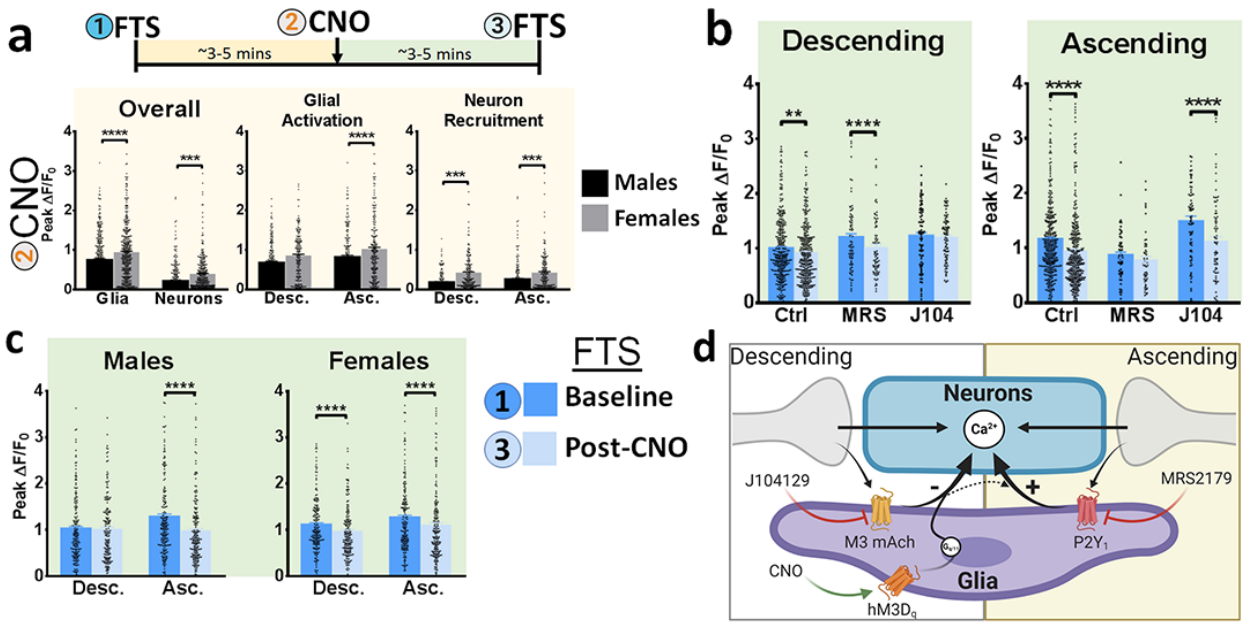

Figure 2.5. Reciprocal modulation of enteric glial and neuronal activity varies with ENS circuitry. a, *Top inset*: Myenteric ganglia were stimulated with either ascending or descending FTS before and after CNO application. *Bottom-left panel*: Unpaired CNO-induced effects on glial activation and neuronal recruitment in male and female mice. CNO provokes a more robust Ca^{2+} response in female glia compared with male glia. Similarly, the magnitude of the neuronal Ca^{2+} response evoked by CNO-induced glial activation is greater in females than in males. *Bottom-middle & -right panels*: Glial and neuronal CNO responses are further sub-stratified according to circuit pathway. In females but not males, glia associated with the ascending pathway are more robustly activated by CNO. For females, neuronal recruitment by CNO is categorically more robust in both ascending and descending pathways. b, Paired neuronal Ca^{2+} responses evoked by descending and ascending pathway activation prior to and following CNO treatment. Under control conditions, glial stimulation with CNO attenuates neuronal responses in both pathways. The CNO-induced reduction in neuronal recruitment is more pronounced in the ascending pathway than in the descending pathway. *Left panel*: Pretreatment with the M3 cholinergic antagonist, J104129, abolishes this effect in the descending pathway. *Right panel*: Pretreatment with the selective P2Y1 antagonist, MRS2179, preferentially blocks CNO-induced reductions in neuronal responses in the ascending pathway. *c,* Sub-stratifying the effects of CNO on neuronal pathway responses reveals a sex-dependence in the effect of glial activation on neuronal responses. *Left panel*: In males, glial activation with CNO attenuates the neuronal Ca^{2+} response in the ascending circuitry without affecting descending pathway responses. *Right panel*: In females, glial activation by CNO attenuates neuronal responses in both network pathways. d, Mechanistic paradigm highlighting pathway-specific roles of glial purinergic and cholinergic signaling. Neuronal recruitment within the descending circuitry is subject to glial inhibitory control in an M3-dependent manner. As such, cholinergic blockade with J104129 unleashes neuronal recruitment by descending synaptic stimuli. Neurons formerly recruited by the ascending circuitry are subsequently activated by both pathways (see increase in baseline response in Fig. 2.5b, *left panel*). In contrast, glial purinergic signaling preferentially bolsters neuronal responses within the

Figure 2.5 (cont'd)
ascending circuitry. Abrogating $P2Y_1$ activation with MRS2179 uncouples neurons from this pathway (see decrease in baseline response in Fig. 2.5b, *right panel*), allowing for unopposed activation by the descending circuitry. These effects are concordant with alterations in population recruitment dynamics described in Fig. 2.3g.

DISCUSSION

Our results demonstrate the existence of cell-specific signaling between subpopulations of enteric glia, neurons, and synapses in ENS circuits. Enteric glia and neurons interact in a cell- and synapse-specific manner, and enteric glia display functional heterogeneity based on selective signaling with particular neuron subtypes and synapses belonging to overlapping ascending and descending motility pathways of the ENS. Synaptic pathway specificity among enteric neuron-glia communication is dictated partly by neurotransmitters such as ACh and ATP. Cholinergic signaling functionally specifies glia to the descending circuitry and this network plays an important role in repressing the excitability of descending neural pathways, with some degree of cross-inhibition imposed upon the ascending pathway. Glial recruitment by purinergic signaling functions to enhance excitability in ascending circuit pathways and constrain activity within descending networks. The balance between purinergic and cholinergic signaling may differentially control specific circuit activity through selective signaling between particular enteric neurons and glia.

Different sets of enteric glia are recruited by ascending and descending neural pathways, and glial activation has differential reciprocal effects that are neural pathway specific. These observations suggest that enteric glia, like astrocytes, are circuit-specific cells. Pathway- and synapse-specific signaling between astrocytes and neurons is becoming an increasingly well-developed concept in the brain, but whether neuroglia display similar properties in the periphery has remained unclear. In the basal ganglia, astrocytes modulate homotypic interactions between D1- or D2-dopaminergic populations of neurons[5]. In this context, astrocytes convey signals between neurons that are wired within a specific network, an observation consistent with prior findings highlighting a role for astrocytic CB1 receptor activation in homosynaptic potentiation[30]. Elsewhere, astrocytes of the *nucleus accumbens* were shown to respond to dopaminergic neuronal input by releasing purines, which, in turn, act on post-synaptic neurons, resulting in

depressed excitatory neurotransmission and the onset of addiction[31]. There is also compelling evidence that incoming synaptic information is decoded by mouse hippocampal astrocytes to cause the release of context-appropriate gliotransmitters that modulate synaptic potentiation and depression between CA3 and CA1 neurons[32]. While such synapse specificity has not been observed in the peripheral nervous system, enteric glia are known to share an impressive array of molecular markers with their CNS counterparts, including expression of fate markers such as GFAP[33] and various neurotransmitter receptors[34]. Thus, enteric glia possess much of the same signaling machinery used for synaptic transmission by astrocytes within brain circuits. Additionally, it has been postulated that the ENS could represent an early evolutionary precursor to the CNS[35]. If this proves to be the case, enteric glia may represent the earliest evolved neuroglia specialized to modulate synaptic transmission in a cell- and synapse-specific manner. Therefore, these data could have broad implications and provide insights into the fundamental rules that govern neuron-glia communication in the periphery and the brain.

Although the properties of separate enteric neuronal subtypes are generally well characterized[15], very little is known about how these neuronal subtypes and enteric glia interact within organized networks to coordinate gastrointestinal motility. As such, decoding how enteric glia modulate neural circuit activity in the ENS is a critical next step towards formulating a comprehensive model of how gastrointestinal motor circuits control gut motility. In this regard, one striking observation that emerged from our study is that ascending synaptic activity provoked more robust Ca^{2+} responses than descending synaptic activity. The ascending circuitry primarily utilizes acetylcholine as an excitatory neurotransmitter to activate targets located in orally situated ganglia[15,20]. In contrast, neurotransmission within the descending neural circuitry is more varied in that it also involves nitrergic[36] and purinergic release[20,27,28]. Recruitment of these inhibitory transmitter systems might therefore constitute a major effector function of cholinergic signaling within the descending pathway, thus accounting for the lower Ca^{2+} response in this circuit.

However, since ascending tract stimulation also recruited greater numbers of neurons and glia, we suspect that neuro-glial wiring of ascending and descending circuits is fundamentally different. While our data ultimately support both possibilities, the salient interpretation remains that enteric glia are functionally dedicated to specific microcircuits within the ENS.

Patterns of intestinal motility are controlled by synaptic signaling within the ENS, mediated in part by cholinergic and purinergic neurotransmitters[24,28]. Purines and ACh are responsible for fast synaptic transmission between enteric neurons[28] and neuron-to-glia communication in myenteric motor networks[12,26]. Our evidence here shows that the neuron-to-glia arm of cholinergic and purinergic transmission functions to establish motor networks and regulate their activity. Purines released by enteric neurons act on P2Y1 receptors expressed by neighboring enteric glia[12,37] and mechanisms downstream of glial activation regulate colonic contractility[14]. Our data show that this effect is mediated through specific positive interactions of ascending neural networks and restrictive effects that constrain activity within the descending pathway. It should be noted that the decrease in the magnitude of ascending neuronal Ca^{2+} responses observed in the presence of purinergic blockade (**Fig. 2.3a**) is seemingly at odds with population recruitment dynamics. However, this apparent discrepancy can be reconciled by the fact that the main effect of MRS2179 is a selective reduction in neuronal recruitment within the ascending circuitry, which accounts for the reduction in neurons recruited by “Both” pathways; this latter recruitment, in turn, can only be accomplished by descending pathways. Since ascending signaling is abolished by MRS2179 but descending signaling proceeds unperturbed, the result is an apparent increase in the proportion of neurons associated with the descending circuitry that reality does not reflect a *bona fide* change in the number of neurons wired to this pathway. These data likely explain the observed decrease in neurogenic contractions and colonic motility under conditions in which intercellular glial signaling mediated by connexin-43 is perturbed[14]. Neuronal ACh release and glial recruitment during synaptic communication also enhance colonic contractility[26], but

apparently do so through inhibitory effects. Here, the actions of ACh at glial M3 receptors constrain glial recruitment within the descending pathway and dampen activity in descending networks. Thus, disrupting either purinergic or cholinergic mechanisms of glial recruitment can lead to widespread changes in neural networks. Together, these observations show that receptor-dependent glial signaling promotes intestinal motility by enhancing ascending motor pathways, dampening descending motor pathways, and restricting the neural network recruited during a stimulus.

Our gain-of-function DREADD model enabled us to selectively activate enteric glia and thereby dissect the glia-to-neuron arm of the enteric motor reflex. We found that glial activation with CNO was sufficient to directly recruit neurons through circuit-specific interactions that were differentially mediated by glial purinergic and cholinergic signaling. While the consistent result of glial activation appears to be a global reduction in neuronal excitability, how this effect is achieved within each pathway is governed by the neurotransmitters involved. In the presence of MRS2179, neuronal excitability in the ascending pathway is reduced to such an extent that glial activation fails to attenuate neuronal responses any further. This “floor effect” is absent in the descending neural circuitry, where glial activation with CNO continues to repress neuronal responses. This further highlights a glial purinergic bias in the ascending pathway. In contrast, glial repression of descending neural activity is abolished by J104129 but preserved within the ascending pathway. This highlights a glial cholinergic bias in the descending pathway, though it is unclear why cross-inhibition of the ascending pathway is unaffected. As is the case for hippocampal astrocytes, however, it is possible that enteric glia decode some frequency or amplitude domain of neuronal firing in mounting specific interactions with the ascending circuitry[32]. Alternatively, it is also possible that glial cross-inhibition of the ascending neural circuitry is orchestrated through synaptically distinct networks that are altogether different from those that mediate repression of the descending circuitry (**Fig. 2.5d**).

Functional gastrointestinal and motility disorders display a strong female bias[21,38], and enteric glial ablation models show sex-dependent effects on motility[22]. Our data suggest that these effects could be due to intrinsic differences in the excitability of female glia and neurons. The factors responsible for driving these differences are not yet clear but hormones could be responsible. Similar positive effects of hormones on cholinergic neurotransmission are observed in the rat forebrain, where estrogen promotes choline acetyltransferase expression[39,40]. Recent single-cell transcription data also show that expression of the type 1 estrogen receptor (ESR1) is enriched in intrinsic primary afferent neurons (IPANs) and possibly ascending excitatory interneurons[41]. IPANs drive activity in ascending and descending reflex pathways as well as activity in the corresponding population of glia that responded to both pathways, and likely correspond to the neuronal population that responded to stimuli in either direction in this study. Estrogen-dependent effects on IPANs would, therefore, have large effects on neuron and glial excitability in enteric motor pathways.

Understanding how simple synapse-level interactions give rise to complex, network-level behaviors remains a fundamental problem in neuroscience. Neurons have long been considered the main active cell type within the ENS circuitry, giving rise to a neurocentric paradigm that has tended to overlook the role of enteric glia as key regulators of gut motility. Our data show that circuit-specific enteric glia regulate neural pathways that control intestinal motility. By functioning as logic gates, enteric glia modify neural network activity through purinergic and cholinergic mechanisms. We therefore postulate that cholinergic recruitment of glia represses the descending circuit pathway, and that its concurrent and exclusive cross-inhibition of the ascending circuitry can protect against states of ENS hyperexcitability. Likewise, we suspect that glial P2Y1 activation positively modulates ascending neural circuit activity and that this can offset the inhibitory effects of purinergic signaling, which dominates the descending neural pathway[28]. Thus, the complexity that emerges at the network level far outstrips what can be gleaned from a neurocentric

description of the ENS circuitry in which neurons are thought to act in isolation. Ultimately, the elegant “division of labor” between cholinergic and purinergic signaling provides valuable insights into how two distinct cell populations can form a connectome[42] in which shared neurotransmitters orchestrate complex physiological processes such as motility.

APPENDIX

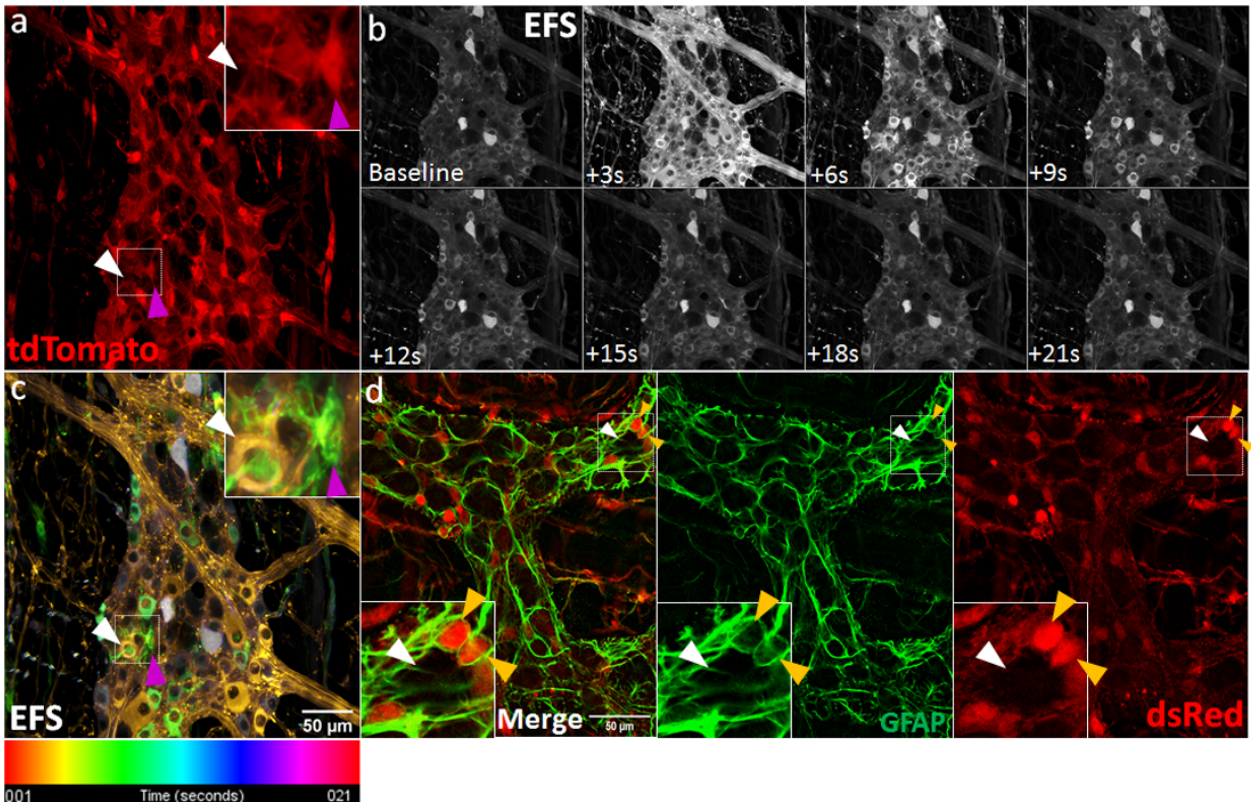

Figure 2.6. Broad glial recruitment following stimulation of neurons with EFS. a, *In situ* expression of native tdTomato signal within the myenteric plexus of *Wnt1Cre::GCamp5g*-tdTomato mice is highly localized to glial cell bodies (magenta arrowheads) and nearly entirely absent from the adjacent neuron (white arrowhead). b, Confocal time-lapse montage of Ca^{2+} responses consequent to application of +70V EFS (at 10 Hz). The rapid rise in intracellular Ca^{2+} level peaks within the first 1–2 s following application of the stimulus. Time intervals are larger since images were obtained as a 3D stack across multiple planes spanning the depth of the ganglion. c, Temporal color projection of EFS-induced Ca^{2+} responses within the same ganglion showing an initial phase of neuronal activation (white arrowheads) followed by glial recruitment approximately 3 s later. d, Immunohistochemical characterization of GFAP (green channel) expression in a fixed myenteric plexus highlights glial processes and provides a cross sectional view of glial cell bodies (orange arrowheads; *middle panel*). Residual tdTomato expression was probed with a dsRed antibody, which demonstrates exquisite overlap with putative glial cell bodies (red channel). The nearby enteric neuron (white arrowhead) expresses nearly undetectable levels of dsRed signal, although some neurons exhibit low levels of dsRed.

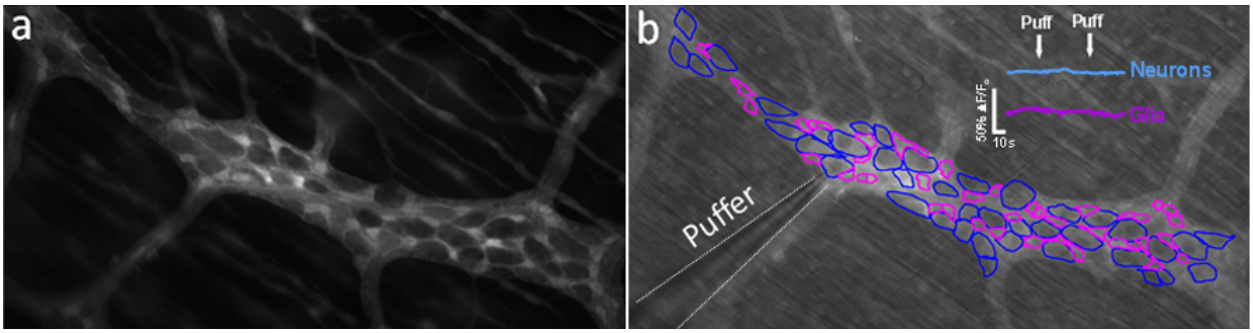

Figure 2.7. Puffing a drug-free solution does not provoke Ca^{2+} responses. a, Native expression of tdTomato signals delineates locations of glia within the myenteric plexus. b, Baseline GCamp5g signals showing that application of drug-free Kreb's buffer directly to the ganglion surface does not provoke Ca^{2+} responses within glia (magenta ROIs) or neurons (blue ROIs). The shadow of the glass microelectrode used to puff solutions onto the ganglion is visible under dim lighting (*bottom left of FOV*; highlighted for clarity). *Top-right insets*: Time-courses of fluorescence signals in the corresponding populations of glia and following application of drug-free solution at 30 and 60 s.

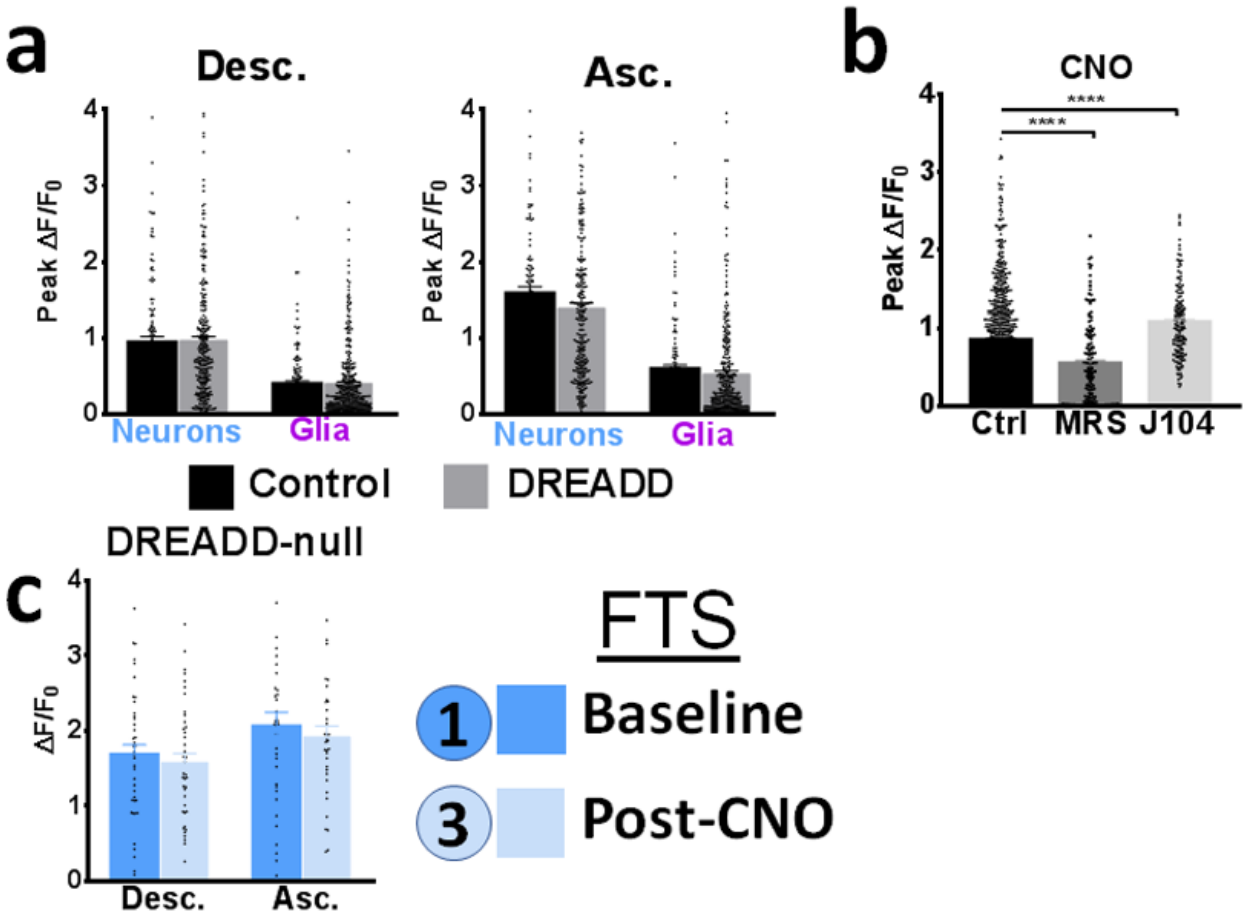

Figure 2.8. Preservation of directional pathway responses in a DREADD model. a, Neuronal and glial Ca^{2+} responses evoked by FTS are not different between DREADD and control WT mice, demonstrating that circuit pathway wiring is not affected by the GFAP::hM3Dq cross. b, Overall CNO-induced glial activation is attenuated by pretreatment with the selective P2Y1 antagonist, MRS2179. Conversely, the selective M3 cholinergic antagonist, J104129, augments glial recruitment by CNO. These data represent non-stratified agonist-evoked glial responses from all pathways, and thus constitute the broader data set from which pathway responses are derived. c, CNO does not abolish peak neuronal Ca^{2+} responses in WT mice, confirming that repeated FTS using our experimental parameters does not lead to run-down of neuronal responses.

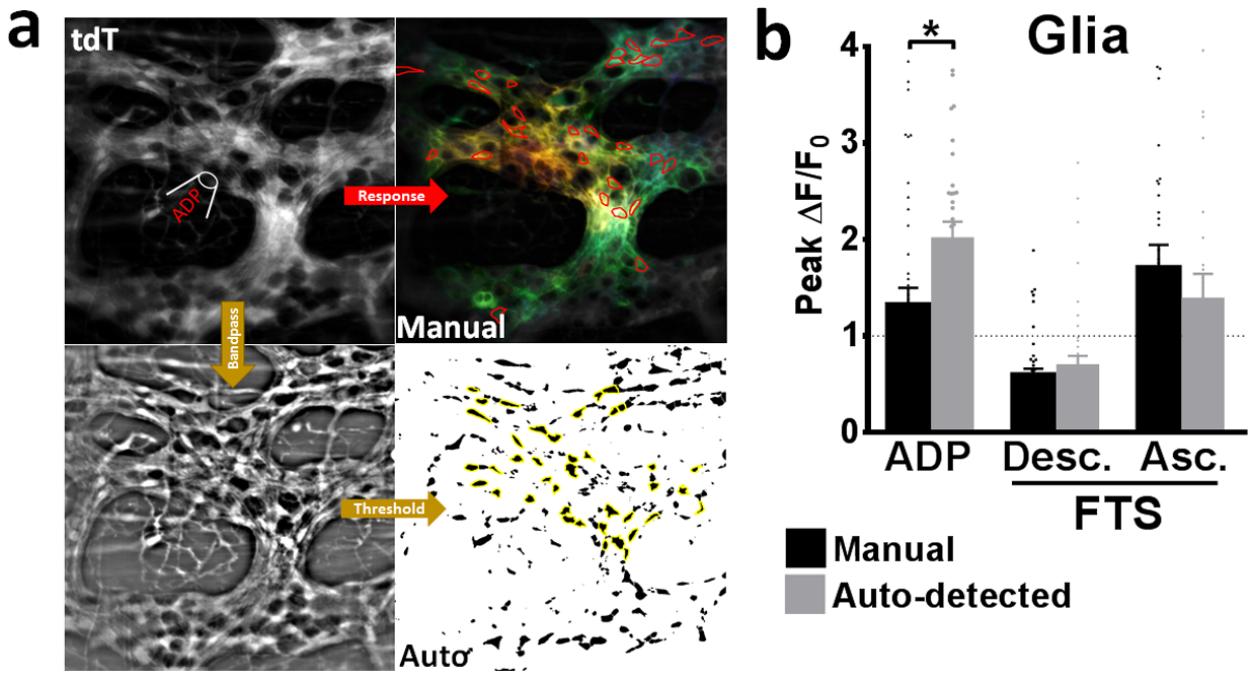

Figure 2.9. Automated detection and analysis of glial ROIs based on tdTomato channel masks. a, A tdTomato mask was used to auto-generate regions of interest for analysis of glial responses (*bottom-left and -right panels*). While traditional approaches rely on functional stimulation of enteric glia with ADP to identify glia (red ROIs), the resultant Ca^{2+} visualized using this approach provides an inconsistent and subjective basis for identifying glia. In the auto-detection method, a band-pass filter is applied to enhance local features. The filtered image is thresholded and the resultant binary mask provides a consistent and objective means for identifying tdTomato+ cell bodies, which correspond to enteric glia (see above). b, Auto-detecting glia using the tdTomato mask identifies cells with ADP-response dynamics more closely resembling expected values compared with the manual approach. This likely reflects greater glial-selectivity and a decreased mis-detection rate of enteric neurons, which exhibit weaker responses to ADP (*$P < 0.05$ by two-way Student's t-test).

REFERENCES

REFERENCES

1. Gundersen, V., Storm-Mathisen, J. & Bergersen, L. H. Neuroglial Transmission. *Physiol. Rev.* **95**, 695–726 (2015).

2. Gulbransen, B. D. Enteric Glia. *Colloq. Ser. Neuroglia Biol. Med. From Physiol. to Dis.* **1**, 1–70 (2014).

3. Colón-Ramos, D. A., Margeta, M. A. & Shen, K. Glia promote local synaptogenesis through UNC-6 (netrin) signaling in C. elegans. *Science (80-.).* **318**, 103–106 (2007).

4. Christopherson, K. S. *et al.* Thrombospondins are astrocyte-secreted proteins that promote CNS synaptogenesis. *Cell* **120**, 421–433 (2005).

5. Martín, R., Bajo-Grañeras, R., Moratalla, R., Perea, G. & Araque, A. *Circuit-specific signaling in astrocyte-neuron networks in basal ganglia pathways*. *Science* vol. 349 http://science.sciencemag.org/ (2015).

6. Martin-Fernandez, M. *et al.* Synapse-specific astrocyte gating of amygdala-related behavior. *Nat. Neurosci.* **20**, 1540–1548 (2017).

7. Chai, H. *et al.* Neural Circuit-Specialized Astrocytes: Transcriptomic, Proteomic, Morphological, and Functional Evidence. *Neuron* **95**, 531-549.e9 (2017).

8. Yu, X. *et al.* Reducing Astrocyte Calcium Signaling In Vivo Alters Striatal Microcircuits and Causes Repetitive Behavior. *Neuron* **99**, 1170-1187.e9 (2018).

9. Spencer, N. J. & Hu, H. Enteric nervous system: sensory transduction, neural circuits and gastrointestinal motility. *Nature Reviews Gastroenterology and Hepatology* vol. 17 338–351 (2020).

10. Fung, C. & Vanden Berghe, P. Functional circuits and signal processing in the enteric nervous system. *Cell. Mol. Life Sci.* **1**, 3 (2020).

11. Broadhead, M. J., Bayguinov, P. O., Okamoto, T., Heredia, D. J. & Smith, T. K. Ca 2+ transients in myenteric glial cells during the colonic migrating motor complex in the isolated murine large intestine. *J. Physiol.* **590**, 335–350 (2012).

12. Gulbransen, B. D. & Sharkey, K. A. Purinergic Neuron-to-Glia Signaling in the Enteric Nervous System. *Gastroenterology* **136**, 1349–1358 (2009).

13. McClain, J. L., Fried, D. E. & Gulbransen, B. D. Agonist-Evoked Ca2+ Signaling in Enteric Glia Drives Neural Programs That Regulate Intestinal Motility in Mice. *Cmgh* **1**, 631–645 (2015).

14. McClain, J. L. *et al.* Ca2+ responses in enteric glia are mediated by connexin-43 hemichannels and modulate colonic transit in mice. *Gastroenterology* **146**, (2014).

15. Furness, J. B. The enteric nervous system and neurogastroenterology. *Nat. Rev. Gastroenterol. Hepatol.* **9**, 286–294 (2012).

16. Broadhead, M. J., Bayguinov, P. O., Okamoto, T., Heredia, D. J. & Smith, T. K. Ca 2+ transients in myenteric glial cells during the colonic migrating motor complex in the isolated

murine large intestine. *J. Physiol.* **590**, 335–350 (2012).

17. Gulbransen, B. D. *et al.* Activation of neuronal P2X7 receptor-pannexin-1 mediates death of enteric neurons during colitis. *Nat. Med.* **18**, 600–604 (2012).

18. Gomes, P. *et al.* ATP-dependent paracrine communication between enteric neurons and glia in a primary cell culture derived from embryonic mice. *Neurogastroenterol. Motil.* **21**, (2009).

19. Brown, I. A. M., McClain, J. L., Watson, R. E., Patel, B. A. & Gulbransen, B. D. Enteric Glia Mediate Neuron Death in Colitis Through Purinergic Pathways That Require Connexin-43 and Nitric Oxide. *CMGH* **2**, 77–91 (2016).

20. Costa, M., Brookes, S. J. H. & Hennig, G. W. Anatomy and physiology of the enteric nervous system. in *Gut* vol. 47 iv15–iv19 (BMJ Publishing Group, 2000).

21. Oshima, T. & Miwa, H. Epidemiology of functional gastrointestinal disorders in Japan and in the world. *J. Neurogastroenterol. Motil.* **21**, 320–329 (2015).

22. Rao, M. *et al.* Enteric Glia Regulate Gastrointestinal Motility but Are Not Required for Maintenance of the Epithelium in Mice. *Gastroenterology* **153**, 1068-1081.e7 (2017).

23. LePard, K. J., Messori, E. & Galligan, J. J. Purinergic fast excitatory postsynaptic potentials in myenteric neurons of guinea pig: Distribution and pharmacology. *Gastroenterology* **113**, 1522–1534 (1997).

24. Galligan, J. J., Lepard, K. J., Schneider, D. A. & Zhou, X. Multiple mechanisms of fast excitatory synaptic transmission in the enteric nervous system. *J. Auton. Nerv. Syst.* **81**, 97–103 (2000).

25. Decker, D. A. & Galligan, J. J. Cross-inhibition between nicotinic acetylcholine receptors and P2X receptors in myenteric neurons and HEK-293 cells. *Am. J. Physiol. - Gastrointest. Liver Physiol.* **296**, (2009).

26. Delvalle, N. M., Fried, D. E., Rivera-Lopez, G., Gaudette, L. & Gulbransen, B. D. Cholinergic activation of enteric glia is a physiological mechanism that contributes to the regulation of gastrointestinal motility. *Am. J. Physiol. - Gastrointest. Liver Physiol.* **315**, G473–G483 (2018).

27. Johnson, P. J., Shum, O. R., Thornton, P. D. J. & Bornstein, J. C. Evidence that inhibitory motor neurons of the guinea-pig small intestine exhibit fast excitatory synaptic potentials mediated via P(2X) receptors. *Neurosci. Lett.* **266**, 169–172 (1999).

28. LePard, K. J. & Galligan, J. J. Analysis of fast synaptic pathways in myenteric plexus of guinea pig ileum. *Am. J. Physiol. - Gastrointest. Liver Physiol.* **276**, (1999).

29. Agulhon, C. *et al.* Modulation of the autonomic nervous system and behaviour by acute glial cell Gq protein-coupled receptor activation in vivo. *J. Physiol.* **591**, 5599–5609 (2013).

30. Navarrete, M. & Araque, A. Endocannabinoids potentiate synaptic transmission through stimulation of astrocytes. *Neuron* **68**, 113–126 (2010).

31. Corkrum, M. *et al.* Dopamine-Evoked Synaptic Regulation in the Nucleus Accumbens Requires Astrocyte Activity. *Neuron* **105**, 1036-1047.e5 (2020).

32. Covelo, A. & Araque, A. Neuronal activity determines distinct gliotransmitter release from a single astrocyte. *Elife* **7**, (2018).

33. Jessen, K. R. & Mirsky, R. Glial cells in the enteric nervous system contain glial fibrillary acidic protein. *Nature* **286**, 736–737 (1980).

34. Jessen, K. R., Saffrey, M. J. & Burnstock, G. The enteric nervous system in tissue culture. I. Cell types and their interactions in explants of the myenteric and submucous plexuses from guinea pig, rabbit and rat. *Brain Res.* **262**, 17–35 (1983).

35. Furness, J. B. & Stebbing, M. J. The first brain: Species comparisons and evolutionary implications for the enteric and central nervous systems. *Neurogastroenterology and Motility* vol. 30 (2018).

36. Gould, T. W., Swope, W. A., Heredia, D. J., Corrigan, R. D. & Smith, T. K. Activity within specific enteric neurochemical subtypes is correlated with distinct patterns of gastrointestinal motility in the murine colon. *Am. J. Physiol. - Gastrointest. Liver Physiol.* **317**, G210–G221 (2019).

37. Boesmans, W. *et al.* Structurally defined signaling in neuro-glia units in the enteric nervous system. *Glia* **67**, 1167–1178 (2019).

38. Chang, F.-Y. *et al. Prevalence of functional gastrointestinal disorders in Taiwan: questionnaire-based survey for adults based on the Rome III criteria*. *594 Asia Pac J Clin Nutr* vol. 21 (2012).

39. Gibbs, R. B. *Fluctuations in relative levels of choline acetyltransferase mRNA in different regions of the rat basal forebrain across the estrous cycle: Effects of estrogen and progesterone*. *Journal of Neuroscience* vol. 16 https://www.jneurosci.org/content/16/3/1049.short (1996).

40. Singer, C. A., McMillan, P. J., Dobie, D. J. & Dorsa, D. M. *Effects of estrogen replacement on choline acetyltransferase and trkA mRNA expression in the basal forebrain of aged rats*. *Brain Research* vol. 789 https://www.jneurosci.org/content/16/5/1860.short (1998).

41. Zeisel, A. *et al.* Molecular Architecture of the Mouse Nervous System Resource Molecular Architecture of the Mouse Nervous System. *Cell* **174**, 999-1014.e22 (2018).

42. Swanson, L. W. & Lichtman, J. W. From Cajal to Connectome and beyond. *Annu. Rev. Neurosci.* **39**, 197–216 (2016).

43. McClain, J. L. & Gulbransen, B. D. The acute inhibition of enteric glial metabolism with fluoroacetate alters calcium signaling, hemichannel function, and the expression of key proteins. *J. Neurophysiol.* **117**, 365–375 (2017).

44. Lewis, A. E., Vasudevan, H. N., O'Neill, A. K., Soriano, P. & Bush, J. O. The widely used Wnt1-Cre transgene causes developmental phenotypes by ectopic activation of Wnt signaling. *Dev. Biol.* **379**, 229–234 (2013).

45. Danielian, P. S., Muccino, D., Rowitch, D. H., Michael, S. K. & McMahon, A. P. Modification of gene activity in mouse embryos in utero by a tamoxifen-inducible form of Cre recombinase. *Curr. Biol.* **8**, 1323–1326 (1998).

46. Spencer, N. J., Dickson, E. J., Hennig, G. W. & Smith, T. K. Sensory elements within the circular muscle are essential for mechanotransduction of ongoing peristaltic reflex activity in guinea-pig distal colon. *J. Physiol.* **576**, 519–531 (2006).

47. Johnson, S. M., Katayama, Y., Morita, K. & North, R. A. *Mediators of slow synaptic potentials in the myenteric plexus of the guinea-pig ileum*. *The Journal of Physiology* vol.

320 https://www.ncbi.nlm.nih.gov/pmc/articles/PMC1244040/ (1981).

48. Mao, Y., Wang, B. & Kunze, W. Characterization of myenteric sensory neurons in the mouse small intestine. *J. Neurophysiol.* **96**, 998–1010 (2006).

49. Schindelin, J. *et al.* Fiji: An open-source platform for biological-image analysis. *Nature Methods* vol. 9 676–682 (2012).

50. Boesmans, W. *et al.* Imaging neuron-glia interactions in the enteric nervous system. *Front. Cell. Neurosci.* (2013) doi:10.3389/fncel.2013.00183.

CHAPTER 3: ENTERIC GLIAL LPAR1 MODULATES GUT MOTILITY IN MICE AND IS REDUCED IN CHRONIC INTESTINAL PSEUDO-OBSTRUCTION IN HUMANS

ABSTRACT

Chronic intestinal pseudo-obstruction (CIPO) is a devastating form of functional gut failure that is idiopathic in nearly 50% of cases. The enteric nervous system (ENS) controls gut motility through intrinsic neurocircuits that are dynamically regulated by enteric glia, though the role of enteric glia in the pathogenesis of CIPO has never been studied. Biolipid mediators of inflammation acting through the type I lysophosphatidic acid receptor (LPAR1) could drive ENS alterations leading to CIPO, a pathway involved in sensitization of peripheral pain neurocircuits. Here, we used a combination of genetic, immunohistochemical, functional and *in vivo* pharmacological approaches to show that enteric glial-specific LPAR1 expression is conserved across species and dramatically reduced in CIPO. Blocking LPAR1 activation in mice attenuates GI motility and leads to obstruction, recapitulating symptoms of CIPO. Thus, our study provides novel insight into the role of enteric glial LPAR1 as a regulator of GI motility and a potential therapeutic target in the treatment of obstructive bowel diseases.

INTRODUCTION

Chronic intestinal pseudo-obstruction (CIPO) is a severe form of functional gut failure characterized by recurrent episodes of intestinal sub-occlusion that occur in the absence of mechanical blockade[1]. Systemic diseases of the neuro-musculature controlling gut motility account for secondary forms of CIPO, though most cases are idiopathic. In these patients, histological examination typically reveals non-specific neuropathic[2], myopathic or mesenchymopathic[3,4] alterations in the gut wall. Clinically, CIPO is associated with substantial morbidity and poor quality of life owing to a lack of effective treatment options[5], which range from the use of prokinetic agents[6,7] to gut transplantation[8] in dire cases. These diagnostic and therapeutic shortcomings highlight major gaps in the management of CIPO that directly result from a poor understanding of the pathophysiological basis of this disease.

The motility of the GI tract is controlled by the enteric nervous system (ENS), an autonomous division of the peripheral nervous system embedded within the gut wall[9]. Enteric neurons of the ENS coordinate the recruitment of ascending-excitatory and descending-inhibitory motor pathways[10]. Thus, loss of enteric neurons heralds dire consequences for gut motility and is a defining histological feature of neuropathic forms of CIPO[2]. Although immune cell infiltrates can be observed in the ENS of some of these patients[11], it is important to note that neuronal degeneration can still occur without overt signs of tissue inflammation. This suggests that some broader mechanism that is common to both pathways may ultimately drive the pathogenesis of CIPO.

Enteric neurons receive input from surrounding populations of enteric glia, which sense neurotransmitters[12,13] and secrete gliotransmitters[14,15] to regulate neuronal function. Enteric glia contribute to neuronal death through purinergic mechanisms during acute colitis[16] but also express major histocompatibility complex type 2 (MHCII)[17,18], highlighting a potential role for these cells as a bridge between acute and chronic inflammatory processes within the ENS. Biolipids

contribute to acute inflammation by activating the type I lysophosphatidic acid receptors (LPAR1)[19,20], a receptor that is highly expressed in cultured enteric glia[21,22] but that has unknown roles in the intact ENS. Many functional GI disorders (FGIDs) are triggered by infectious inflammatory insults[23] that promote long-term neuroplastic changes favoring ENS hyperexcitability[24]. Satellite glia[25] and Schwann cells[26] orchestrate strikingly similar events during the onset of neuropathic pain, which requires LPAR1 to initiate sensitization of peripheral pain pathways[27]. Thus, it is plausible that enteric glia employ similar LPAR1-dependent mechanisms to consolidate acute inflammatory stimuli into long-term ENS changes leading to CIPO.

We hypothesized that enteric glial LPAR1 is important in the control of gut motility and tested this by assessing LPAR1 expression in the human ENS. Here, we report that human enteric glia express LPAR1 and that its expression is reduced in CIPO, a disease defined by critical failure in gut motility. We further demonstrate that glial LPAR1 expression is highly conserved in the mouse ENS and that pharmacological manipulation of this receptor drastically affects gut motility *in vivo*. Thus, our study serves to model functional GI obstruction in the mouse and unveils novel mechanistic insights that could inform the treatment of obstructive diseases of the GI tract.

MATERIALS AND METHODS

Human sample collection

Full thickness colon (n=6) or ileum (n=5) (one patient had both ileum and colon) tissue was obtained from adults (n=10; 8 females; age range: 22-73 years) with a diagnosis of CIPO established via clinical assessment, radiological tests (i.e., mainly abdominal CT scan) and small bowel manometry at St. Orsola-Malpighi Hospital from 2014 to 2019 (see below section: *Clinical features of patients* for further details).

Comparable tissue samples (n=4 ileum; n=4 colon), obtained from n=4 patients (2 females; age range: 48-73 years) (asymptomatic for previous GI symptoms) and referred to surgery for non-complicated GI tumors, were used as controls.

Tissue specimens from each patient and control were immediately fixed in cold neutral 4% formaldehyde (Kaltek, Padua, Italy), paraffin- embedded, cut into 5-µm-thick sections, and mounted serially on poly-L-lysine-coated slides (Thermo Fisher Scientific, Braunschweig, Germany).

All the experimental procedures were approved by the Ethics Committee of St. Orsola-Malpighi Hospital for handling and analysis of tissue samples from patients with severe gut dysmotility (EM/146/2014/O).

Clinical features of patients

Patients with CIPO secondary to infectious, neurological, metabolic, systemic autoimmune, and paraneoplastic conditions as well as cases secondary to known genetic abnormalities were excluded. Thus, all patients included in this study were idiopathic in origin. Anorexia nervosa was also specifically excluded in all patients with malnutrition by a psychiatric examination.

The clinical diagnosis of CIPO was established on the basis of a chronic (>3 months), severe symptom complex mimicking mechanical small bowel obstruction, and (at least on one occasion) radiological evidence of air-fluid levels or dilated small bowel loops.

Prior to laparoscopic surgery for tissue collection, patients completed a clinical questionnaire reporting the following data, symptoms and signs: age, sex, BMI, symptoms onset, number of sub-obstructive episodes that occurred prior to surgery, abdominal distension, abdominal pain, nausea, vomiting, fullness, early satiety, constipation, diarrhea, esophageal involvement (ie, motor abnormalities assessed by standard esophageal manometry), gastroparesis (established by scintigraphic gastric emptying), small intestine bacterial overgrowth (SIBO) (determined by glucose/lactulose breath test), urinary symptoms, and small bowel dilation (detectable at abdominal CT scan or MRI). Medications used by each subject were also recorded. These features were summarized in Table 1.

In 4 patients with CIPO, the ileum was the main site of the disease with at least 3/4 patients reporting symptoms of nausea, vomiting, abdominal fullness, early satiety, diarrhea, or constipation. Of these ileum biopsies, only one derived from a male patient while the remaining three were from female patients. In a separate group of 6 patients with CIPO, the disease was localized to the colon. All patients with colonic CIPO reported experiencing constipation while diarrhea was only reported by one patient. In addition, 4 patients with colonic CIPO reported experiencing mild-to-moderate grade abdominal pain while 1 patient reported experiencing severe abdominal pain. Importantly, the body mass index (BMI) of patients with CIPO affecting the ileum (16.28 ± 1.18, $n=4$) was lower than that of patients where CIPO affected the colon (20.40 ± 0.39, $n=6$; $p=0.033$) suggesting differences in long-term nutritional status between the two groups.

Animal Use

All experiments were conducted according to guidelines established by the National Institutes of Health (NIH) Guide for the Care and Use of Animals. All protocols were subject to rigorous institutional oversight administered by the Michigan State University Institutional Animal Care and Use Committee (IACUC).

Deparaffinization and antigen retrieval

Human tissues were deparaffinized and subjected to heat-induced epitope retrieval using a modified version of techniques described elsewhere[49]. Briefly, deparaffinization involved fully submerging slides in two changes of xylene followed by one change of 1:1 xylene:ethanol solution. At this stage, slides were submerged for 10min during each submersion step. Tissues were then hydrated by submerging slides in two changes of 100% ethanol for 3 minutes, 95% ethanol for 1 minute, 90% ethanol for 1 minute and 80% ethanol for 1 minute before being gently rinsed in distilled water. Antigen retrieval was performed by submerging slides for 40 mins in a dish containing sodium citrate buffer solution (10mM sodium citrate, 0.05% Tween-20, pH 6.0), which was preheated on a hotplate to a constant temperature of 95-100^{o}C. Samples were then removed and allowed to cool to room temperature before conducting immunohistochemical studies.

Animal models

Transgenic *Wnt1^{Cre};GCaMP5g-tdT* mice generated on a C57/Bl6 background were used to study calcium (Ca^{2+}) responses in the ENS. As described previously, Cre recombinase in Wnt1+ cells of the neural crest drives the expression of the fluorescent Ca^{2+} sensor, GCamp5g, in both neurons and glia while the tdTomato reporter is only expressed in glia. This allows Ca^{2+}

responses to be readily distinguished between these two cell populations. For all experiments, male and female animals were used between 10 and 14 wks of age and were housed in a temperature-regulated facility where they were exposed to a 12 hr light:dark cycle and provided *ad libitum* access to standard chow and water. Mouse genotypes were verified commercially by Transnetyx Inc. (Cordova, TN). For immunohistochemistry and motility-related experiments, WT C57/Bl6 mice were used.

Mouse colonic tissue isolation and processing

Mice were euthanized by cervical dislocation followed by decapitation in accordance with guidelines established by the Michigan State University institutional ethics policy. Fresh colon tissue was collected in cold Dulbecco's Modified Eagle Medium (DMEM) before being further processed for use in Ca^{2+} imaging, immunohistochemistry, or colonic migrating motor complex (CMMC) studies. For Ca^{2+} imaging studies only, the DMEM solution was supplemented with 3 µM nicardipine to paralyze the muscular apparatus and enable recording of ENS responses.

Tissue dissection and fixation

Isolated colonic tissue was longitudinally slit open along the mesenteric border and pinned out using inset pins in a 35mm dish coated with Sylgard™. The tissue was then fixed with Zamboni's fixative overnight at 4°C for subsequent immunohistochemical studies. For Ca^{2+} imaging studies, the epithelium was removed and whole-mount circular muscle-myenteric plexus (CMMP) preparations were generated by flipping the tissue and removing the longitudinal muscle layer by microdissection[50]. In the resultant preparation, the myenteric plexus maintains its structural integrity as the thick circular muscle layer is not damaged.

Immunohistochemistry

Following overnight fixation in Zamboni's buffer, mouse colonic tissue was further micro-dissected according to techniques described previously. In brief, the epithelium was removed along with the circular smooth muscle layer thereby generating a longitudinal muscle-myenteric plexus (LMMP) preparation. At this point, a 1x1 cm segment of tissue was then cut out and washed three times in phosphate buffered saline (PBS) containing 0.1% Triton X-100. For both human and fixed mouse tissues, samples were incubated for 40 mins with a blocking solution containing 4% normal goat serum, 0.4% Triton X-100 and 1% bovine serum albumin dissolved in PBS. Tissues were then incubated overnight at 4^{o}C with the following antibodies: chicken anti-GFAP (1:1000; Cat#ab4674, Abcam, Cambridge, UK), rabbit anti-LPAR1 (1:250; Cat#ab23698, Abcam, Cambridge, UK)[51], guinea-pig anti-PGP9.5 (1:500; Cat#GP14104, Neuromics, Edina, MN), biotinylated anti-HuC/D (1:200; Cat#A21272, Invitrogen, Carlsbad, CA) or rabbit anti-doublecortin (1:200; Cat#ab18723, Abcam, Cambridge, UK). On the day of imaging, samples were incubated with the following fluorescently-conjugated secondary antibodies for 2 h: Alexa 488 donkey anti-chicken (Cat#703-545-155, Jackson, Westgrove, PA), Alexa 488 donkey anti-rabbit (Cat#711-545-152; Jackson, Westgrove, PA), Alexa 594 donkey anti-rabbit (Cat#711-585-152; Jackson, Westgrove, PA), Alexa 594 donkey anti-guinea pig (Cat# 706-585-148; Jackson, Westgrove, PA), Alexa 594 goat anti-chicken (Cat#103-585-155; Jackson, Westgrove, PA), streptavidin-Alexa 594 (Cat#016-580-084; Jackson, Westgrove, PA), Alexa 647 donkey anti-rabbit (Cat#711-605-152; Jackson, Westgrove, PA) and/or streptavidin Dylight Alexa 405 (Cat# 016-470-084; Jackson, Westgrove, PA). All secondary antibodies were used at a dilution of 1:400. Prior to imaging, tissues were mounted in 4',6-diamidino-2-phenylindole (DAPI) fluoromount G (Cat#0100-20; Southern Biotech, Birmingham, AL).

The specificity of rabbit anti-LPAR1 antibody has been confirmed elsewhere[51] but was further demonstrated here by conducting a pre-adsorption assay between the primary antibody

and its immunizing peptide sequence (Cat#10006984, Cayman, Ann Arbor, MI) according to manufacturer instructions. Briefly, this entailed incubating the anti-LPAR1 antibody with the immunizing peptide (GGYLPFRDPNSEENSNDIAL) in a 1:1 ratio (v/v) for 1 h at room temperature with occasional mixing. The antibody-peptide cocktail was then diluted to the usual 1:250 antibody dilution and the remaining protocol proceeded as previously described.

Ca^{2+}-imaging studies

Ca2+ imaging studies were conducted in CMMP preparations[50], which were perfused with Kreb's buffer (37°C) at a constant rate (2–3 mL/min). The perfusate was removed using a Peri-Star Pro peristaltic pump (World Precision Instruments Inc.). Unless otherwise specified, all imaging studies were conducted on on an upright Olympus BX51WI fixed-stage microscope (Center Valley, PA). Ganglia were viewed at 20x through a wide-field water-immersion objective lens (Olympus XLUMPLFLN20xW, 1.0 numerical aperture). The fluorescent tdTomato reporter was highly expressed in resident glial cells. Illumination for fluorescence imaging was provided by a DG4 Xenon light source (Sutter Instrument, Novato, CA).

GCamp5g photoexcitation was filtered through a 485/20-nm band-pass filter, and emitted light was filtered through a 515-nm long-pass filter. tdT signal was excited by light filtered through a 535/20-nm band-pass filter and reflected tdT signals were filtered through a 610/75-nm band-pass emission filter[16]. Imaging data were acquired at a frame rate of 1 frame per second using a Neo sCMOS camera (Andor, South Windsor, CT). In some cases, confocal video fluorimetry was performed using a confocal spinning-disk microscope (Nikon A1R HD25; Nikon, Tokyo, Japan), providing higher spatiotemporal resolution of Ca^{2+} responses, which were imaged through a 20x Nikon objective lens (CFI Apochromat LWD Lambda20xC WI, 0.95 numerical aperture). Confocal images were captured using a Nikon DS-Ri2 digital camera (Nikon, Tokyo, Japan) and recorded using NIS-Elements C software (Nikon). For epifluorescence and confocal fluorescence imaging

studies, all data were saved on a personal computer running Windows 10 (Microsoft Corporation, WA) and MetaMorph (Molecular Devices, Sunnyvale, CA) and exported as *.tiff* stacks for analysis with Fiji software (NIH)[52].

Electrical field stimulation

Electrical field stimulation (EFS) was used to activate neurons using electricity. This was accomplished by applying depolarizing pulses to the tissue using two platinum wires using a GRASS S9E Electrical Stimulator (Quincy, MA) with the parameters: +70V, 10Hz and 0.1 ms duration.

Local drug application

ADP or 18:1 LPA were applied locally to the ganglion surface to provoke agonist responses. To do this, glass capillary applicators were fabricated with a pipette puller (P-87 Flaming-Brown Micropipette Puller, Sutter Instruments Corporation, Novato, CA, USA) and back-filled with drug, dissolved in Kreb's buffer. Drugs were then applied using very gentle positive pressure that was applied with a 1-mL syringe connected to a pipette holder. This approach delivered picoliter volumes of drug and only affected the ganglion within the field of view. We confirmed that the shear fluid stress associated with drug application did not activate neurons or glia under these conditions (not shown).

Solutions and chemicals

DMEM was obtained from Life Technologies (Carlsbad, CA). Unless otherwise noted, all reagents were obtained from Sigma (St. Louis, MO). The composition of Kreb's solution used during imaging experiments was as follows: 121mM Na^+, 4.9mM K^+, 25mM $NaCO_3^-$, 1.2mM Mg^{2+}, 2.5mM $CaCl_2$, 1.2mM $NaHPO_3^-$ 11mM D-glucose, and 1mM pyruvate. Kreb's solution was titrated

to pH 7.4 with NaOH. 1-oleoyl-2-hydroxy-sn-glycero-3-phosphate (18:1 LPA; Avanti Polar Lipids, Inc., Alabaster, AL) was dissolved in 50% ethanol (v/v) according to manufacturer instructions, and care was taken to avoid surpassing its critical micelle concentration[53]. AM966 (Cayman Chemical Company, Ann Arbor, MI; Cat#22048) was dissolved in DMSO to a final stock concentration of 50mM.

Data analysis and statistics

All analyses were conducted in Fiji[52]. Briefly, background-subtracted videos were stabilized using the StackReg plugin (http://bigwww.epfl.ch/thevenaz/stackreg/). The tdT channel imaged at each experiment's outset served to identity the location of glial cells and was used to generate corresponding regions of interest (ROIs), which were converted into binary masks that guided analysis. To do this, Fiji's band-pass filter function was used to filter the tdT image and the resultant image was auto-thresholded. Neuronal ROIs were identified by exclusion of glial ROIs, and manually selected based on morphological features. All glial and neuronal ROIs were saved. Ca^{2+} responses were measured using these ROIs and exported to Microsoft Excel (Microsoft Corporation, WA). Most Ca^{2+} responses are reported as fold-change in mean cellular fluorescence intensity relative to baseline florescence intensity ($\Delta F/F_o$) within a given cell. Unless otherwise noted, values are presented as means ± standard error of the mean (SEM). Unless otherwise stated, sample size denotes the number of cells responding under those experimental conditions with the number of mice utilized is included where appropriate. For all experiments, approximately 30–40 neurons and a comparable number of glia were studied per ganglion, with at least 1–2 ganglia utilized per mouse under each recording condition. Grubb's test was used to compute statistical outliers, which were excluded from the final analysis only if the confidence threshold of $\alpha=0.05$ was surpassed. In most instances, statistical testing involved unpaired two-tailed Student's *t*-tests comparing $\Delta F/F_o$ values between different conditions. Welch's correction

was applied as needed when data variability was unequal between the groups being compared. Final figures were produced with GraphPad Prism 5 (GraphPad Software Inc., La Jolla, CA), and custom illustrations were designed in BioRender software (https://biorender.com/).

AM966 injections and carmine transit studies

Age-matched males and females were randomly assigned to one of 4 possible treatment groups: low-dose AM966 (22 mg/kg), medium-dose AM966 (33 mg/kg), high-dose AM966 (43 mg/kg) or vehicle[38]. WT C57/Bl6 mice were then injected intraperitoneally with the LPAR1 antagonist, AM966 (Cat#22048; Cayman, Ann Arbor, MI) q24 for 3 days, or vehicle. The vehicle control consisted of DMSO dissolved in sunflower oil which at most delivered a DMSO dosage far below the 10 ml/kg upper limit reported for mice[54]. Mouse weights were measured longitudinally over the duration of the experiment, beginning on the first day of injections. Drug dosages were selected based on previous *in vivo* reports of the systemic effects and pharmacokinetic properties of AM966 in mice as well as *in vitro* studies on the binding affinity of AM966 at the LPA1 receptor.

After 3-days of continuous exposure to AM966, the *in vivo* effect of sustained, sub-chronic LPAR1 blockade was assessed by determining the whole-bowel transit of Carmine red dye. As described elsewhere[14,55], mice were administered 200 µL of 6% Carmine red solution in water supplemented with 0.5% methylcellulose by oral gavage. After 1 h, mice were euthanized, and the entire GI tract was carefully but rapidly removed and laid out at neutral length on an all-white surface. The Carmine red wavefront was then grossly visualized within the gut lumen as a discrete, bright-red bolus that was immediately trailed by a dye-free bowel segment, and its distance relative to the gastric fundus was measured. Additional parameters that were noted included total bowel length, splenic weight, location of the ileocecal pouch and the presence of strictures or serosal hemorrhages. The colonic regions of these tissue were then collected in drug-

free DMEM for subsequent fixation and further immunohistochemical characterization of ENS architecture.

Colonic migrating motor complexes (CMMCs)

Colonic motility was assessed in response to LPA1R receptor activation ex vivo. Briefly, whole intact colon was rapidly collected in drug-free DMEM/F-12, maintained at 37^{o}C. The oral and aboral ends of the colon were then mounted in place on a stainless-steel holding rod after lumen contents were flushed. Two force transducers (Grass Instruments), connected via hooks, were gently inserted into the gut wall approximately 2cm apart. The baseline tension was calibrated to 0.5g and spontaneous CMMC production was monitored for a period of 20min before experiments were conducted. The last 5min of this acclimatization period was used as a baseline for analysis, which was conducted in LabChart 8 (ADInstruments, Colorado Springs, CO). Agonists was added cumulatively to the bath and the resultant changes in CMMC amplitude was measured in relation to baseline.

RESULTS

LPAR1 serves pathogenic roles in central and peripheral neurocircuits but its function in the ENS is unclear. Here, we examined the function of type I lysophosphatidic acid receptor (LPAR1) in enteric glia and showed that LPAR1 expression is conserved in the intact ENS, where it drives calcium (Ca^{2+}) responses in enteric glia. We then demonstrate clinically relevant reductions in LPAR1 in chronic intestinal pseudo-obstruction (CIPO) and corroborated this *in vivo* by selectively blocking LPAR1 to provoke obstruction. These data provide insights into the pathophysiological mechanisms of CIPO and identify a novel therapeutic target in the treatment of human GI obstructions.

LPAR1 expression is conserved in human and murine enteric glia

We began by assessing potential signaling mechanisms contributing to ENS dysfunction in CIPO by screening genetic expression of G-protein coupled receptors (GPCR) in human and murine myenteric glia. Using two publicly available databases of the ENS translatome[28,29] (**Fig 3.1a**), we found that enteric glia robustly express *LPAR1* in nearly all enteric glia of the human large intestine (**Fig 3.1b**). In the mouse, expression of *Lpar1* was also restricted to enteric glia in small and large intestines (**Fig 3.1c**). While cultured guinea pig enteric glia express LPAR1[21,22], this finding had not been confirmed in the intact ENS until now. Importantly, LPAR1 gene expression was null in nearly all enteric neurons in both species indicating that its ENS roles are likely glial-mediated (**Appendix Figure 3.6**). It should be noted that of the six LPAR subtypes[30], the remaining $LPAR_{2\text{-}5}$ subtypes were undetectable in both human and murine enteric glia (not shown).

These findings were consistent with results from another recent study characterizing the molecular architecture of the mouse nervous system[28]. Here, glial *Lpar1* expression exceeded the levels of glial fibrillary acidic protein (*Gfap*), *Sox10* and the type 1 P2 purinergic receptor

(*P2ry1;* **Fig 3.1d**), which was surprising since these are canonical glial markers used in the identification of enteric glia[31]. Lastly, our own prior investigation of the ENS colonic translatome[32] also demonstrated high *Lpar1* expression in enteric glia (**Fig 3.1e**). This finding was complemented by robust expression of the gene for lysophosphatidic acid-generating enzyme[30], ectonucleotide pyrophosphatase type 2 (*Enpp2*). *Lpar1* and *Enpp2* gene expression were dramatically reduced in the mouse during the acute phase of dinitrobenzenesulfonic acid (DNBS)-induced colitis, supporting a possible role for altered glial LPAR1 signaling in the pathogenesis of dysmotility following an inflammatory insult.

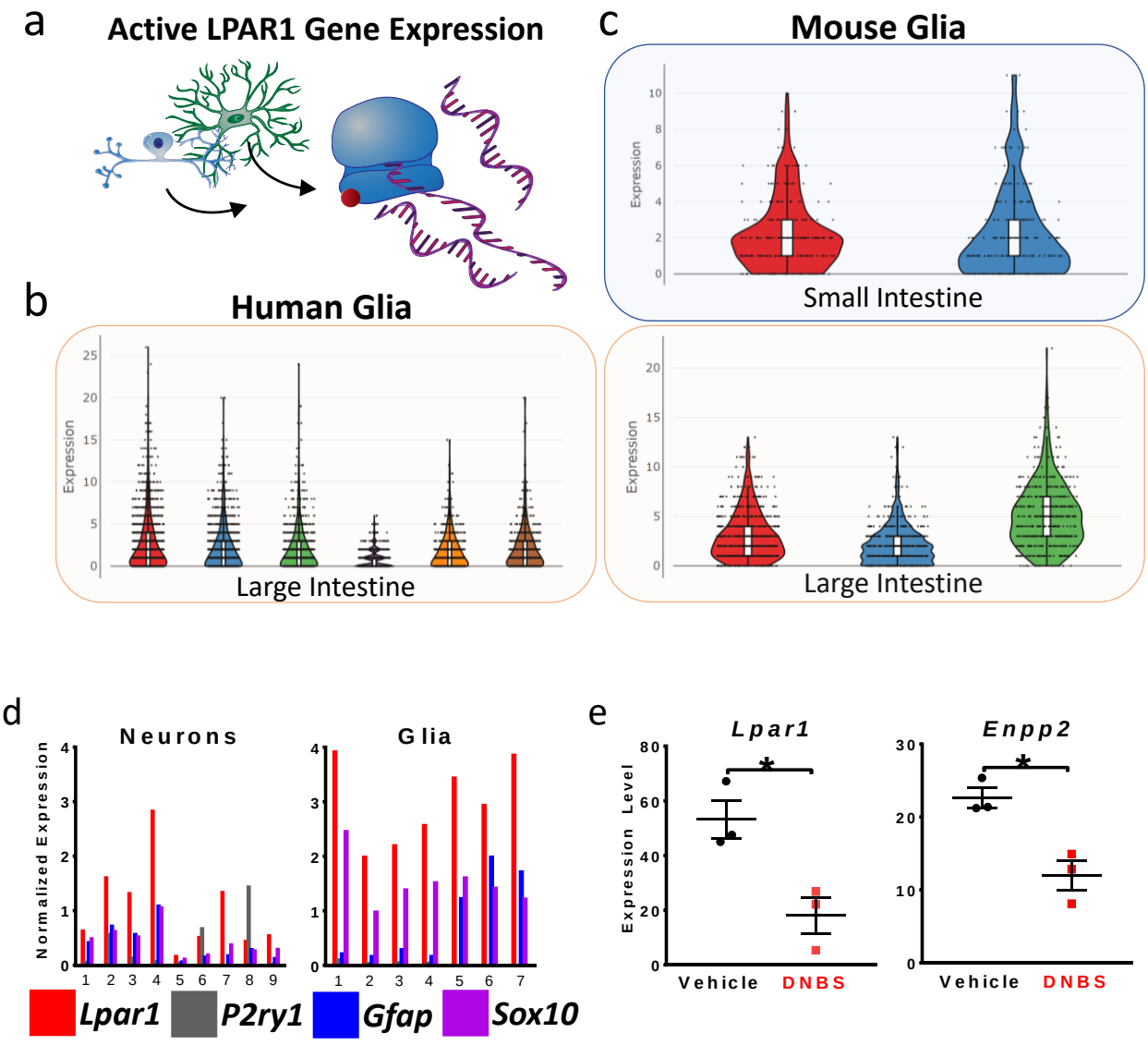

Figure 3.1. LPAR1 expression is highly conserved in murine enteric glia. a, RNAsequencing conducted by our group and others provide cell-specific insight into the expression of LPAR1 gene levels in enteric glia. b, c, Within the human large intestines (b), *LPAR1* is highly expressed in enteric glia. In the mouse small and large intestine (c), *Lpar1* expression is also high in all enteric glial sub-types. d, *Left panel*: *Lpar1* is expressed in some enteric neuronal subtypes, but typically at much lower levels compared to glia. These neurons also demonstrate expression of glial markers. *Right panel*: *Lpar1* expression exceeds the levels of canonical markers used to identify enteric glia (*P2ry1*, *Gfap*, *Sox10*). e, As measured by ribotag RNA sequencing, acute DNBS-mediated colitis reduces glial expression of both *Lpar1* (*left panel*) and the ecto-enzyme, *Enpp2* (*right panel*), which catalyzes production of lysophospholipids acting at LPAR1.

LPAR1 activation provokes glial Ca^{2+} responses

Our findings show conserved genetic expression of *Lpar1* in enteric glia but not neurons, suggesting that it serves an indispensable role in the regulation of ENS physiology. Thus, we proceeded to directly confirm protein-level LPAR1 expression within the intact murine myenteric plexus by immunohistochemistry (**Fig 3.2a** and **Appendix Figure 3.7**) and found high levels of LPAR1 that was restricted to GFAP-positive enteric glia and absent from neurons, which express the neuronal marker HuC/D. Functionally, LPAR1 evokes Ca^{2+} responses in cultured guinea-pig enteric glia[21,22] but the physiological applicability of those *in vitro* findings remain unclear. Thus, we tested the effect of LPAR1 activation in the intact myenteric plexus of transgenic mice expressing the fluorescent Ca^{2+} indicator, GCamp5g, in enteric neurons and glia. In this model, the fluorescent tdTomato reporter is expressed in enteric glia but undetectable in neurons[16,33,34] allowing us to distinguish responses in each population (**Fig 3.2b**).

We initially stimulated the intact myenteric plexus with electrical field stimulation (EFS) to broadly activate neurons. Because enteric neurons are electrically excitable (**Figs 3.2c-e**), applying +70V of depolarization (at a frequency of 10Hz) provoked a Ca^{2+} response measuring $\Delta F/F_o$=1.67±0.03 (n=1064 neurons) relative to baseline (**Fig 3.2n**). These experimental parameters mobilize physiological levels of intracellular Ca^{2+} in neurons, which releases neurotransmitters that activate nearby enteric glia. Thus, EFS-mediated neuronal responses were accompanied by a glial response measuring $\Delta F/F_o$=0.92±0.03 (n=886 glia) and exhibiting similar activation kinetics. Under these conditions, neurons recruited approximately 82.19±3.64% of neighboring glia, highlighting the profound degree to which neuronal responses can influence glial activation states.

To establish a framework for interpreting the effects of LPAR1 activation in the intact ENS, we characterized glial Ca^{2+} responses to focally applied adenosine diphosphate (ADP; **Fig 3.2f**). ADP is a potent agonist of the P2Y1 purinergic receptor (P2Y1R), which is highly expressed on

enteric glia[16]. Thus, ADP acts to specifically activate glia-to-neuron signaling, which in turn modulates neuronal activity. ADP evoked glial Ca^{2+} responses measuring $\Delta F/F_o$=1.65±0.099 (n=239 glia; **Figs 3.2g-l,n**). The fact that Ca^{2+} responses propagated along the network of glial cells confirms the predominantly glial-specific effect of this agonist. Lastly, ADP-mediated glial responses were accompanied by a delayed phase of neuronal recruitment that was offset by ~1-2s, measured $\Delta F/F_o$=0.555±0.05 (n=239 neurons) and activated 38.23±7.65% of neurons overall.

After characterizing typical neuronal and glial response patterns to EFS and ADP, we studied the direct effect of 18:1 LPA on the intact ENS (**Figs 3.2j-m**). 18:1 LPA was selected as it is the most highly produced and longest-lived of the various LPA species generated during inflammation[35], making it an ideal candidate for studying the role of glial LPAR1 in the pathogenesis of CIPO. Application of 1μM LPA elicited Ca^{2+} responses that were ~67% greater in magnitude in glia (n=333 cells) compared to neurons (n=312 cells, p<0.0001; **Fig 3.2o**). By comparison, 10μM LPA evoked Ca^{2+} responses in glia measuring $\Delta F/F_o$=1.085±0.064 (n=350 cells), which were greater than the effect in neurons ($\Delta F/F_o$=0.676±0.056, n=311 cells; p<0.0001). Despite the apparently greater glial Ca^{2+} responses evoked at 10μM LPA, however, there was no difference in the proportion of neurons recruited at this concentration (36.09±9.58% of 311 cells from 9 mice) compared to 1μM LPA (26.06±6.22% of 312 cells from 9 mice; p=0.393). In terms of overall glial specificity, LPA-mediated Ca^{2+} responses were confined to the glial network (**Fig 3.2m**). Together, these findings demonstrate that LPAR1 drives glial Ca^{2+} responses *in situ* and may recruit enteric neurons.

Because of the well-established female-predilection for CIPO and the fact that most of our human biopsy specimens derived from female patients, we stratified LPA-mediated glial Ca^{2+} responses by sex (**Fig 3.2p**) and found that male enteric glia exhibited more robust Ca^{2+} responses following application of 1μM LPA ($\Delta F/F_o$=1.27±0.103, n=180 cells) compared to females ($\Delta F/F_o$=0.861±0.103, n=153 cells; p=0.0053). While this glial sex-effect was not observed at higher concentrations of LPA, neuronal responses to 10μM LPA were also greater in males

($\Delta F/F_o$=0.962±0.089, n=170 cells) compared to females ($\Delta F/F_o$=0.331±0.043, n=141 cells; $p<0.0001$). Despite the lack of consistency between the LPA doses at which sex differences emerge in neurons and glia, these data suggest some degree of sex-specificity with regards to the effects of LPAR1 in the ENS.

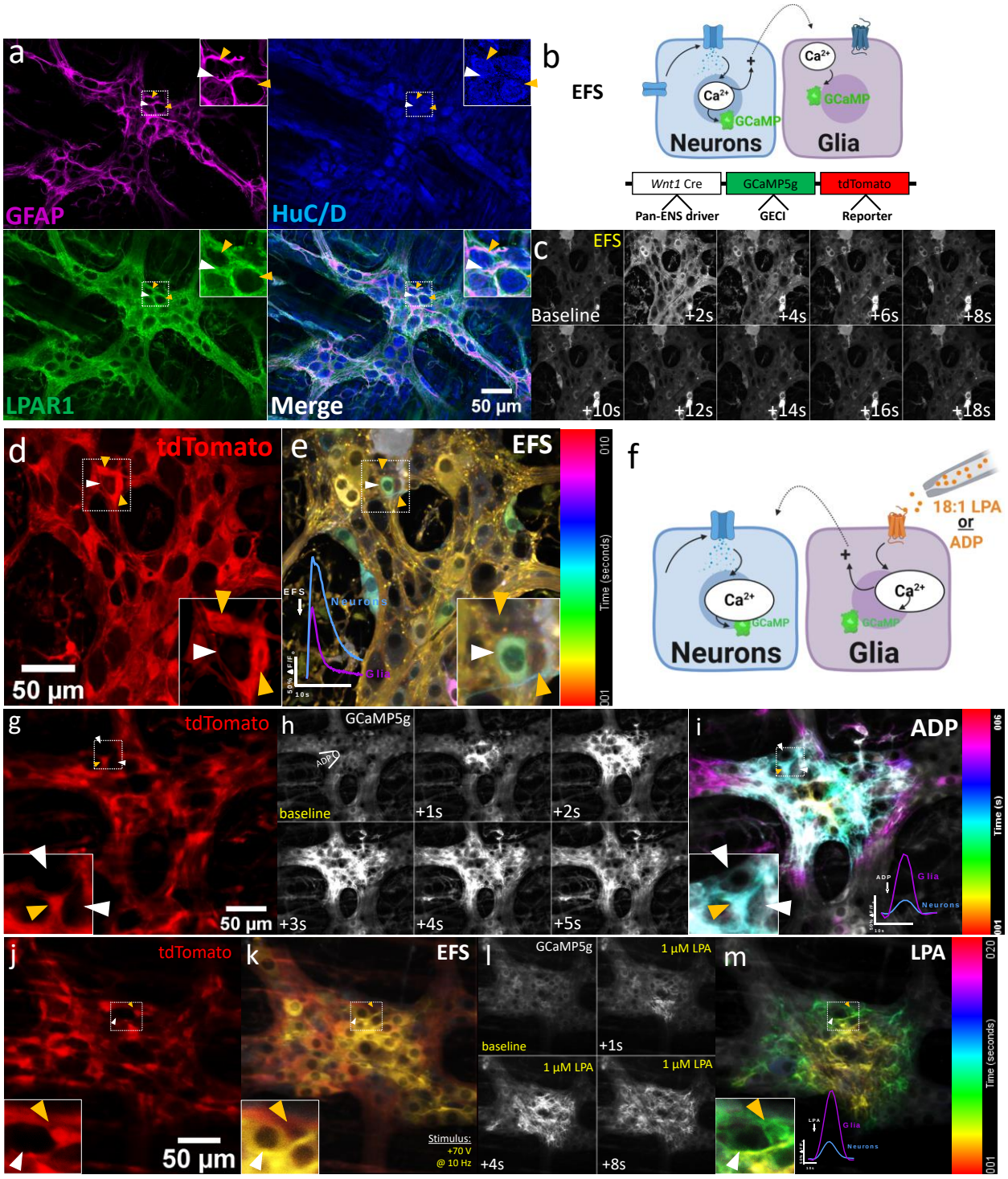

Figure 3.2. LPAR1 activation drives Ca^{2+} responses in murine enteric glia. a, Immunohistochemical staining of fixed murine myenteric plexus reveals high levels of LPAR1 protein expression (green) that dramatically overlaps with GFAP (magenta). Both GFAP and LPAR1 expression are nearly entirely absent from adjacent enteric neurons, which express high levels of the neuronal marker HuC/D (blue). b, Experimental paradigm used to drive broad neuronal responses in the myenteric plexus. Application of electrical field stimulation (EFS) stimulates neuronal Ca^{2+} responses and triggers downstream glial activation. c, Confocal

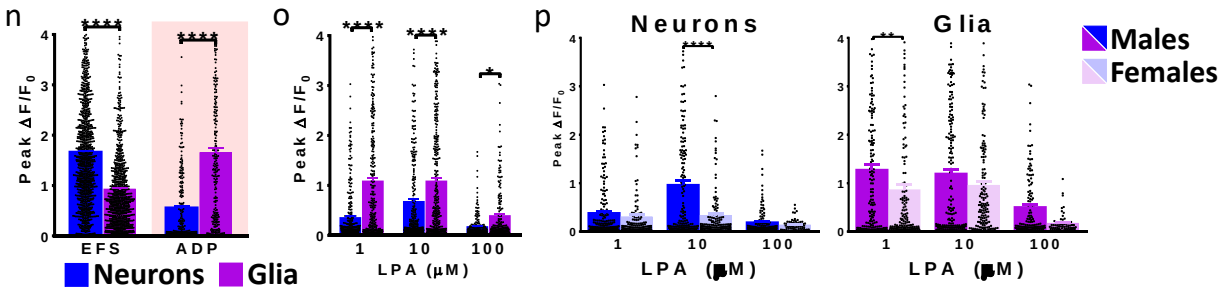

Figure 3.2 (cont'd)

fluorescence montage depicting Ca^{2+} responses provoked by EFS. d, tdTomato reporter is highly expressed in enteric glia (orange arrowhead) and absent from enteric neurons (white arrowhead). e, Color-coded temporal projection depicting robust Ca^{2+} responses following EFS. Much of the response remains localized to the neuronal population, although there is some glial activation (bottom left inset). f, Ganglia were treated with 18:1 LPA or ADP, which is a P2Y1R agonist that activates enteric glia. g, h, i, Focal application of ADP stimulates Ca^{2+} responses (i, orange arrowhead) that overlap with tdTomato expression in enteric glia (g). j-m, Glia expressing high levels of tdTomato (j) do not exhibit robust Ca^{2+} responses following EFS (k) but are robustly activated by focal application of 18:1 LPA (l). The LPA-mediated Ca^{2+} response remains confined to the glial network and is largely absent from neighboring populations of neurons (white arrowheads). n, Summary of EFS and ADP-mediated Ca^{2+} responses in enteric neurons and glia. o, Focal application of LPA provokes robust Ca^{2+} responses that are more dramatic in enteric glia compared to enteric neurons. p, LPA provokes greater Ca^{2+} responses in male glia but this effect is only observed at 1μM drug concentration. Similarly, only 10μM LPA provokes greater $Ca2^{+}$ responses in male neurons.

Glial LPAR1 expression is reduced in human ileum and colon during CIPO

Our findings show that LPAR1 drives Ca^{2+} responses within the intact ENS and that its genetic expression is restricted to enteric glia and conserved across different species. While this suggests that glial LPAR1 plays an indispensable role in GI physiology, its exact relevance to GI motility remains unclear. We therefore proceeded to investigate the putative role of glial LPAR1 in the pathogenesis of CIPO.

Full thickness sections of ileum and colon from healthy controls and patients with CIPO (**Fig 3.3a,b**) were co-labeled with antibodies against LPAR1 and PGP9.5 to identify enteric neurons. LPAR1 immunolabeling was robust throughout the myenteric plexus of the human ileum (**Fig 3.3c**) and colon (**Fig 3.3e**) in samples from healthy controls (n=4). In agreement with labeling in mice, LPAR1 staining was undetectable in neurons and intense in glia surrounding PGP9.5+ neuronal cell bodies, confirming restricted expression of LPAR1 protein to enteric glia in humans.

Samples from individuals with CIPO exhibited significantly less LPAR1 and PGP9.5 labeling in the ileum (**Fig 3.3c,d**) and colon (**Fig 3.3e,f**) myenteric plexus. Cross-sectional LPAR1 staining in the CIPO myenteric plexus was ~41% lower in the ileum (n=4, $p<0.0001$; **Fig 3.3d**) and ~27% lower in the colon (n=6, $p=0.004$; **Fig 3.3f**). Measurements of the ENS cross-sectional architecture did not reveal differences in ganglion size or cellularity between CIPO and healthy tissues (**Appendix Figure 3.8**). Overall, these data confirm that LPAR1 is highly expressed by enteric glia in humans and that glial LPAR1 signaling may be altered in patients with CIPO.

a

Patient Characteristics								
	Sample size, n (male:female)		BMI (mean ±SEM)		Age at (yrs ± SEM): Symptom onset		Tissue biopsy	
	Ileum	Colon	Ileum	Colon	Ileum	Colon	Ileum	Colon
Control	4	4	n.d.	n.d.			n.d.	n.d.
CIPO	4, (1M:3F)	6, (1M:5F)	16.28 ± 1.18	20.40 ± 0.39	36.75 ± 10.40	33.20 ± 3.63	51.50 ± 21.5	36.60 ± 3.27

b

CIPO Clinical Features (# reporting/total)								
	Pain							
	Mild-Moderate	Severe	Nausea	Vomiting	Fullness	Early Satiety	Constipation	Diarrhea
Colon	4/6	1/6	3/6	2/6	3/6	2/6	6/6	1/6
Ileum	n.d.	n.d.	4/4	3/4	3/4	3/4	3/4	3/4

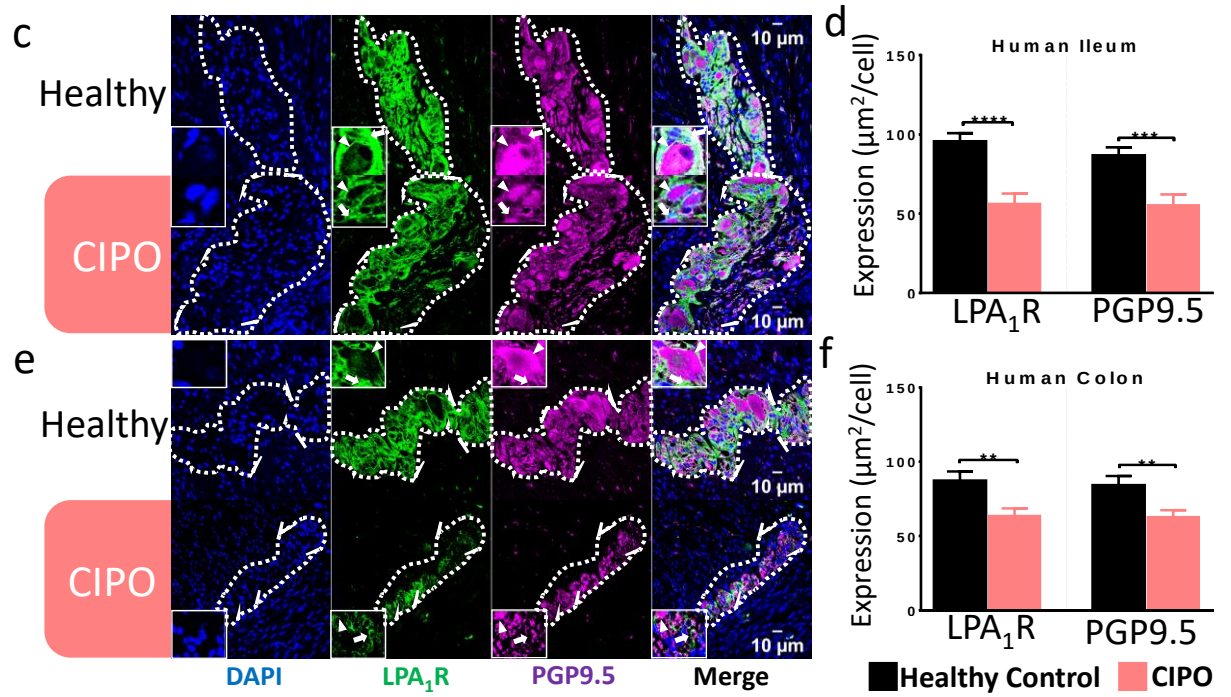

Figure 3.3. Glial expression of human LPAR1 is reduced in CIPO. a, b, Summary of general patient characteristics (a) and clinical severity of CIPO (b) in those CIPO subjects from whom biopsy specimens were obtained. c, *Top row*: In healthy human ileum, LPAR1 (green channel) is robustly and uniformly expressed in enteric glial cells (white arrow) throughout the myenteric ganglion. By comparison, LPAR1 expression is nearly entirely absent from adjacent enteric neurons (white arrowhead), which express high levels of the neuronal marker PGP9.5 (magenta channel). *Bottom row*: In CIPO, LPAR1 and PGP9.5 expression is dramatically reduced in glia and neurons, respectively. d, Semi-quantification of cross-sectional protein expression reveals drastic reductions in LPAR1 and PGP9.5 level in CIPO relative to healthy controls. e, *Top row*: In healthy human colon, LPAR1 (green channel) and PGP9.5 (magenta channel) are robustly and uniformly expressed in the myenteric plexus. Like the ileum, LPAR1 is highly localized to regions surrounding neurons, indicating glial-specific expression in the human colon. *Bottom row*: LPAR1 and PGP9.5 expression is dramatically reduced in CIPO. f, Semi-quantificaiton of cross-sectional protein expression confirms significant reductions in myenteric LPAR1 and PGP9.5 levels in CIPO.

LPAR1 modulates gut motility

Although the marked reduction in glial LPAR1 expression is a novel and important histological finding in CIPO, the role of LPAR1 in GI motility remains circumstantial. If LPAR1 contributes to the pathogenesis of CIPO, we expect that manipulating LPAR1 signaling should produce a CIPO-like effect in mice. We consequently tested this by modulating LPAR1 activation *ex vivo* and *in vivo* and evaluating its effect on GI motility.

We assessed lower GI tract motility by measuring the effect of 18:1 LPA on colonic migrating motor complexes (CMMCs; **Fig 3.4a**). CMMCs are spontaneous inter-digestive patterns of colonic contractions that propagate in an oral-to-aboral direction and are dependent on the circuitry of the myenteric plexus[12,36]. Although the exact mechanisms regulating CMMC formation remain unclear[37], measuring CMMCs provides insight into the effect of LPA on the ENS-dependent GI motility. As such, application of LPA evoked a concentration-dependent reduction in colonic contractility in both the proximal (IC_{50}=19.2μM) and distal colon (IC_{50}=46.6μM, n=5**; Fig 3.4c**).

Given the drastic reductions in glial LPAR1 protein expression in CIPO, we characterized the effect selective LPAR1 blockade with AM966[38] on GI transit *in vivo* to determine if this could recapitulate the obstruction seen in CIPO. In vehicle-injected mice, carmine red dye traversed 35.24±1.21cm (n=5) of the total GI tract. Compared to controls, dye transit was drastically reduced in mice following exposure to medium (33mg/kg: 18.50±4.81cm, n=5; p=0.0014) or high (43mg/kg: 13.67±1.66cm, n=3; p=0.0014) doses of AM966 (**Fig 3.4f**).

Interestingly, AM966 provoked ~10% reduction in total body weight that was consistent between the low (23mg/kg), medium (33mg/kg) and high (43mg/kg) dose treatment groups (**Fig 3.4e**). This weight loss followed a consistent time course in all three drug treatment groups, plateauing by day 3. Remarkably, 2 of the 5 mice treated with high-dose AM966 were found dead on day 3 and post-mortem necropsies performed in these mice revealed consistent, small bowel

distension that was accompanied by a continuous pattern of transmural hemorrhaging that spared the colon (**Fig 3.4d**). Furthermore, the fecal pellets recovered in the colons of these mice were large and impacted, indicating that colonic transit was also dysregulated but that the overall effect was greatest in the ileum (not shown). This experimental finding is consistent with the overall presentation of small bowel ischemia observed in the surgical setting during bowel obstructions, including CIPO. Interestingly, mice treated with low-dose AM966 experienced a similar degree of weight loss as their medium or high dose-treated counterparts but did not exhibit reductions in carmine red transit.

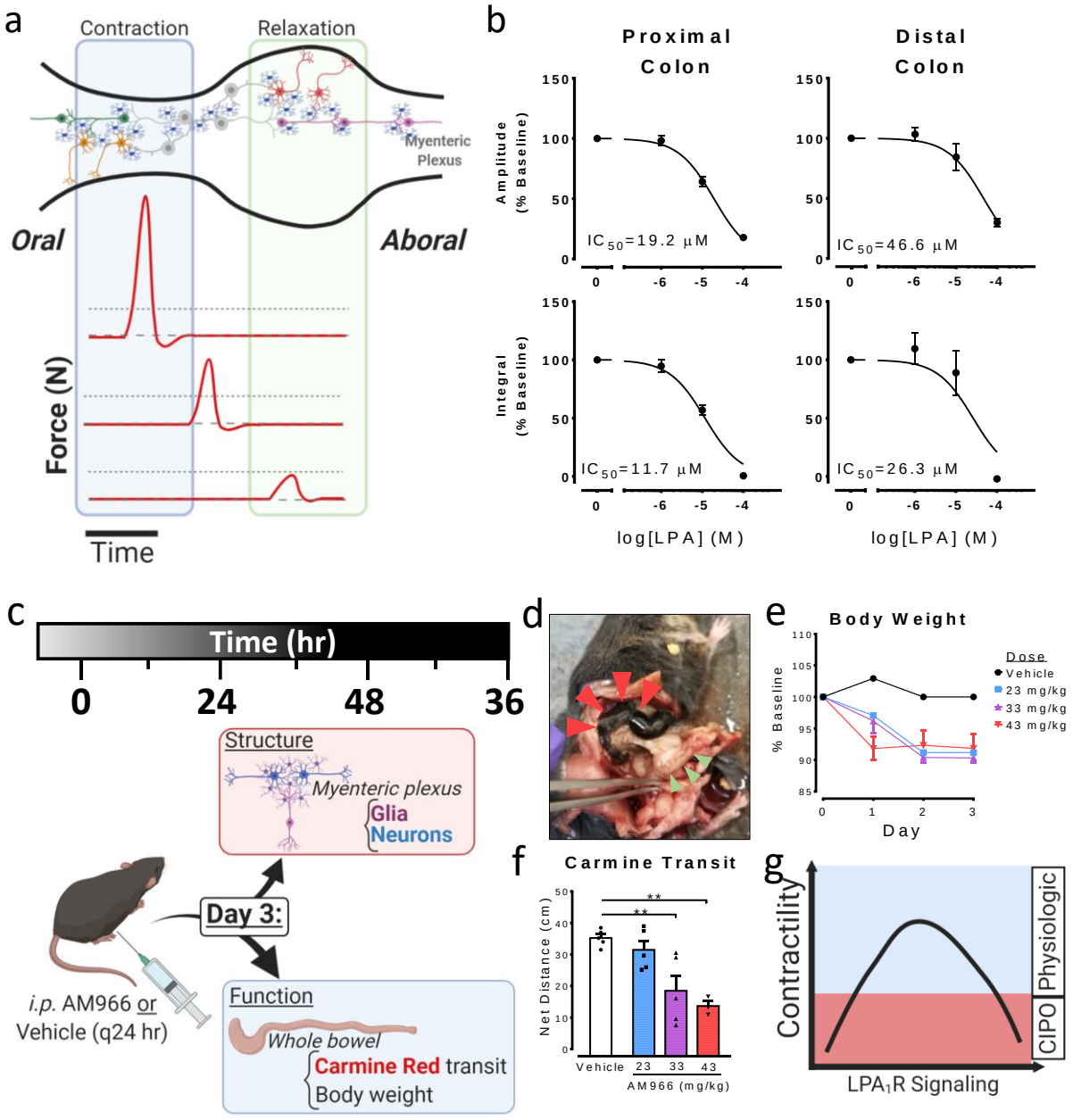

Figure 3.4. LPAR1 modulates whole bowel motility. a, Propagation of colonic migrating motor complexes (CMMCs) is mediated by the intrinsic circuitry of the myenteric plexus. Modulating glial LPAR1 may alter the contractile force of CMMCs. b, Acute stimulation of LPAR1 with bath-applied 18:1 LPA attenuates CMMCs in a concentration-dependent manner. c, Experimental paradigm illustrating *in vivo* pharmacological blockade of LPAR1 signaling. d, Mice treated with AM966 exhibited a sustained and isolated weight loss that plateaued by Day 3. e, In some cases, injection of 43mg/kg AM966 induced selective necrosis of the small bowel (red arrowheads) without grossly affecting colonic tissue appearance (green arrowheads). f, Carmine red transit was reduced in AM966-treated mice in a dose-dependent manner. g, Schematic diagram illustrating role of LPAR1 in gut motility. Excessive activation or blockade of LPAR1 is sufficient to alter several different parameters of GI motility.

In vivo blockade of LPAR1 is sufficient to drive ENS pathology

Our animal and CMMC studies indicate that LPAR1 signaling modulates GI motility and that deviations from some physiologically ideal set-point leads to GI dysmotility affecting small and large bowel motility. To corroborate the ENS specificity of these findings, we characterized architectural changes in the myenteric plexus of AM966 injected mice using immunohistochemistry.

Compared to vehicle-treated mice, low-dose AM966 did not affect ENS expression of GFAP or Hu C/D (**Fig 3.5a,b**). In these cases, GFAP staining exhibited a uniformly reticulated pattern with Hu-positive neurons evenly distributed within this network. Doublecortin staining, which delineates the location of nascent neurons[39], was relatively consistent between these two treatment groups and exhibited a linear punctate pattern resembling the varicosities of extrinsic autonomic nerves fiber tracts. Importantly, myenteric plexus structure was unaffected by low-dose AM966 as demonstrated by the qualitatively normal GFAP staining pattern.

Compared to vehicle controls, mice injected with medium-dose AM966 displayed ~96% increase in GFAP staining intensity ($p<0.01$), which was accompanied by drastically altered glial cell morphology in which cells adopted an astrocyte-like appearance. This marked change in glial architecture is a hallmark of cell stress and commonly observed under culture conditions. These histological findings are consistent with features of enteric gliosis and were further accompanied by a ~43% reduction in HuC/D expression (<0.001). Given that doublecortin staining was not affected, however, this likely reflects loss of mature enteric neurons without overt effects on the proliferating pool of enteric neurons.

High-dose AM966 exhibited similar ENS alterations characterized by glial process retraction and profound cytoskeletal disarray. Doublecortin staining was not affected at high dose AM966 treatment even though HuC/D staining was reduced by ~47% ($p<0.001$) compared to control. Like in the medium dose-treated group, there was no difference in ENS cellularity

compared to vehicle controls suggesting a lack of inflammatory cell influx or cellular hyperproliferation – findings consistent with the absence of systemic inflammation following AM966 injection noted elsewhere (**Appendix Figure 3.9**). Taken together, these data suggest that *in vivo* blockade of LPAR1 promotes enteric glial dysfunction and loss of mature but not immature enteric neurons within this timeframe of drug exposure.

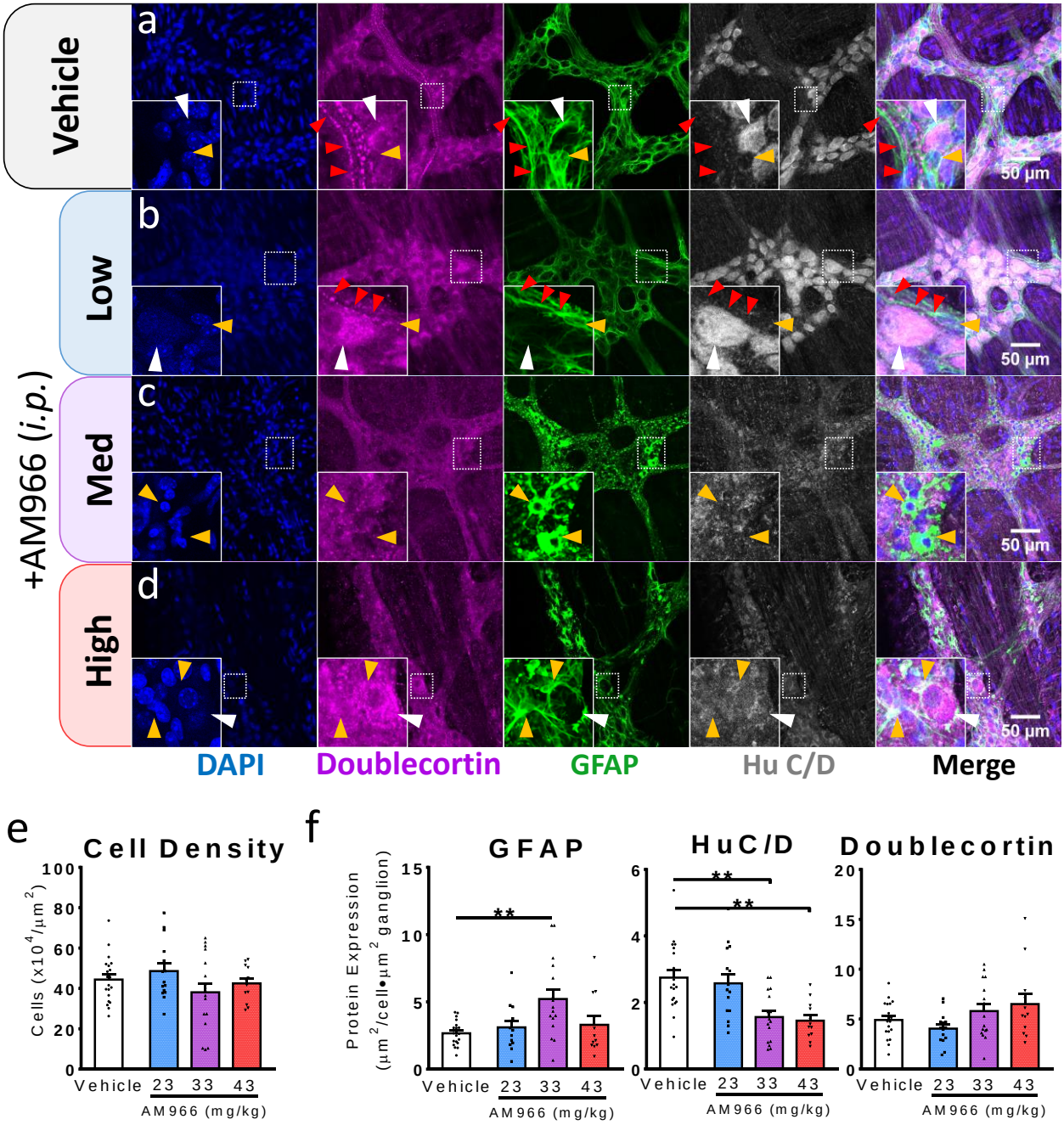

Figure 3.5. Pharmacological blockade of LPAR1 is sufficient to drive ENS pathology. a, b, In vehicle-treated colonic tissue, doublecortin staining can be visualized in fiber tracts coursing through the myenteric plexus alongside GFAP-positive fibers (a). This staining pattern is largely conserved in animals injected with low-dose AM966 (b) but is generally absent at higher doses. c, d, Both moderate (c) and high doses (d) of AM966 injection promote widespread gliosis in the myenteric plexus with accompanying loss of enteric neurons. This pathological pattern is characterized by diffuse, hyperintense GFAP staining (green channel) and reduced HuC/D expression patterns. e, The ENS changes are not accompanied by alterations in ganglion cellularity, suggesting that cell survival in the ENS is otherwise not acutely affected by AM966 treatment. f, Doublecortin expression levels are not affected by AM966 although neuronal HuC/D staining significantly decreases following injection of moderate and high doses of AM966.

DISCUSSION

Chronic intestinal pseudo-obstruction (CIPO) is a debilitating form of gut failure that is idiopathic in ~50% of cases. Histological examination of the gut in CIPO reveals neuropathic, myopathic and mesenchymopathic alterations of unknown etiology, with immune-mediated mechanisms playing a role in only some of these cases[1]. Here, we demonstrate conserved expression of the type I lysophosphatidic acid receptor (LPAR1) in enteric glia in mice and humans. In mice, LPAR1 drives Ca^{2+} responses in enteric glia while in humans, glial LPAR1 protein expression is reduced in CIPO. Selective blockade of LPAR1 in mice promotes decreased bowel transit, GI obstruction, and ENS alterations that collectively recapitulate the clinical findings of human CIPO. Together, these findings support an entirely novel role for enteric glial LPAR1 in the regulation of GI motility and the pathogenesis of CIPO.

LPAR1 is pleiotropically expressed[30] and whole-body knockout studies have shown its role in the GI tract includes regulation of tight junction protein expression in the colon[40]. While the motility-related effects of LPAR1 could therefore have been due to barrier disruptions, it is unlikely that this is the case for several reasons. Firstly, enteric glia serve well-known roles in modulating epithelial barrier function[41] and so the compromised barrier integrity and susceptibility to DSS-induced colitis noted in this study could have been amenable to dysregulations enteric glial LPAR1 activity *per se*. In addition, our *in vivo* experiments showed that AM966 triggers fulminant jejuno-ileitis that completely spares the colon. Given the putative role of colonic LPAR1 in maintaining the epithelial barrier, it was surprising that we did not observe any gross abnormalities within the colons of AM966-treated mice. Lastly, whole-body LPAR1 knockout drastically impairs feeding behaviors[42] and the wound healing response[43], raising the possibility that the GI phenotype observed was due to altogether due to extrinsic factors.

Although LPAR1 blockade in mice caused obstruction and recapitulated the clinical findings of CIPO, stimulating LPAR1 attenuated CMMCs but also provoked Ca^{2+} responses in

glia. This apparent contradiction between the effects of LPAR1 stimulation and blockade can be reconciled by the fact that LPAR1 activation drives internalization of the receptor into early endosomes[44,45]. Physiologically, this likely serves to dampen receptor activity when local agonist concentrations are exceedingly high, as is the case during acute inflammation. Moreover, LPAR1-endosomes activate non-canonical signaling programs that promote long-term changes in structural gene expression[44]. Thus, in the presence of high LPA concentration, the ensuing receptor internalization can shift the second messenger cascade away from $G_{q/11}$ and towards G_{13}, which in turn can initiate changes in cell morphology[46]. Alternatively, it is also possible that glial LPAR1 affects enteric neuronal subtypes involved in regulation of smooth muscle tone. In the feline lower esophageal sphincter (LES), for instance, LPA potentiates relaxation of the lower esophageal sphincter by blocking presynaptic uptake of nitric oxide[47]. Thus, it is possible that the reduction in colonic motility that we observed could be due to a similar effect on nitrergic neurons.

Our data provide compelling evidence that LPAR1 is robustly expressed in enteric glia and may contribute to motility disturbances in mice and humans. The mechanism through which this occurs is unclear, however, but may be dictated the intensity and duration of the stimulus. In the CNS and periphery, neuroglial LPAR1 has developmental and pathological roles involving control of neurocircuit architecture. For instance, LPAR1 guides Schwann cell myelination of motor neurons[48] while satellite glial LPAR1 initiates neuropathic pain by promoting cytoskeletal retraction[25]. Thus, enteric glial LPAR1 activity may serve a similar role in maintaining the structural integrity of the ENS – a possibility that is supported by the profound decay in ENS architecture seen in AM966-injected mice. One corollary of this is that glial LPAR1 is constitutively active in maintaining ENS architecture, though we suspect that basal levels of interstitial LPA are exceedingly low and tightly regulated.

Given that many functional GI disorders (FGIDs) feature a remote history of acute infectious enteritis and that biolipids, including 18:1 LPA, are robustly generated during the acute phase of inflammation, activation of enteric glial LPAR1 may serve as the bridge linking early

tissue damage to long term remodeling of ENS architecture. This would be consistent with the function of glial LPAR1 in shaping the neural landscape during development, but also with its purported role in re-sculpting peripheral neurocircuitry during disease. In accordance with this, the reductions in *Lpar1* and *Enpp2* gene expression observed following acute colitis may constitute an early perturbance that, if sustained, lead to the histopathological changes seen in CIPO patients. Indeed, tissue levels of 18:1 LPA remain uniquely elevated in mice following partial ligation of the sciatic nerve weeks following the initial injury[35]. It is therefore conceivable that persistence of LPA in the ENS could potentiate the initial tissue damage. If confirmed, this would imply that FGID severity is governed by the degree and persistence of glial LPAR1 dysregulation and that CIPO simply lies on the extreme end of this spectrum. Whether glial LPAR1 is dysregulated in the context of other GI dysmotilities, however, is an important next step that should be further investigated.

The finding that enteric glial LPAR1 expression is conserved across different species suggests that this receptor fulfills a critical role in GI physiology. Considering our clinical and functional data, this role likely involves modulation of gut motility possibly through long-term regulation of ENS architecture and acute modulation of Ca^{2+} handling dynamics. Ultimately, our study identifies a novel role for enteric glia in the pathogenesis of GI dysmotility and unveils a new target that may be of diagnostic and therapeutic benefit in the clinical management of CIPO.

APPENDIX

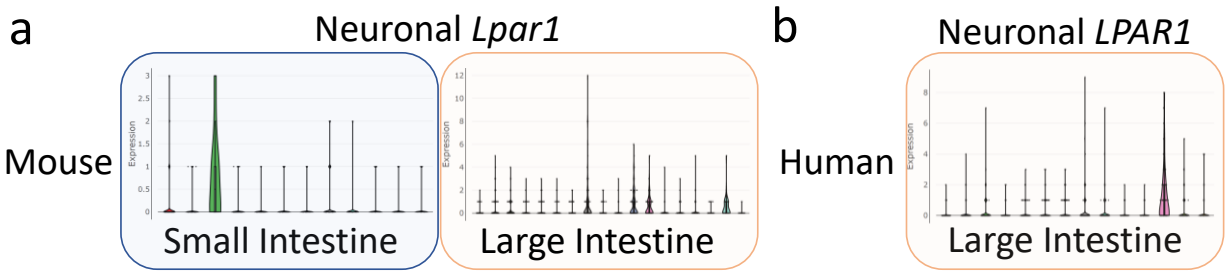

Figure 3.6. LPAR1 gene expression in enteric neurons. a, Murine enteric neurons express nearly undetectable levels of *Lpar1*, except for one subtype (*left panel*, green violin plot). This pattern of low *Lpar1* expression is evident in both small and large intestinal tissue regions. b, Similarly low levels of LPAR1 gene expression is observed within enteric neurons of the human large intestine. Data are compiled from a single-cell RNA-sequencing database from Zeisel et. al., (2018). Plots were generated using the online database located at (http://mousebrain.org/genesearch.html).

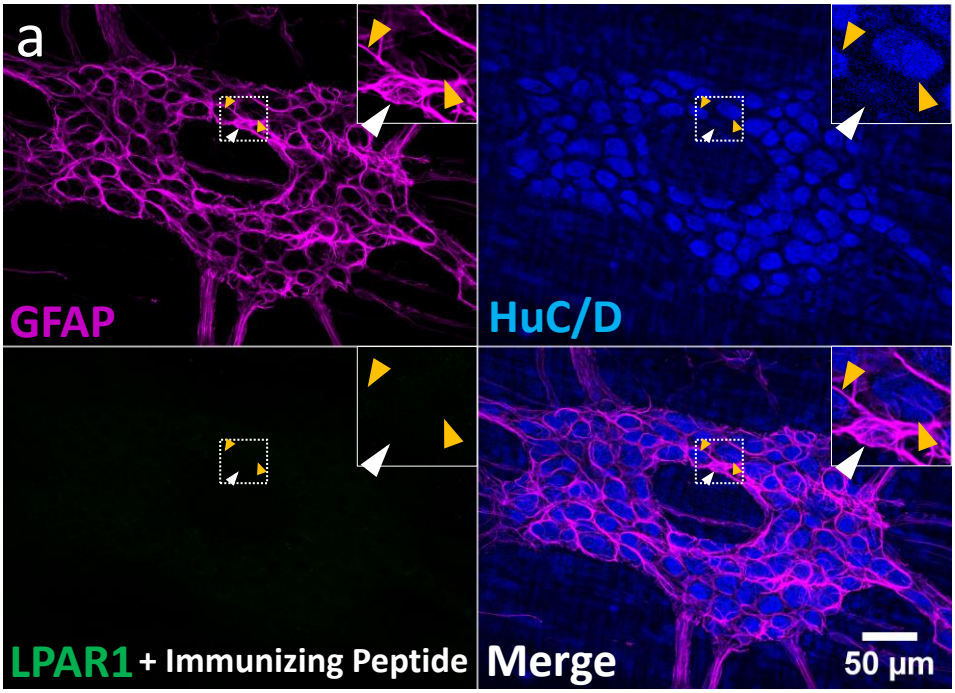

Figure 3.7. Specificity of LPAR1 antibody. LPAR1 staining is entirely abrogated when the probing antibody is blocked with the immunizing peptide, suggesting specificity in the staining pattern.

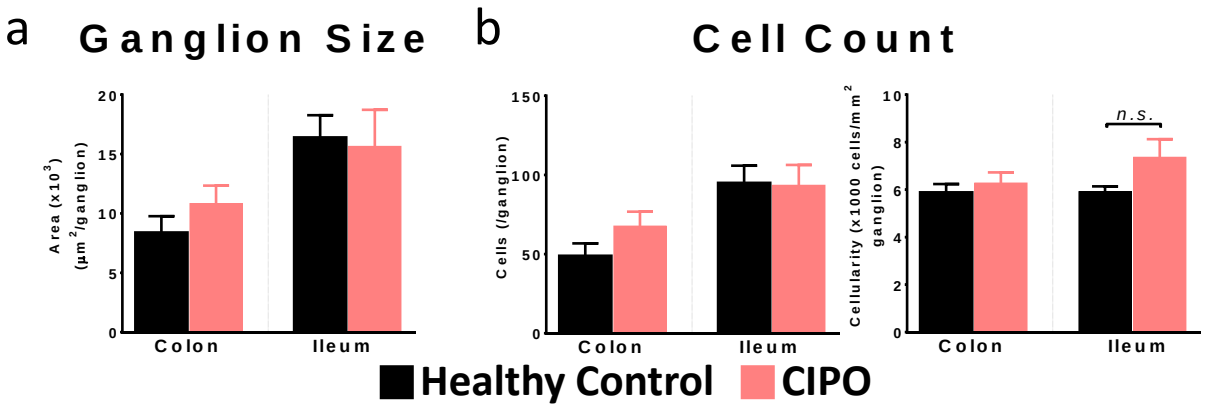

Figure 3.8. Morphological characteristics of human ileum and colon. a, The cross-sectional area of the myenteric plexus is not different between CIPO and healthy controls. This pattern is true in both the ileum and colon. b, Ganglionic cellularity, measured by quantifying the number of cells within a given ganglion (left panel) or number of cells per mm^2 ganglionic area (*right panel*) provided two distinctive measures showing no difference between the ganglionic cellularity observed in the ENS of healthy individuals and patients with CIPO.

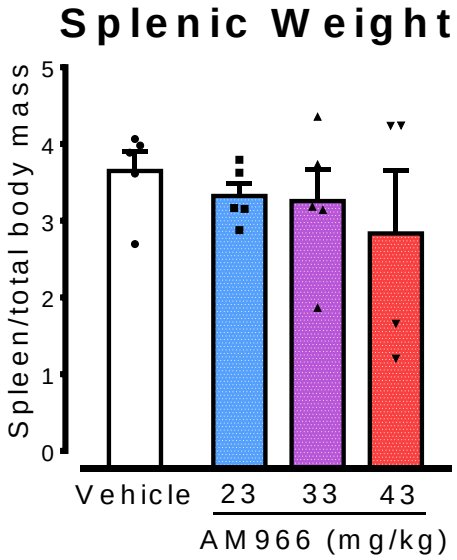

Figure 3.9. Effect of AM966 injection on splenic weight. Sub-chronic treatment with *ip* AM966 did not result in changes in splenic mass, which was normalized to the final body weight of each mouse at the time of death. This suggests that the overall effects, including reductions in body weight, were not likely to be driven by a broad systemic inflammatory response.

REFERENCES

REFERENCES

1. De Giorgio, R., Cogliandro, R. F., Barbara, G., Corinaldesi, R. & Stanghellini, V. Chronic Intestinal Pseudo-Obstruction: Clinical Features, Diagnosis, and Therapy. *Gastroenterol. Clin. North Am.* **40**, 787–807 (2011).

2. De Giorgio, R. *et al.* New insights into human enteric neuropathies. in *Neurogastroenterology and Motility* vol. 16 143–147 (Blackwell Publishing Ltd, 2004).

3. Streutker, C. J., Huizinga, J. D., Campbell, F., Ho, J. & Riddell, R. H. Loss of CD117 (c-kit)- and CD34-positive ICC and associated CD34-positive fibroblasts defines a subpopulation of chronic intestinal pseudo-obstruction. *Am. J. Surg. Pathol.* **27**, 228–235 (2003).

4. Boeckxstaens, G. E., Rumessen, J. J., Wit, L., Tytgat, G. N. J. & Vanderwinden, J.-M. Abnormal distribution of the interstitial cells of Cajal in an adult patient with pseudo-obstruction and megaduodenum. *Am. J. Gastroenterol.* **97**, 2120–2126 (2002).

5. Stanghellini, V. *et al.* Natural history of chronic idiopathic intestinal pseudo-obstruction in adults: A single center study. *Clin. Gastroenterol. Hepatol.* **3**, 449–458 (2005).

6. Longo, W. E. & Vernava, A. M. Prokinetic agents for lower gastrointestinal motility disorders. *Dis. Colon Rectum* **36**, 696–708 (1993).

7. Camilleri, M. *et al.* Effect of Six Weeks of Treatment With Cisapride in Gastroparesis and Intestinal Pseudo obstruction. *Gastroenterology* **96**, 704–712 (1989).

8. Sogawa, H. *et al.* Twenty Years of Gut Transplantation for Chronic Intestinal Pseudo-obstruction. *Ann. Surg.* **XX**, (2019).

9. Furness, J. B. The enteric nervous system and neurogastroenterology. *Nat. Rev. Gastroenterol. Hepatol.* **9**, 286–294 (2012).

10. Spencer, N. J. & Hu, H. Enteric nervous system: sensory transduction, neural circuits and gastrointestinal motility. *Nature Reviews Gastroenterology and Hepatology* vol. 17 338–351 (2020).

11. De Giorgio, R. *et al.* Inflammatory neuropathies of the enteric nervous system. *Gastroenterology* **126**, 1872–1883 (2004).

12. Broadhead, M. J., Bayguinov, P. O., Okamoto, T., Heredia, D. J. & Smith, T. K. Ca 2+ transients in myenteric glial cells during the colonic migrating motor complex in the isolated murine large intestine. *J. Physiol.* **590**, 335–350 (2012).

13. Gulbransen, B. D. & Sharkey, K. A. Purinergic Neuron-to-Glia Signaling in the Enteric Nervous System. *Gastroenterology* **136**, 1349–1358 (2009).

14. McClain, J. L., Fried, D. E. & Gulbransen, B. D. Agonist-Evoked Ca2+ Signaling in Enteric Glia Drives Neural Programs That Regulate Intestinal Motility in Mice. *Cmgh* **1**, 631–645 (2015).

15. McClain, J. *et al.* Ca2+ responses in enteric glia are mediated by connexin-43 hemichannels and modulate colonic transit in mice. *Gastroenterology* **146**, 497-507.e1

(2014).

16. Brown, I. A. M., McClain, J. L., Watson, R. E., Patel, B. A. & Gulbransen, B. D. Enteric Glia Mediate Neuron Death in Colitis Through Purinergic Pathways That Require Connexin-43 and Nitric Oxide. *CMGH* **2**, 77–91 (2016).

17. Barcelos Morais Da Silveira, A. *et al.* Enteroglial cells act as antigen-presenting cells in chagasic megacolon. *Hum. Pathol.* **42**, 522–532 (2011).

18. Chow, A. K. & Gulbransen, B. D. Potential roles of enteric glia in bridging neuroimmune communication in the gut. *Am. J. Physiol. - Gastrointest. Liver Physiol.* **312**, G145–G152 (2017).

19. Gaire, B. P., Sapkota, A., Song, M. R. & Choi, J. W. Lysophosphatidic acid receptor 1 (LPA1) plays critical roles in microglial activation and brain damage after transient focal cerebral ischemia. *J. Neuroinflammation* **16**, 170 (2019).

20. Lin, C. I. *et al.* Lysophosphatidic acid regulates inflammation-related genes in human endothelial cells through LPA1 and LPA3. *Biochem. Biophys. Res. Commun.* **363**, 1001–1008 (2007).

21. Segura, B. J. *et al.* Lysophosphatidic acid stimulates calcium transients in enteric glia. *Neuroscience* **123**, 687–693 (2004).

22. Zhang, W., Segura, B. J., Lin, T. R., Hu, Y. & Mulholland, M. W. Intercellular calcium waves in cultured enteric glia from neonatal guinea pig. *Glia* **42**, 252–262 (2003).

23. Spiller, R. & Garsed, K. Postinfectious Irritable Bowel Syndrome. *Gastroenterology* **136**, 1979–1988 (2009).

24. Drossman, D. A. Functional gastrointestinal disorders: History, pathophysiology, clinical features, and Rome IV. *Gastroenterology* **150**, 1262-1279.e2 (2016).

25. Robering, J. W. *et al.* Lysophosphatidic acid activates satellite glia cells and Schwann cells. *Glia* **67**, 999–1012 (2019).

26. Inoue, M. *et al.* Initiation of neuropathic pain requires lysophosphatidic acid receptor signaling. *Nat. Med.* **10**, 712–719 (2004).

27. Park, K. A. & Vasko, M. R. Lipid mediators of sensitivity in sensory neurons. *Trends Pharmacol. Sci.* **26**, 571–577 (2005).

28. Zeisel, A. *et al.* Molecular Architecture of the Mouse Nervous System Resource Molecular Architecture of the Mouse Nervous System. *Cell* **174**, 999-1014.e22 (2018).

29. Drokhlyansky, E. *et al.* The Human and Mouse Enteric Nervous System at Single-Cell Resolution. *Cell* **182**, 1606-1622.e23 (2020).

30. Yung, Y. C., Stoddard, N. C. & Chun, J. LPA receptor signaling: Pharmacology, physiology, and pathophysiology. *Journal of Lipid Research* vol. 55 1192–1214 (2014).

31. Jessen, K. R. & Mirsky, R. Glial cells in the enteric nervous system contain glial fibrillary acidic protein. *Nature* **286**, 736–737 (1980).

32. Delvalle, N. M. *et al.* Communication Between Enteric Neurons, Glia, and Nociceptors Underlies the Effects of Tachykinins on Neuroinflammation. *Cmgh* **6**, 321–344 (2018).

33. Lewis, A. E., Vasudevan, H. N., O'Neill, A. K., Soriano, P. & Bush, J. O. The widely used Wnt1-Cre transgene causes developmental phenotypes by ectopic activation of Wnt signaling. *Dev. Biol.* **379**, 229–234 (2013).

34. Danielian, P. S., Muccino, D., Rowitch, D. H., Michael, S. K. & McMahon, A. P. Modification of gene activity in mouse embryos in utero by a tamoxifen-inducible form of Cre recombinase. *Curr. Biol.* **8**, 1323–1326 (1998).

35. Santos-Nogueira, E. *et al.* Activation of lysophosphatidic acid receptor type 1 contributes to pathophysiology of spinal cord injury. *J. Neurosci.* **35**, 10224–102035 (2015).

36. Hibberd, T. J. *et al.* Neurogenic and myogenic patterns of electrical activity in isolated intact mouse colon. *Neurogastroenterol. Motil.* **29**, 1–12 (2017).

37. Smith, T. K. & Koh, S. D. A model of the enteric neural circuitry underlying the generation of rhythmic motor patterns in the colon: The role of serotonin. *Am. J. Physiol. - Gastrointest. Liver Physiol.* **312**, G1–G14 (2017).

38. Swaney, J. S. *et al.* A novel, orally active LPA 1 receptor antagonist inhibits lung fibrosis in the mouse bleomycin model. *Br. J. Pharmacol.* **160**, 1699–1713 (2010).

39. Liu, M. T., Kuan, Y. H., Wang, J., Hen, R. & Gershon, M. D. 5-HT4 receptor-mediated neuroprotection and neurogenesis in the enteric nervous system of adult mice. *J. Neurosci.* **29**, 9683–9699 (2009).

40. Lin, S. *et al.* Lysophosphatidic Acid Receptor 1 Is Important for Intestinal Epithelial Barrier Function and Susceptibility to Colitis. *Am. J. Pathol.* **188**, 353–366 (2018).

41. Savidge, T. C. *et al.* Enteric Glia Regulate Intestinal Barrier Function and Inflammation Via Release of S-Nitrosoglutathione. *Gastroenterology* **132**, 1344–1358 (2007).

42. Contos, J. J. A., Fukushima, N., Weiner, J. A., Kaushal, D. & Chun, J. Requirement for the lp(A1) lysophosphatidic acid receptor gene in normal suckling behavior. *Proc. Natl. Acad. Sci. U. S. A.* **97**, 13384–13389 (2000).

43. Yun, C. C. & Kumar, A. Diverse roles of LPA signaling in the intestinal epithelium. *Exp. Cell Res.* **333**, 201–207 (2015).

44. Varsano, T., Taupin, V., Guo, L., Baterina, O. Y. & Farquhar, M. G. The PDZ Protein GIPC Regulates Trafficking of the LPA1 Receptor from APPL Signaling Endosomes and Attenuates the Cell's Response to LPA. *PLoS One* **7**, (2012).

45. Alcántara-Hernández, R., Hernández-Méndez, A., Campos-Martínez, G. A., Meizoso-Huesca, A. & García-Sáinz, J. A. Phosphorylation and internalization of lysophosphatidic acid receptors LPA1, LPA2, and LPA3. *PLoS One* **10**, (2015).

46. Cai, H. & Xu, Y. The role of LPA and YAP signaling in long-term migration of human ovarian cancer cells. *Cell Commun. Signal.* **11**, 31 (2013).

47. Lee, J. W., Kim, C. H., Wang, Y. Y., Yan, X. M. & Sohn, U. D. Lysophosphatidic acid presynaptically blocks NO uptake during electric field stimulation-induced relaxation via LPA1 receptor in cat lower esophageal sphincter. *Arch. Pharm. Res.* **34**, 169–176 (2011).

48. Mogha, A., D'Rozario, M. & Monk, K. R. G Protein-Coupled Receptors in Myelinating Glia. *Trends in Pharmacological Sciences* vol. 37 977–987 (2016).

49. Shi, S. R., Chaiwun, B., Young, L., Cote, R. J. & Taylor, C. R. Antigen retrieval technique

utilizing citrate buffer or urea solution for immunohistochemical demonstration of androgen receptor in formalin-fixed paraffin sections. *J. Histochem. Cytochem.* **41**, 1599–1604 (1993).

50. Spencer, N. J., Dickson, E. J., Hennig, G. W. & Smith, T. K. Sensory elements within the circular muscle are essential for mechanotransduction of ongoing peristaltic reflex activity in guinea-pig distal colon. *J. Physiol.* **576**, 519–531 (2006).

51. Liszewska, E. *et al.* Lysophosphatidic acid signaling during embryo development in sheep: Involvement in prostaglandin synthesis. *Endocrinology* **150**, 422 (2009).

52. Schindelin, J. *et al.* Fiji: An open-source platform for biological-image analysis. *Nature Methods* vol. 9 676–682 (2012).

53. Li, Z., Mintzer, E. & Bittman, R. The critical micelle concentrations of lysophosphatidic acid and sphingosylphosphorylcholine. *Chem. Phys. Lipids* **130**, 197–201 (2004).

54. Gad, S. C., Cassidy, C. D., Aubert, N., Spainhour, B. & Robbe, H. Nonclinical vehicle use in studies by multiple routes in multiple species. *Int. J. Toxicol.* **25**, 499–521 (2006).

55. Grubišić, V., Kennedy, A. J., Sweatt, J. D. & Parpura, V. Pitt-Hopkins Mouse Model has Altered Particular Gastrointestinal Transits In Vivo. *Autism Res.* **8**, 629–633 (2015).

CHAPTER 4: KEY FINDINGS AND FUTURE DIRECTIONS

KEY FINDINGS

Neuroglia are increasingly recognized for their role in regulating synaptic activity[1,2]. This concept has garnered particular attention in the CNS, where astrocytes have been found to regulate brain circuit activity through synapse-specific mechanisms[3–6]. This newfound precision in glial modulation of neural activity has dramatic implications for our understanding brain function overall but has otherwise remained an isolated observation thought to be unique to the highly evolved CNS.

In Chapter 1, we demonstrated that glia in the gut's enteric nervous system (ENS) regulate the neural circuits controlling gut motility in a synapse-specific and sex-dependent manner. While the neural circuitry of the ENS has been well described in isolation[7,8], no one has provided a comprehensive and functionally validated framework describing how these neurons engage with enteric glia—which surround them in abundance. Rather than studying discrete neural or glial responses, we investigated how these two cell populations interact with each other in an intact "connectome"[9]. Using novel chemogenetic and optogenetic mouse lines, we show that enteric glia function as logic gates to delegate the flow of information through overlapping neural networks of the GI tract. These interactions are precise and deliberate, ultimately showcasing how responses within an integrated network far outstrip the functional complexity seen at the single-cell level.

This truer-to-life model of the gut's neurocircuitry reconciles decades-old descriptions of ENS neurochemical coding with functional roles that are physiologically and clinically meaningful. The scope and impact of these findings are therefore potentially immense, as they not only allow for all-cause gut dysmotilities to be reframed as connectopathies in which network-level perturbances drive disease, but they also showcase the evolutionary basis of how brain networks are potentially regulated in states of health and disease.

In Chapter 2, we provided new evidence for the functional role of glial LPAR1 in the control of GI motility and the pathogenesis of CIPO. Using multiple approaches, we demonstrated that LPAR1 expression is highly conserved in enteric glia but absent from enteric neurons in both mice and humans. We subsequently replicate CIPO-like symptoms in mice by pharmacologically blocking LPAR1 activity with the specific antagonist, AM966. The collective genetic, immunohistochemical, functional and *in vivo* experimental approaches all support a novel, pathologically relevant role for enteric glial LPAR1 as a regulator of GI motility. This study consequently highlights a fundamentally novel disease mechanism that could be targeted in the development of treatments for CIPO.

FUTURE DIRECTIONS

Patterns of GI motility vary drastically between different gut segments (mixing in the ileum vs propulsive in the colon). At the same time, these motility programs must be dynamic, modifiable, and appropriate for the physiological state (fed vs inter-digestive) or pathological burden (infection vs tolerance). Understanding how network-level dysfunction in the ENS precipitates motility disturbances can serve to reframe our understanding of FGIDs as "connectopathies" resulting from aberrant interactions between the synaptic elements of the ENS neurocircuitry. Thus, future experiments should seek to clarify the impact of inflammatory insults on the networked activity of the ENS. Specifically, using a post-inflammatory model of DNBS colitis to recapitulate the phenotypic alterations in ENS excitability can provide a useful tool for characterizing the connectopathic alterations in the post-inflamed gut. Furthermore, it would be pertinent to characterize putative differences in these alterations between sexes as this could shed insight into why females tend to exhibit a greater predilection for functional GI dysmotilities[10].

Lastly, the role of glial LPAR1 in maintaining ENS architecture should be more closely investigated. I suspect that the role of glial LPAR1 in the developing ENS is analogous to the CNS

– that is, control of axonal guidance and neurite outgrowth. Constitutive signaling via this pathway may be basally required for ongoing maintenance of ENS structure in the adult thus representing a continuation of its developmental role. In this regard, dysregulation of glial LPAR1 might constitute the “first strike” that initiates rapid architectural demise in the ENS that through other mechanisms eventually leading to derangements in GI motility. The kinetics of glial LPAR1 singaling and the pharmacodynamics (regulation of cell surface expression levels) may dictate this process. Lastly, the use of mouse models permitting the conditional, glial-specific deletion of LPAR1 (recently described LPAR1$^{flox/flox}$)[11] may also prove valuable in further clarifying the role of glial LPAR1 in the regulation of GI motiliyt.

The effects of LPAR1 activation (or blockade) on the acute, chronic and post-inflammatory phases of DNBS-colitis should also be explored as a starting point for assessing the translational potential of LPAR1 modulation in the context of GI motility disorders. I anticipate that low-grade stimulation with an LPAR1 incapable of driving receptor internalization might be protective during acute inflammation, while LPAR1 blockade might be protective during chronic phases of inflammation (when LPA agonist is present in abundance).

Additional *in vitro* experiments should be conducted to assess the effect of focal LPA concentration gradients on the morphological outgrowth, survival, and function of cultured populations of enteric glia. I anticipate that enteric glial LPAR1 activation, at the right agonist concentration range, would facilitate glial survival, minimize cell stress, and overall promote plexiform growth of the cells.

REFERENCES

REFERENCES

1. Verkhratsky, A., Parpura, V., Dean, M. & Gan, M. Introduction to Neuroglia Introduction to Neuroglia Colloquium series on neuroglia in Biology and mediCine from physiology to disease Colloquium series on neuroglia in Biology and mediCine from physiology to disease.

2. Gundersen, V., Storm-Mathisen, J. & Bergersen, L. H. Neuroglial Transmission. *Physiol. Rev.* **95**, 695–726 (2015).

3. Martín, R., Bajo-Grañeras, R., Moratalla, R., Perea, G. & Araque, A. *Circuit-specific signaling in astrocyte-neuron networks in basal ganglia pathways*. *Science* vol. 349 http://science.sciencemag.org/ (2015).

4. Martin-Fernandez, M. *et al.* Synapse-specific astrocyte gating of amygdala-related behavior. *Nat. Neurosci.* **20**, 1540–1548 (2017).

5. Chai, H., Diaz-Castro, B., Shigetomi, E., Neuron, E. M.- & 2017, undefined. Neural circuit-specialized astrocytes: transcriptomic, proteomic, morphological, and functional evidence. *Elsevier*.

6. Yu, X. *et al.* Reducing Astrocyte Calcium Signaling In Vivo Alters Striatal Microcircuits and Causes Repetitive Behavior. *Neuron* **99**, 1170-1187.e9 (2018).

7. Furness, J. B. The enteric nervous system and neurogastroenterology. *Nat. Rev. Gastroenterol. Hepatol.* **9**, 286–294 (2012).

8. Furness, J. B. Types of neurons in the enteric nervous system. *J. Auton. Nerv. Syst.* **81**, 87–96 (2000).

9. Swanson, L. W. & Lichtman, J. W. From Cajal to Connectome and beyond. *Annu. Rev. Neurosci.* **39**, 197–216 (2016).

10. Epidemiology, R. C. S. & Schemann, M. Irritable bowel syndrome HHS Public Access. *Nat. Rev. Dis. Prim.* **2**, 16014 (2016).

11. Rivera, R. R., Lin, M.-E., Bornhop, E. C., Chun, J. & Burnham, S. Conditional Lpar1 gene targeting identifies cell types mediating neuropathic pain. *bioRxiv* **858**, 795–5024 (2020).